[Electronic Supplementary Information to accompany *Chem. Commun.* manuscript CC-COM-12-2011-017568]

Enhanced catalytic decomposition of a phosphate triester by modularly accessible bimetallic porphyrin dyads and dimers

Ryan K. Totten,[a] Patrick Ryan,[b] Byungman Kang,[a] Suk Joong Lee,[a,c] Linda J. Broadbelt,[b] Randall Q. Snurr,[b] Joseph T. Hupp,[a,*] and SonBinh T. Nguyen[a,*]

[a]*Department of Chemistry and the Institute for Catalysis in Energy Processes, Northwestern University, 2145 Sheridan Road, Evanston, Illinois 60208-3113, USA.* [b]*Department of Chemical and Biological Engineering, Northwestern University, 2145 Sheridan Road, Evanston, Illinois 60208, USA.* [c]*Current address: Department of Chemistry, Research Institute for Natural Sciences, Korea University, 5 Anam-dong, Sungbuk-gu, Seoul 136-701, Korea*

Table of Contents *Page number*

I. General information. ^{1}H and ^{13}C NMR spectra were recorded on either a Bruker Avance 500 (499.4 MHz for ^{1}H, 125.8 MHz for ^{13}C) spectrometer or a Varian Mercury 400 FT-NMR spectrometer (400.6 MHz for ^{1}H, 100.7 MHz for ^{13}C). ^{1}H NMR data are reported as follows: chemical shift (multiplicity (bs = broad singlet, s = singlet, d = doublet, t = triplet, q = quartet, and m = multiplet), coupling constant and integration). ^{1}H and ^{13}C chemical shifts are reported in ppm downfield from tetramethylsilane (TMS, δ scale) using the residual solvent resonances as internal standards. ^{31}P NMR spectra were recorded on a Varian INOVA 400 FTNMR spectrometer (161.9 MHz for ^{31}P) and externally referenced to 85% phosphoric acid solution in D_2O.

Matrix-assisted laser desorption ionization time-of-flight (MALDI-ToF) mass spectra were recorded on a Bruker Autoflex III spectrometer using reflective positive MALDI ionization method with either 2-hydroxy-1-naphthoic acid for Zn-containing compounds or pyrene matrices for Al-containing compounds. The use of non-acidic pyrene matrix is critical for porphyrin containing Al-OMe: if the acidic 2-hydroxy-1-naphthoic acid matrix is used, complete demetallation occurs. When the pyrene matrix was used, demetallion was not observed but significant loss of the OMe axial ligand does occur. High-resolution electrospray ionization mass spectrometric (HRESIMS) data were obtained by staff members in the Integrated Molecular Structure Education and Research Center (IMSERC), Northwestern University (Evanston, IL, USA).

UV-vis spectra were obtained in CH_2Cl_2 or $CHCl_3$ on a Varian Cary 500 spectrophotometer. Fluorescence emission spectra were obtained in a mixture of $CHCl_3$/MeOH (1:1 v/v) on a Jobin Yvon FluoroLog fluorometer (λ_{ex} = 442 nm, λ_{em} = 500 – 800 nm, slit width = 3 nm) (HORIBA Jobin Yvon Inc., Edison, NJ, USA).

II. General procedures and materials. All air- or water-sensitive reactions were carried out under nitrogen using oven-dried glassware. All synthetic and catalytic experiments concerning porphyrin and porphyrin derivatives were carried out under light-deficient conditions: the hood lights were turned off and the reaction flasks are covered with aluminum foil to further minimize light exposure. Isolated porphyrin products were stored at low temperatures (-10 °C) in foil-covered vials. All flash-chromatography was carried out using silica gel (MP Silitech 60-200 mesh) under a positive pressure of nitrogen, unless otherwise noted. Analytical thin layer chromatography (TLC) was performed using glass-backed silica gel 60 F_{254} plates (Merck EMD-571507). Visualization of the TLC results was achieved by observation under UV light (254 nm).

Tetrahydrofuran and dichloromethane (Fisher Scientific) were dried over neutral alumina in a Dow-Grubbs solvent system[S1] installed by Glass Contours (now SG Water, Nashua, NH, USA). All other reagents were purchased from the Aldrich Chemical Company (Milwaukee, WI, USA) and used without further purification, unless otherwise noted. Deuterated solvents were purchased from Cambridge Isotope Laboratories (Andover, MA, USA) and used without further purification.

III. Preparation of porphyrins possessing di-*tert*-butylphenyl substituents.

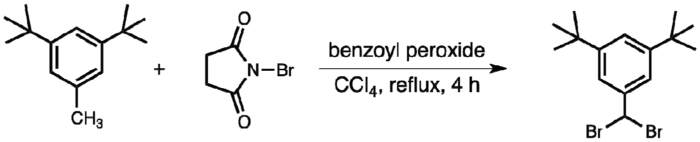

1

3,5-Di-*tert*-butyl(dibromomethyl)benzene (1). This compound was synthesized following a modified literature procedure.[S2] Into a 250 mL round-bottom flask equipped with a magnetic stir bar and a water-cooled reflux condenser were combined 3,5-di-*tert*-butyltoluene (10.0 g, 48.8 mmol), *N*-bromosuccinimide (17.4 g, 97.6 mmol), benzoyl peroxide (0.1 g, 0.5 mmol), and CCl_4 (90 mL). The resulting suspension was then brought to reflux and kept there for 4 h. After cooling to room temperature, the reaction mixture was filtered and concentrated under reduced pressure to afford a yellow oil. The crude product (17.7 g, 48.8 mmol, 99% yield) was used without any further purification in the next step.

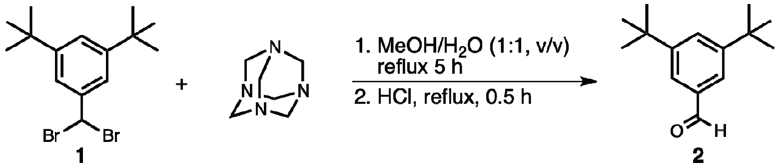

3,5-Di-*tert*-butylbenzaldehyde (2). This compound was synthesized following a modified literature procedure.[S2] Into a 250 mL round-bottom flask equipped with a magnetic stir bar and a water-cooled reflux condenser were combined compound **1** (crude mass 17.7 g, 48.8 mmol), hexamethylenetetramine (28.5 g, 202.0 mmol), and a mixture of methanol/water (80 mL, 1:1 v/v). The resulting mixture was then brought to reflux and then kept there for 5 h. Concentrated aqueous HCl (25 mL of a 37 wt% solution) was added dropwise and the reaction mixture was allowed to reflux for an additional 0.5 h. After cooling to room temperature, the solution was extracted into CH_2Cl_2 (3 × 60 mL) and the combined organic extracts were dried over Na_2SO_4, filtered, and concentrated under reduced pressure. Purification via silica gel column chromatography (column dimensions = 60 mm × 250 mm, eluent = hexanes/CH_2Cl_2 10:1 v/v) gave a crude product, which was recrystallized from EtOH/water (1:1 v/v) to give pure **2** (8.2 g, 37.6 mmol, 77% yield) as a white crystalline solid. Spectroscopic data for **2** was in good agreement with literature data.[S2] ^{1}H NMR (499.4 MHz, $CDCl_3$): δ 1.4 (s, 18H, C(C*H*$_3$)$_3$, 7.74 (m, 3H, Ar-*H*), 10.03 (s, 1H, C*H*O). {^{1}H}^{13}C NMR (125.8 MHz, $CDCl_3$): δ 31.4, 35.2, 124.4, 129.1, 136.4, 152.0, 193.4.

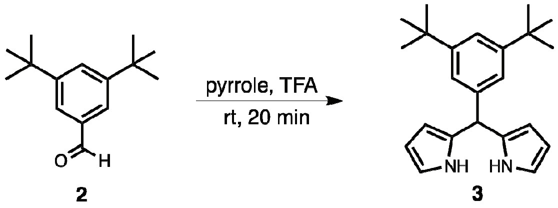

(3,5-Di-*tert*-butylphenyl)-2,2'-dipyrromethane (3). This compound was synthesized following a modified literature procedure.[S3] Compound **2** (3.0 g, 13.7 mmol) was combined with freshly distilled pyrrole (95 mL) in a 250 mL round-bottom flask equipped with a magnetic stir bar. This mixture was degassed with a stream of N_2 for 10 minutes. Trifluoroacetic acid (0.1 mL, 1.4 mmol) was then added and the reaction mixture was stirred under N_2 at room temperature for 20 minutes. The reaction mixture was diluted with CH_2Cl_2 (300 mL) before washing with aq. NaOH (150 mL of a 0.1 M solution). After drying over Na_2SO_4, the solvent was removed under reduced pressure. Excess pyrrole was removed by vacuum distillation at 60 °C and 20 mm Hg. The resulting tarry residue was purified by silica gel column chromatography (column dimensions = 60 mm × 250 mm, eluent = hexanes/ EtOAc/triethylamine 7:2:1 v/v/v). The second fraction was collected, evaporated to dryness, and redissolved in hot methanol/water (5:1 v/v) and stored at -10 ºC overnight. The solution was decanted into water (100 mL) and then extracted into CH_2Cl_2 (3 × 60 mL). After drying over Na_2SO_4, the CH_2Cl_2 layer was concentrated to dryness under reduced pressure to give a pale yellow oil that solidified at -10 °C (3.4 g, 10.3 mmol, 75% yield). Spectroscopic data for **3** was in good agreement with literature data.[S3] ^{1}H NMR (499.4 MHz, $CDCl_3$): δ 1.26 (s, 18H, C(C*H*$_3$)$_3$, 5.43 (s, 1H, C*H*), 5.91 (bs, 2H, pyrrole C*H*), 6.13 (dd, J_1 = 7.5 Hz, J_2 = 3.5 Hz, 2H, pyrrole C*H*), 6.67 (m, 2H, pyrrole C*H*), 7.04 (d, J = 2 Hz, 2H, Ar-*H*), 7.29 (d, J = 2 Hz, 1H, Ar-*H*), 7.91 (bs, 2H, N*H*). {^{1}H}^{13}C NMR (125.8 MHz, $CDCl_3$): δ 31.7, 35.0, 44.7, 107.3, 108.5, 117.2, 121.1, 122.9, 133.1, 141.0, 151.1.

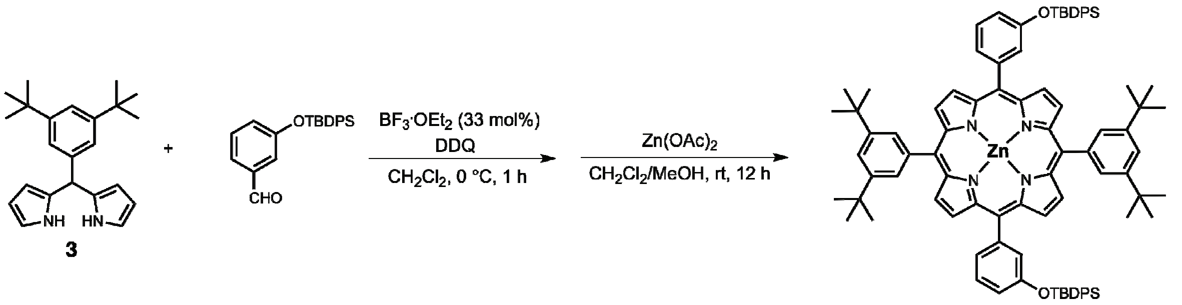

[5,15-bis-(3-*tert*-butyldiphenylsiloxyphenyl)-10,20-bis-(3,5-di-*tert*-butylphenyl)porphyrinato]zinc(II). Compound **3** (3.0 g, 9.0 mmol) and 3-*tert*-butyldiphenylsiloxybenzaldehyde (3.2 g, 9.0 mmol) were combined with CH_2Cl_2 (900 mL) in a 2 L round-bottom flask equipped with a magnetic stir bar. The resulting mixture was degassed with N_2 for ten minutes and cooled to 0 ºC before $BF_3{\cdot}Et_2O$ (0.4 mL, 3.0 mmol) was added. After stirring under N_2 for 1 h at 0 ºC, DDQ (4.1 g, 18.0 mmol) was added as a solid and the resulting mixture was warmed to room temperature and stirred for an additional 2 h. A solution of $Zn(OAc)_2$ (2.5 g, 13.5 mmol) in MeOH (30 mL) was then added, and the combined mixture was allowed to stir for 12 h more before being evaporated to dryness using a rotary evaporator. The remaining crude product was purified by silica gel column chromatography (column dimensions = 60 mm × 250 mm, eluent = hexanes/CH_2Cl_2 5:2 v/v) to give the desired porphyrin as a purple solid (1.3 g, 0.9 mmol, 20% yield). ^{1}H NMR (499.4 MHz, $CDCl_3$): δ 1.20 (m, 18H, Si-C(CH_3)$_3$, 1.54 (m, 36H, C(CH_3)$_3$, 7.23 (m, 2H, Ar-*H*), 7.43 (m, 14H, Ar-*H*), 7.73 (m, 4H, Ar-*H*), 7.88, (m, 10H, Ar-*H*), 8.11 (m, 4H, Ar-*H*), 8.72 (s, 2H, β-*H*), 8.75 (t, $J = 4.5$ Hz, 2H, β-*H*), 8.93 (t, $J = 4.5$ Hz, 2H, β-*H*), 9.02 (s, 2H, β-*H*). {^{1}H}^{13}C NMR (125.8 MHz, $CDCl_3$): δ 19.8, 26.8, 32.0, 35.3, 119.3, 120.5, 120.9, 126.6, 127.2, 128.1, 128.4, 129.9, 130.2, 131.9, 132.4, 133.1, 135.9, 142.0, 144.2, 148.7, 150.1, 150.5, 154.1. MALDI-ToF (reflective positive mode): Calcd for $C_{92}H_{96}N_4O_2Si_2Zn$: 1408.64, found: *m/z* 1408.18 [M]$^+$. UV-vis (nm, ($\varepsilon \times 10^4$ /M^{-1}cm^{-1})): 422 (39), 550 (1.5), 590 (0.3). See Fig. S1 for NMR spectra.

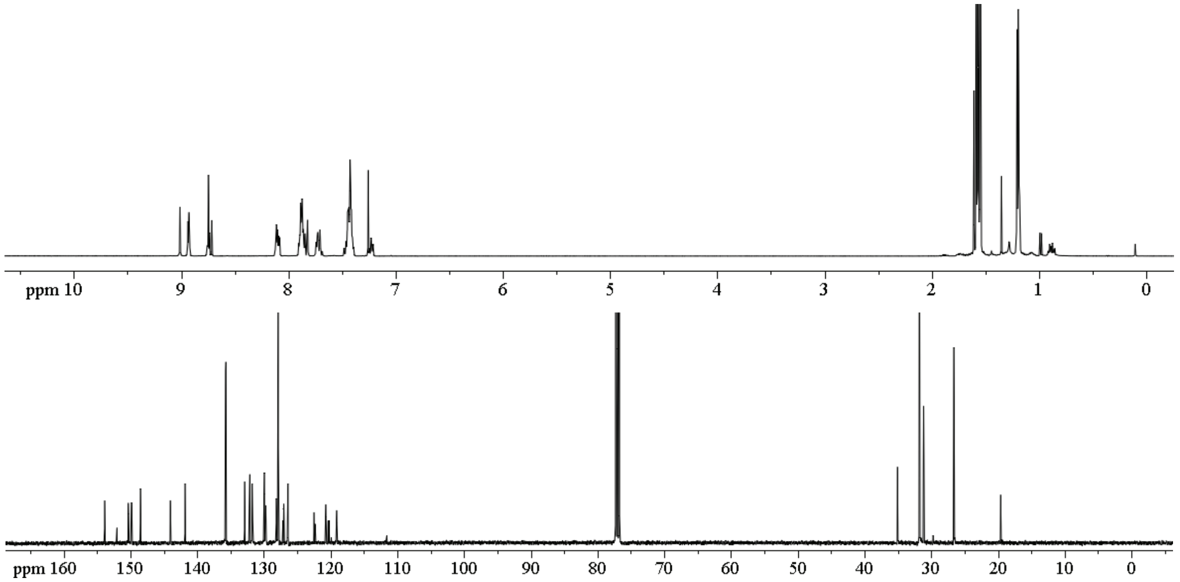

Fig. S1 The ^{1}H (top) and ^{13}C NMR (bottom) spectra for [5,15-bis-(3-*tert*-butyldiphenylsiloxyphenyl)-10,20-bis-(3,5-di-*tert*-butylphenyl)porphyrinato]zinc(II).

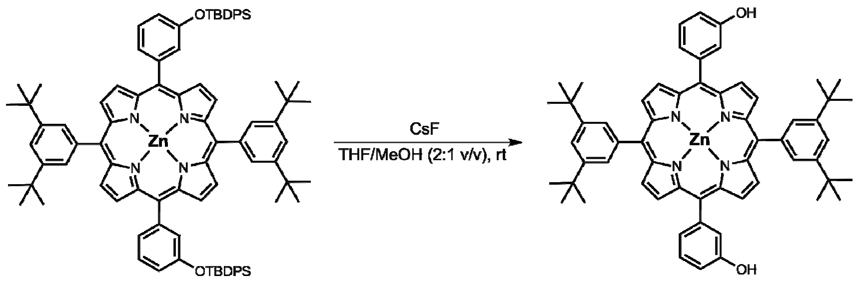

Zn1

[5,15-bis-(3-hydroxy-phenyl)-10,20-bis-(3,5-di-*tert*-butylphenyl)porphyrinato]zinc(II) (Zn1). To a THF/MeOH (300 mL, 2:1 v/v) solution of [5,15-bis-(3-*tert*-butyldiphenylsiloxyphenyl)-10,20-bis-(3,5-di-*tert*-butylphenyl)porphyrinato]zinc(II) (1.3 g, 0.9 mmol) in a 500 mL round-bottom flask equipped with a magnetic stir bar was added a MeOH solution of CsF (0.3 g, 2.0 mmol, 10 mL). The reaction mixture was stirred for 3 h at room temperature before it was evaporated to dryness. The residue was redissolved in CH_2Cl_2 (200 mL) and the resulting solution was washed with water (150 mL), dried over Na_2SO_4, and concentrated to dryness under reduced pressure. The crude product was purified by silica gel column chromatography (column dimensions = 50 mm × 250 mm, 1st fraction: eluent = hexanes/CH_2Cl_2 1:1 v/v, 2nd fraction: eluent = CH_2Cl_2/MeOH 9:1 v/v) to yield **Zn1** as a purple solid (0.8 g, 0.9 mmol, 98% yield). ^{1}H NMR (499.4 MHz, $CDCl_3$): δ 1.55 (s, 36H, C(C*H*$_3$)$_3$), 4.88 (bs, 1H, O*H*), 7.07 (bs, 2H, Ar-*H*), 7.52 (bs, 4H, Ar-*H*), 7.78 (m, 4H, Ar-*H*), 8.12 (bs, 4H, Ar-*H*), 9.01 (t, *J* = 16 Hz, 8H, β-*H*). {^{1}H}^{13}C NMR (125.4 MHz, $CDCl_3$): δ 31.9, 35.2, 114.4, 120.1, 120.9, 121.8, 122.7, 127.7, 129.9, 131.9, 132.5, 141.9, 144.5, 148.7, 150.1, 150.6, 153.6. MALDI-ToF (reflective positive mode): Calcd for $C_{60}H_{60}N_4O_2Zn$: 934.4, found: *m/z* 934.02 $[M]^+$. UV-vis (nm, (ε ×10^4 /$M^{-1}cm^{-1}$)): 423 (30.1), 548 (1.2), 590 (0.3). See Fig. S2 for NMR spectra.

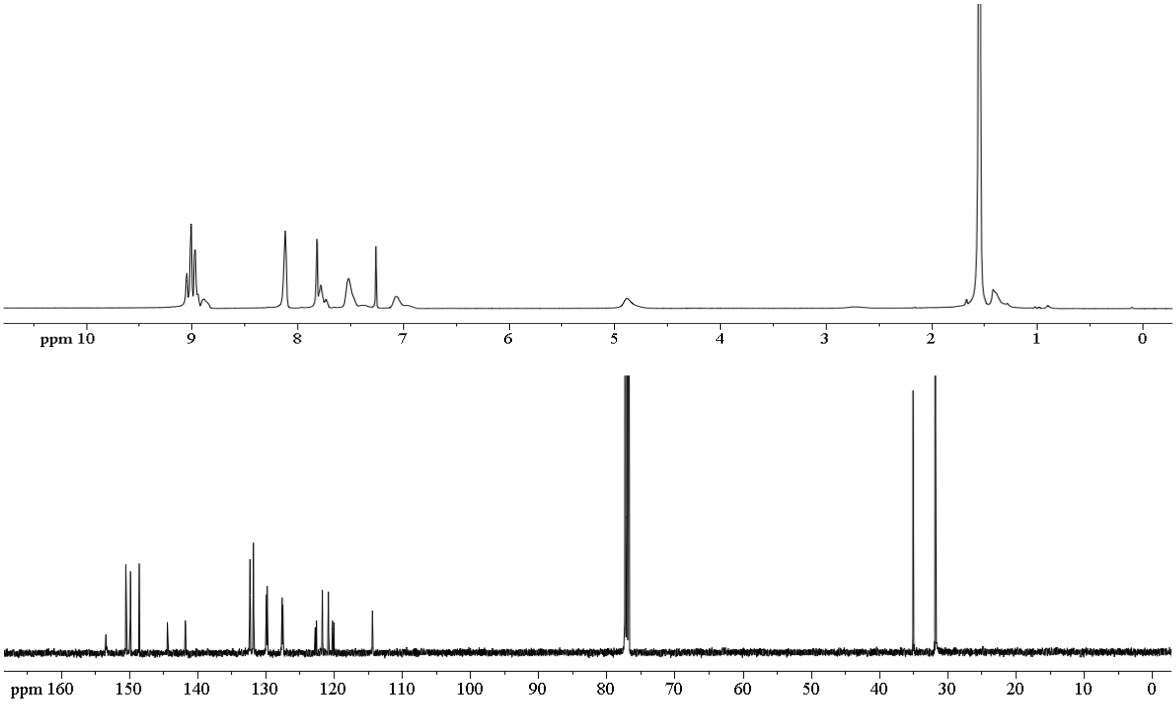

Fig. S2 The ^{1}H (top) and ^{13}C NMR (bottom) spectra for [5,15-bis-(3-hydroxy-phenyl)-10,20-bis-(3,5-di-*tert*-butylphenyl)porphyrinato]zinc(II) (**Zn1**).

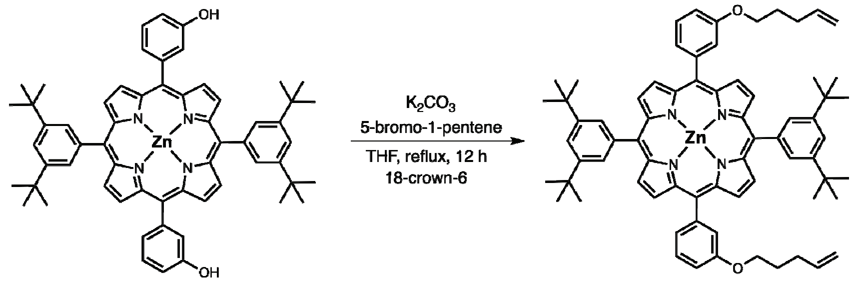

Zn1 **unsat-Zn1**

[5,15-bis-(3-(1-pentenyloxy)phenyl)-10,20-bis-(3,5-di-*tert*-butyl-phenyl)porphinato]zinc(II) (unsat-Zn1). Into a 50 mL round-bottom flask equipped with a magnetic stir bar and a water-cooled reflux condenser were combined anhydrous THF (10 mL), **Zn1** (440 mg, 0.5 mmol), 5-bromo-1-pentene (164 mg, 1.1 mmol), K_2CO_3 (390 mg, 2.8 mmol), and 18-crown-6 (50 mg, 0.2 mmol) and the resulting reaction mixture was refluxed overnight under N_2. After cooling, the reaction mixture was quenched with water (100 mL) and extracted into CH_2Cl_2 (3 × 50 mL). The organic layer was dried over Na_2SO_4, filtered, and concentrated to dryness under reduced pressure. Purification by silica gel column chromatography (column dimensions = 20 mm × 200 mm, eluent = hexanes/CH_2Cl_2 1:1 v/v) yielded **unsat-Zn1** as a purple solid (494 mg, 0.5 mmol, 98% yield). ^{1}H NMR (499.4 MHz, $CDCl_3$): δ 1.61 (s, 36H, C(CH_3)$_3$), 2.02 (m, 4H, CH_2CH$_2$O), 2.32 (m, 4H, CH$_2$=CHCH_2), 4.16 (t, J = 6.5 Hz, 4H, CH$_2$CH_2O), 5.04 (dd, J_1 = 41.5 Hz, J_2 = 10.5 Hz, 2H, CH_2=CHCH$_2$), 5.12 (dd, J_1 = 41.5 Hz, J_2 = 17 Hz, 2H, CH_2=CHCH$_2$), 5.91 (m, 2H, CH$_2$=CHCH$_2$), 7.33 (d, J = 8 Hz, 2H, Ar-H), 7.67 (t, J = 7.5 Hz, 2H, Ar-H), 7.84 (s, 2H, Ar-H), 7.88 (s, 4H, Ar-H), 8.18 (s, 4H, Ar-H), 9.08 (s, 8H, β-H). {^{1}H}^{13}C NMR (125.8 MHz, $CDCl_3$): δ 28.7, 30.3, 31.9, 35.2, 67.6, 114.2, 115.4, 120.9, 127.6, 129.9, 132.4, 138.0, 141.9, 144.4, 148.7, 150.2, 150.7, 157.4. MALDI-ToF (reflective positive mode): Calcd for $C_{70}H_{76}N_4O_2Zn$: 1068.53, found: *m/z* 1068.08 [M]$^+$. UV-vis (nm, (ε ×10^4 /M^{-1}cm^{-1})): 425 (54.4), 552 (1.0), 590 (0.5). See Fig. S3 for NMR spectra.

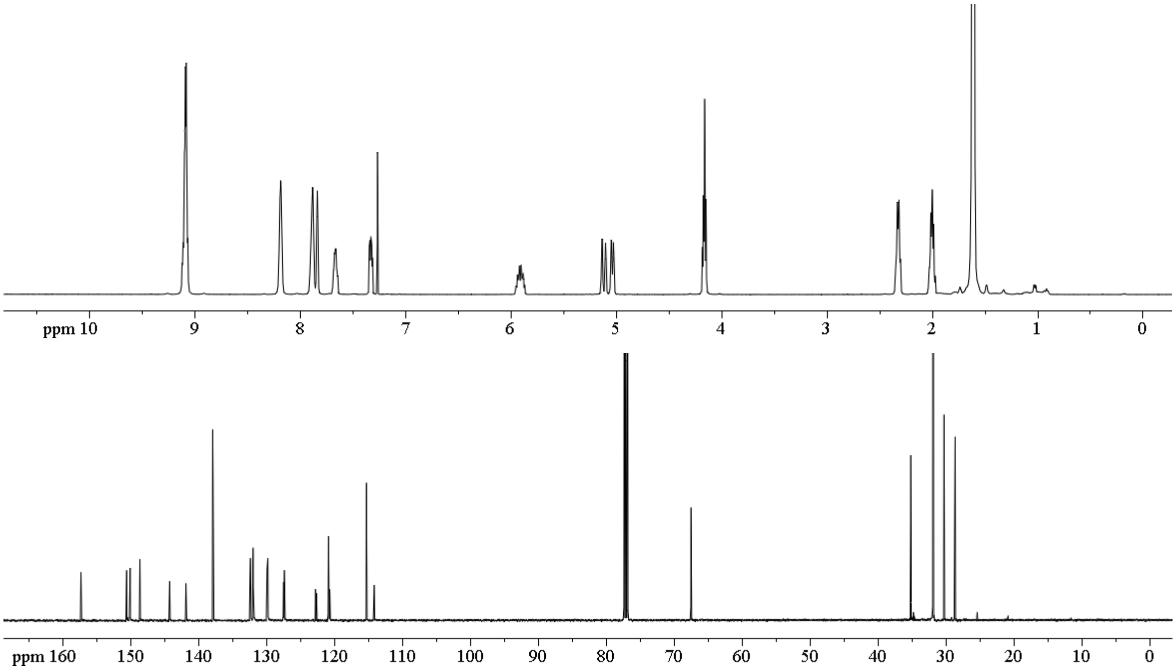

Fig. S3 The ^{1}H (top) and ^{13}C NMR (bottom) spectra for [5,15-bis-(3-(1-pentenyloxy)phenyl)-10,20-bis-(3,5-di-*tert*-butyl-phenyl)porphyrinato]zinc(II) (**unsat-Zn1**).

General demetallation strategy using trifluoroacetic acid (TFA). To a 50 mL flask containing a stirring solution of zinc porphyrin in CH_2Cl_2 (10 mL, ~ 10-50 μmol porphyrin)) was added trifluoroacetic acid (10 equiv). Upon addition of TFA, a color change from red to green was observed. After stirring for 30 min, the reaction mixture was quenched with triethylamine (20 equiv) and the solvent was removed by rotary evaporation. The remaining crude product was purified by silica gel column chromatography (column dimensions = 20 mm × 200 mm, eluent = hexanes/CH_2Cl_2 1:1 v/v) to give the free-base porphyrin as a purple solid.

General metallation strategy using $AlMe_3$. Under a nitrogen atmosphere, a 50 mL Schlenk flask equipped with a magnetic stir bar was loaded with a solution of free-base porphyrin in anhydrous CH_2Cl_2 (10 mL, ~ 10-50 μmol porphyrin). An appropriate amount of a solution of $AlMe_3$ (2 M in heptane) (except when noted, 3 equiv were used in reactions involving porphyrin monomer and 6 equiv were used in reactions involving porphyrin dimer) was then added using a gas-tight syringe. After stirring for 30 min under N_2, MeOH (10 mL) was added to quench the reaction and the mixture was evaporated to dryness under reduced pressure. The residue was subjected to size-exclusion chromatography (Bio-Rad Bio-Beads S-X1, column dimensions = 50 mm × 250 mm, eluent = CH_2Cl_2/MeOH 15:1 v/v) to afford the Al porphyrin as a purple solid.

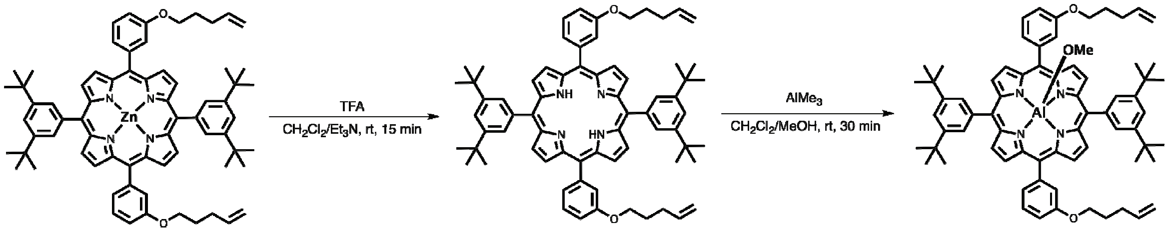

unsat-Zn1 **unsat-H$_2$1** **unsat-Al1**

[5,15-bis-(3-(1-pentenyloxy)phenyl)-10,20-bis-(3,5-di-*tert*-butyl-phenyl)porphyrinato]aluminum(III) methoxide. **Unsat-Zn1** (50 mg, 46.8 μmol) was demetallated according to the general demetallation strategy using TFA. Free-base monomer, **unsat-H$_2$1**, was isolated as a purple solid (46 mg, 45.4 μmol, 97% yield). ^{1}H NMR (499.4 MHz, $CDCl_3$): δ -2.66 (s, 2H, N*H*), 1.59 (s, 36H, C(CH_3)$_3$), 2.02 (q, *J* = 6.5 Hz, 4H, CH_2CH$_2$O), 2.34 (q, *J* = 7 Hz, 4H, CH$_2$=CHCH_2), 4.20 (t, *J* = 6.5 Hz, 4H, CH$_2$CH_2O), 5.04 (dd, J_1 = 42 Hz, J_2 = 10 Hz, 2H, CH_2=CHCH$_2$), 5.12 (dd, J_1 = 42 Hz, J_2 = 17 Hz, 2H, CH_2=CHCH$_2$), 5.92 (m, 2H, CH$_2$=C*H*CH$_2$), 7.35 (dd, J_1 = 7.5 Hz, J_2 = 2.5 Hz, 1H, Ar-*H*), 7.36 (dd, J_1 = 7.5 Hz, J_2 = 2.5 Hz, 1H, Ar-*H*), 7.67 (t, *J* = 8Hz, 2H, Ar-*H*), 7.87 (m, 6H, Ar-*H*), 8.15 (s, 4H, Ar-*H*), 8.96 (s, 8H, β-*H*). {^{1}H}^{13}C NMR (125.8 MHz, $CDCl_3$): δ 28.7, 30.4, 31.9, 35.2, 67.6, 114.3, 115.4, 119.7, 121.2, 121.8, 127.7, 130.0, 138.0, 141.4, 143.8, 148.9, 157.5. MALDI-ToF (reflective positive mode): Calcd for $C_{70}H_{78}N_4O_2$: 1006.61, found: *m/z* 1007.33 [M]$^+$. UV-vis (nm, (ε ×10^4 /$M^{-1}cm^{-1}$)): 425 (45.4), 552 (1.2), 590 (0.3). See Fig. S4 for NMR spectra.

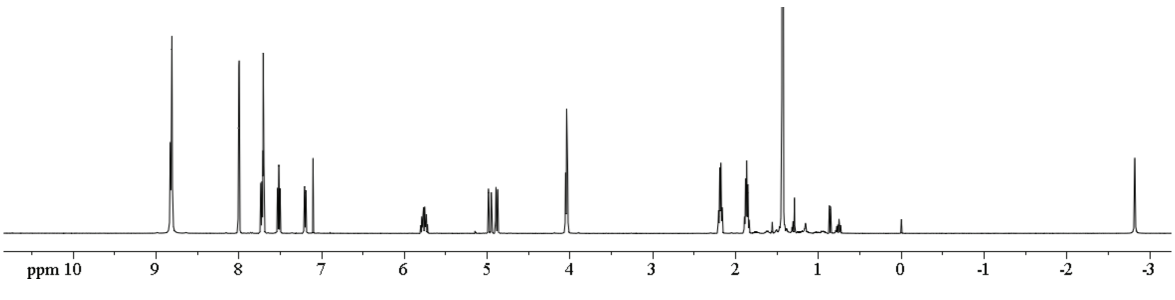

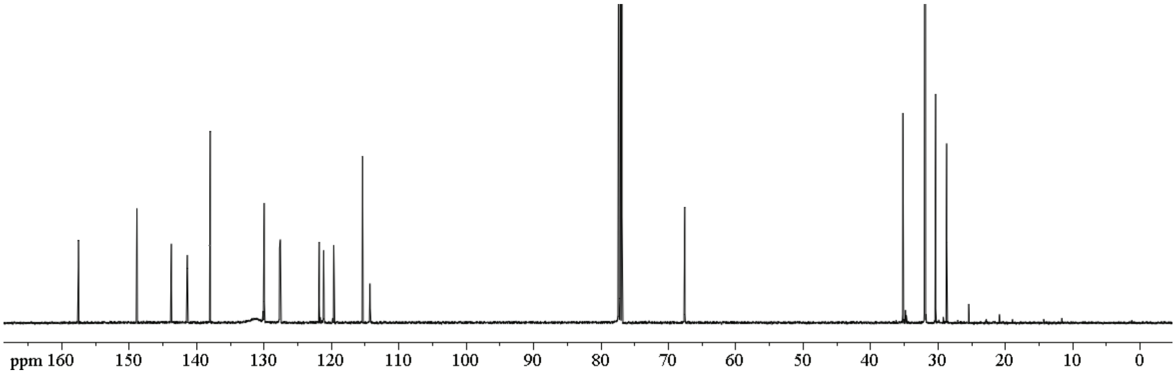

Fig. S4 The ^{1}H (top) and ^{13}C NMR (bottom) spectra for [5,15-bis-(3-(1-pentenyloxy)phenyl)-10,20-bis-(3,5-di-*tert*-butyl-phenyl)]porphine (**unsat-H$_2$1**).

Unsat-H$_2$1 (46 mg, 45.4 µmol) was metallated according to the general metallation strategy using AlMe$_3$. Pure **unsat-Al1** was isolated as a purple solid (47 mg, 44.5 µmol, 98% yield). ^{1}H NMR (499.4 MHz, CDCl$_3$): δ 1.59 (s, 36H, C(CH_3)$_3$), 2.04 (bs, 4H, CH_2CH$_2$O), 2.36 (bs, 4H, CH$_2$=CHCH_2), 4.20 (bs, 4H, CH$_2$CH_2O), 5.05 (dd, J_1 = 42 Hz, J_2 = 10 Hz, 2H, CH_2=CHCH$_2$), 5.14 (dd, J_1 = 42 Hz, J_2 = 17 Hz, 2H, CH_2=CHCH$_2$), 5.92 (m, 2H, CH$_2$=C*H*CH$_2$), 7.35 (dd, J_1 = 7.5 Hz, J_2 = 2.5 Hz, 1H, Ar-*H*), 7.36 (dd, J_1 = 7.5 Hz, J_2 = 2.5 Hz, 1H, Ar-*H*), 7.69 (bs, 2H, Ar-*H*), 7.88 (s, 6H, Ar-*H*), 8.06 (bs, 2H, Ar-*H*), 8.25 (bs, 2H, Ar-*H*), 9.18 (d, J = 12.5 Hz, 8H, β-*H*). {^{1}H}^{13}C NMR (125.8 MHz, CDCl$_3$): δ 28.9, 30.5, 32.1, 35.4, 67.8, 115.6, 120.9, 121.5, 122.5, 127.9, 132.2, 132.8, 138.1, 140.9, 143.3, 149.2, 157.8. MALDI-ToF (reflective positive mode, pyrene matrix): Calcd for C$_{71}$H$_{79}$N$_4$O$_3$Al: 1062.61, found: *m/z* 1063.43 [M]$^+$, 1048.44 [M-CH$_3$]$^+$, 1031.45 [M-OMe]$^+$. ESIMS: Calcd for C$_{71}$H$_{79}$N$_4$O$_3$Al: 1062.61, found: *m/z* 1063.3 [M+H]$^+$. UV-vis (nm, (ε ×10^4 /M^{-1}cm^{-1})): 417 (41.5), 547 (1.5), 584 (0.2). See Fig. S5 for NMR spectra.

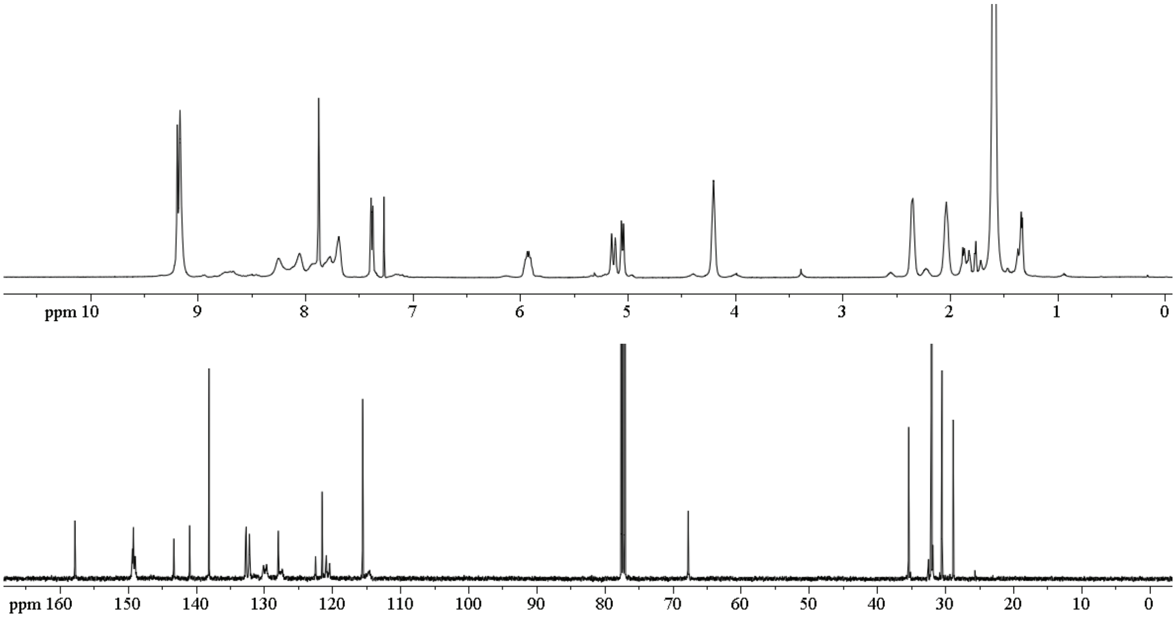

Fig. S5 The ^{1}H (top) and ^{13}C NMR (bottom) spectra for [5,15-bis-(3-(1-pentenyloxy)phenyl)-10,20-bis-(3,5-di-*tert*-butyl-phenyl)porphinato]aluminum(III) methoxide (**unsat-Al1**).

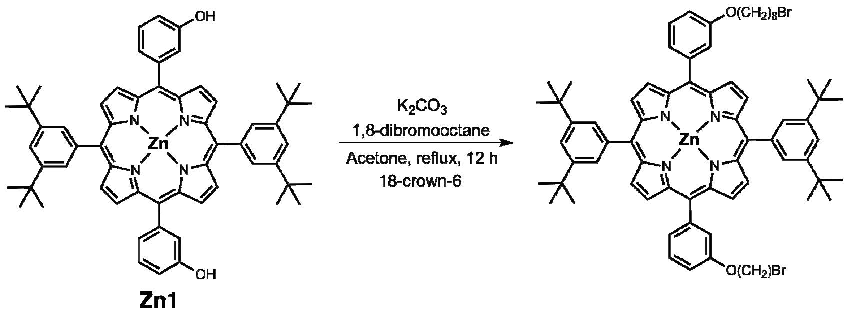

Zn1

[5,15-bis-(3-(1-bromooctanyloxy)phenyl)-10,20-bis-(3,5-di-*tert*-butyl-phenyl)porphinato]zinc(II). Into a 50 mL round-bottom flask equipped with a magnetic stir bar and a water-cooled reflux condenser were combined **Zn1** (50 mg, 53.5 μmol), K_2CO_3 (48 mg, 347.3 μmmol), 18-crown-6 (6 mg, 22.7 μmol), acetone (11 mL), and 1,8 dibromooctane (5.0 g, 18.5 mmol) and the resulting reaction mixture was refluxed overnight under N_2. The reaction mixture was then cooled to room temperature, filtered, and washed with acetone (25 mL). The combined organics were evaporated to dryness under reduced pressure and the remaining residue was purified by silica gel column chromatography (column dimensions = 20 mm × 200 mm, 1st fraction: eluent = hexanes, 2nd fraction: eluent = hexanes/CH_2Cl_2 1:1 v/v) to yield the product as a purple solid (70 mg, 53.0 μmol, 99% yield). ^{1}H NMR (499.4 MHz, $CDCl_3$): δ 1.40 (m, 16H, CH_2), 1.54 (s, 36H, C(CH_3)$_3$, 1.86 (m, 8H, CH_2), 3.37 (t, J = 7 Hz, 4H, CH_2Br), 4.13 (t, J = 7 Hz, 4H, OCH_2), 7.33 (d, J = 8.5 Hz, 2H, Ar-H), 7.63 (t, J = 8 Hz, 2H, Ar-H), 7.81 (t, J = 10 Hz, 6H, Ar-H), 8.11 (s, 4H, Ar-H), 9.02 (s, 8H, β-H). {^{1}H}^{13}C NMR (125.8 MHz, $CDCl_3$): δ 14.4, 22.9, 26.2, 28.3, 28.9, 29.4, 29.6, 30.0, 31.9, 33.0, 34.2, 35.3, 37.3, 68.3, 114.3, 120.9, 122.9, 127.5, 129.9, 132.1, 132.5, 141.9, 144.3, 148.7, 150.3, 150.7, 157.5. MALDI-ToF (reflective positive mode): Calcd for $C_{76}H_{90}N_4O_2Br_2Zn$ 1316.74, found: *m/z* 1316.89 $[M]^+$. UV-vis (nm, (ε ×10^4 /$M^{-1}cm^{-1}$)): 423 (59.6), 551 (0.9), 590 (0.3). See Fig. S6 for NMR spectra.

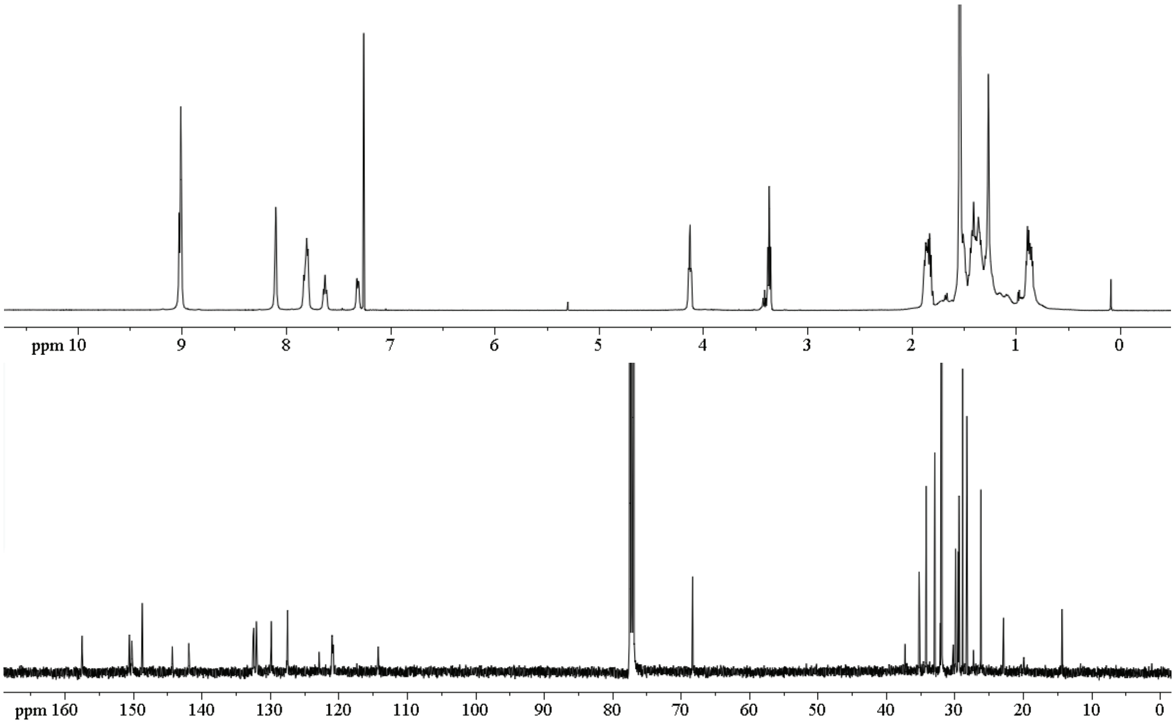

Fig. S6 The ^{1}H (top) and ^{13}C NMR (bottom) spectra for [5,15-bis-(3-(1-bromooctanyloxy)phenyl)-10,20-bis-(3,5-di-*tert*-butyl-phenyl)porphinato]zinc(II).

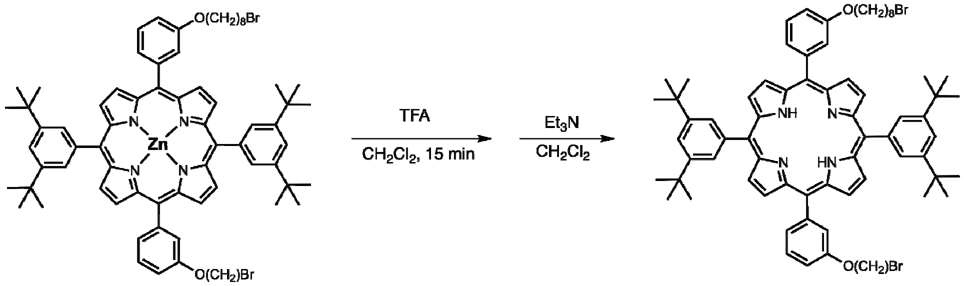

[5,15-bis-(3-(1-bromooctanyloxy)phenyl)-10,20-bis-(3,5-di-*tert*-butyl-phenyl)]porphine. [5,15-bis-(3-(1-bromooctanyloxy)phenyl)-10,20-bis-(3,5-di-*tert*-butyl-phenyl)porphinato]zinc(II) (70 mg, 53.0 μmol) was demetallated according to the general demetallation strategy using TFA. Free-base porphyrin was isolated as a purple solid (64 mg, 51.4 μmol, 97% yield). ^{1}H NMR (499.4 MHz, $CDCl_3$): δ -2.84 (s, 2H, N*H*), 1.41 (m, 16H, CH_2), 1.57 (s, 36H, C(CH_3)$_3$, 1.87 (m, 8H, CH_2), 3.39 (t, J = 7 Hz, 4H, CH_2Br), 4.16 (t, J = 7 Hz, 4H, OCH_2), 7.33 (d, J = 8.5 Hz, 2H, Ar-*H*), 7.65 (t, J = 8 Hz, 2H, Ar-*H*), 7.84 (t, J = 10 Hz, 6H, Ar-*H*), 8.14 (s, 4H, Ar-*H*), 8.94 (s, 8H, β-*H*). {^{1}H}^{13}C NMR (125.4 MHz, $CDCl_3$): δ 26.3, 28.3, 28.9, 29.5, 29.6, 32.0, 33.0, 34.2, 35.3, 68.4, 114.4, 119.7, 121.1, 121.8, 127.6, 130.0, 141.4, 143.8, 148.9, 157.6. MALDI-ToF (reflective positive mode): Calcd for $C_{76}H_{92}Br_2N_4O_2$: 1253.38, found: *m/z* 1253.32 $[M]^+$. UV-vis (nm, (ε ×10^4 /$M^{-1}cm^{-1}$)): 424 (54.4), 552 (1.0), 590 (0.3). See Fig. S7 for NMR spectra.

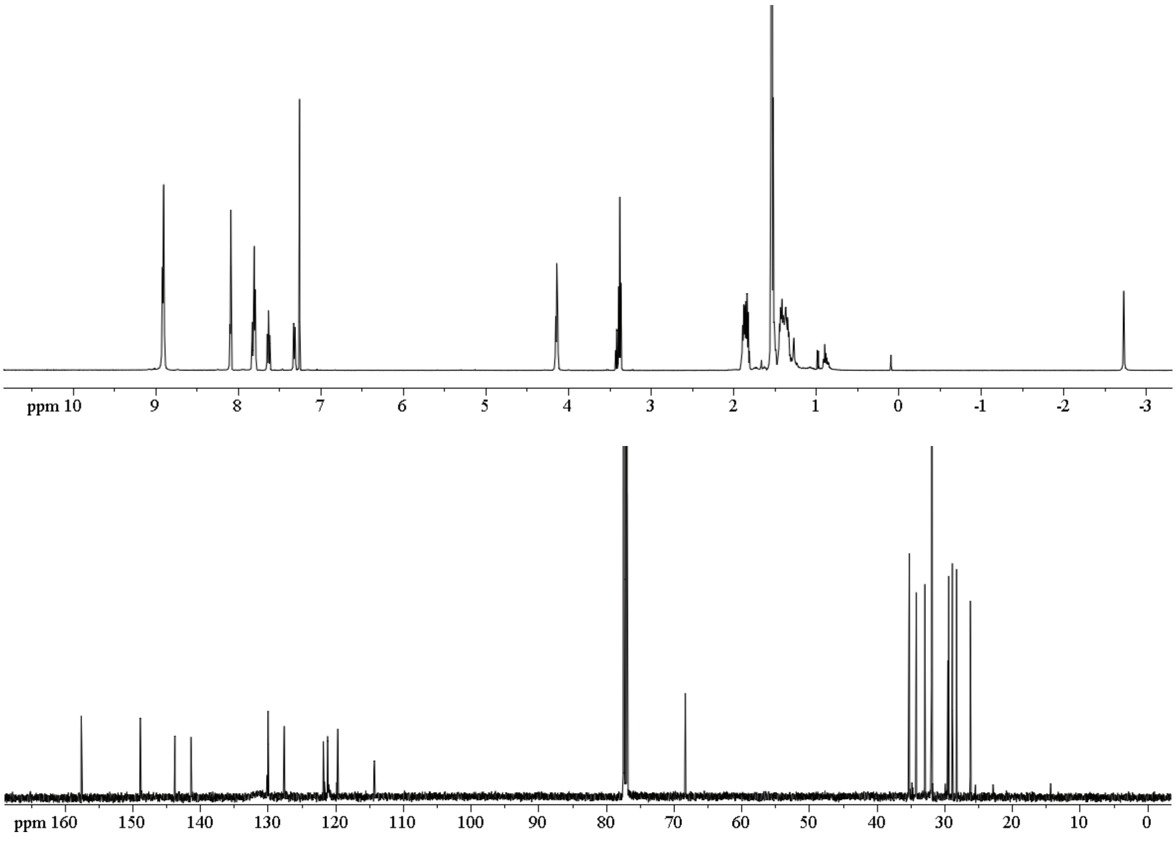

Fig. S7 The ^{1}H (top) and ^{13}C NMR (bottom) spectra for [5,15-bis-(3-(1-bromooctanyloxy)phenyl)-10,20-bis-(3,5-di-*tert*-butyl-phenyl)]porphine.

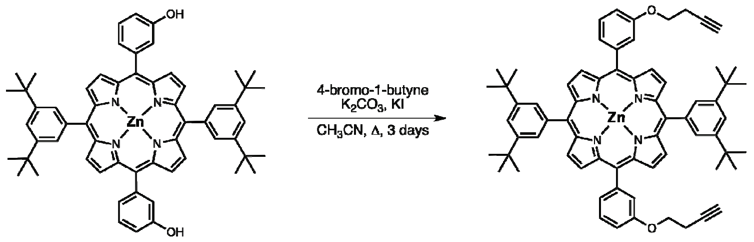

Zn1 **diyne-Zn1**

[5,15-bis-(3-(1-butynyloxy)phenyl)-10,20-bis-(3,5-di-*tert*-butyl-phenyl)porphyrinato]zinc(II). Into a 50 mL round-bottom flask equipped with a magnetic stir bar and a water-cooled reflux condenser were combined **Zn1** (200 mg, 0.2 mmol), 4-bromo-1-butyne (285 mg, 2.1 mmol), K_2CO_3 (296 mg, 2.1 mmol), KI (355 mg, 2.1 mmol), and anhydrous CH_3CN (15 mL) and the resulting reaction mixture was refluxed for 3 days under N_2. After cooling to room temperature, the reaction mixture was filtered and evaporated to dryness by rotary evaporation. The crude residue was redissolved in CH_2Cl_2 (50 mL) and washed with water (3 × 50 mL). The organic layer was dried over Na_2SO_4, filtered, and concentrated to dryness under reduced pressure. TLC analysis (hexanes/CH_2Cl_2 = 3:2 v/v) revealed a mixture of two new porphyrin compounds, which were separated by silica gel column chromatography (column dimensions = 50 mm × 250 mm, eluent = hexanes/CH_2Cl_2 3:2 v/v). A first purple band (131 mg, 0.1 mmol, 59% yield) was cleanly separated from a second purple band (87 mg, 0.1 mmol, 39% yield). Both species have identical UV-vis spectra as well as NMR spectra and MALDI-ToF mass spectra (cf. Figs. S8a and S8b) leading us to suspect at first that they are αα and αβ atropisomers. However, this is inconsistent with the lack of observable atropisomerism in structurally similar compounds (**unsat-Zn1**, **unsat-$H_2$1**, and **unsat-Al1**) that we synthesized in this work. Attempts to interconvert these two compounds by heating in boiling toluene for several hours were not successful, further casting doubt that they are atropisomers.

Based on reactivity in the Glaser-Hay coupling (see p. S21), we assign the first compound isolated from chromatography to be the desired **diyne-Zn1** monomer. ^{1}H NMR (499.4 MHz, $CDCl_3$): δ 1.58 (s, 36H, $C(CH_3)_3$), 2.04 (s, 2H, CC*H*), 2.79 (t, *J* = 7 Hz, 4H, CH_2CH_2CCH), 4.29, (td, J_1 = 2 Hz, J_2 = 7 Hz, 4H, OCH_2), 7.35 (dd, J_1 = 2.5 Hz, J_2 = 8.5 Hz, 2H, Ar-*H*), 7.67 (t, *J* = 8.5 Hz, 2H, Ar-*H*), 7.84 (m, 4H, Ar-*H*), 7.9 (d, *J* = 7 Hz, 2H, Ar-*H*), 8.14 (sextet, *J* = 2 Hz, 4H, Ar-*H*), 9.10 (m, 8H, β-*H*). {^{1}H}^{13}C NMR (125.8 MHz, $CDCl_3$): δ 19.9, 32.0, 35.3, 66.4, 70.2, 80.7, 114.5, 120.6, 121.0, 123.0, 127.6, 128.1, 129.9, 131.9, 132.7, 142.0, 144.5, 148.8, 150.3, 150.7, 156.9. MALDI-ToF (reflective positive mode): Calcd for $C_{68}H_{68}N_4O_2Zn$: 1036.46, found: *m/z* 1035.94 $[M]^+$. UV-vis (nm, (ε ×10^4 /$M^{-1}cm^{-1}$)): 425 (48.6), 550 (0.7), 590 (0.2). See Fig. S8a for NMR spectra and MALDI-ToF mass spectra.

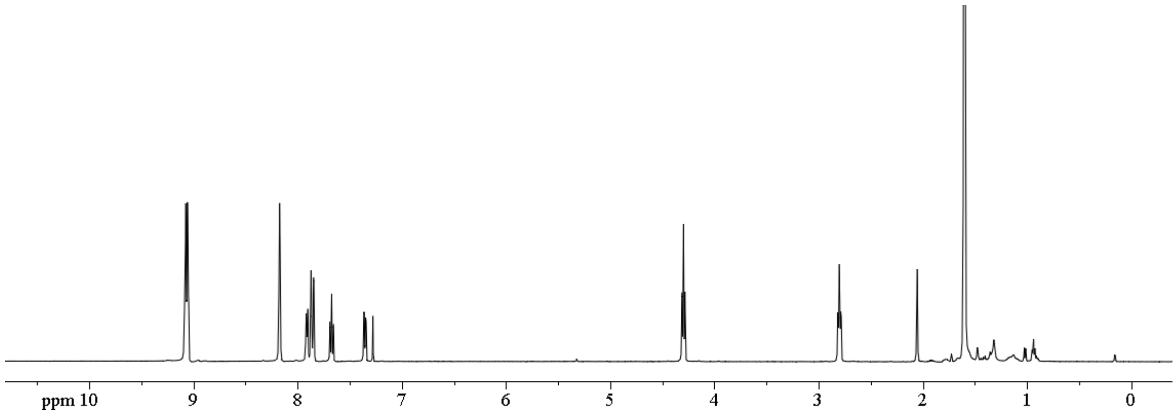

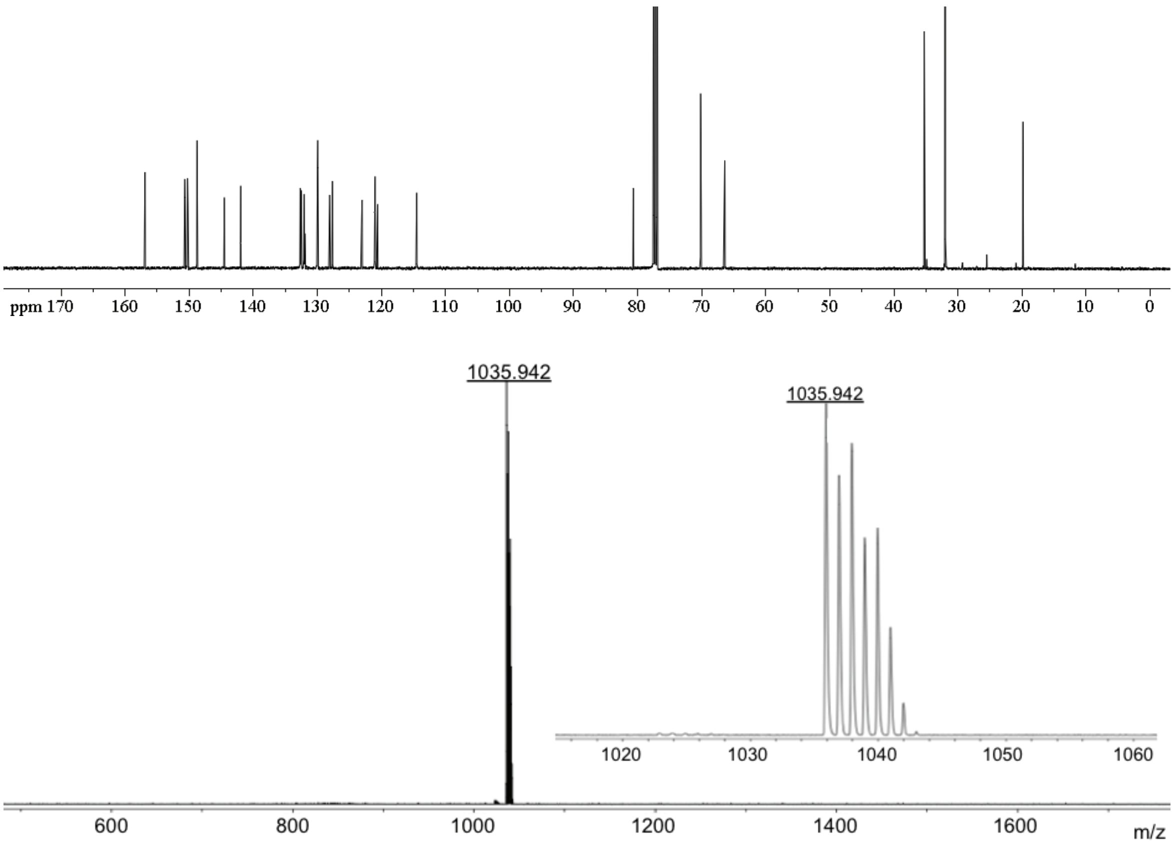

Fig. S8a The ^{1}H NMR (top), ^{13}C NMR (middle), and MALDI-ToF mass (bottom) spectra for [5,15-bis-(3-(1-butynyloxy)phenyl)-10,20-bis-(3,5-di-*tert*-butyl-phenyl)porphyrinato]zinc(II) (**diyne-Zn1**).

Spectral data for the second compound isolated from column chromatography. ^{1}H NMR (499.4 MHz, CDCl$_3$): δ 1.58 (s, 36H, C(C*H*$_3$)$_3$), 2.04 (s, 2H, CC*H*), 2.79 (t, *J* = 7 Hz, 4H, CH$_2$C*H*$_2$CCH), 4.29, (td, J_1 = 2 Hz, J_2 = 7 Hz, 4H, OC*H*$_2$), 7.34 (dd, J_1 = 2.5 Hz, J_2 = 8.5 Hz, 2H, Ar-*H*), 7.67 (t, *J* = 8.5 Hz, 2H, Ar-*H*), 7.84 (m, 4H, Ar-*H*), 7.89 (d, *J* = 7 Hz, 2H, Ar-*H*), 8.15 (sextet, *J* = 2 Hz, 4H, Ar-*H*), 9.10 (m, 8H, β-*H*). {^{1}H}^{13}C NMR (125.8 MHz, CDCl$_3$): δ 19.8, 32.0, 35.3, 66.4, 70.2, 80.6, 114.5, 120.6, 121.0, 122.9, 127.6, 128.1, 130.1, 132.1, 132.7, 142.0, 144.5, 148.8, 150.2, 150.8, 156.8. MALDI-ToF (reflective positive mode): Calcd for $C_{68}H_{68}N_4O_2Zn$: 1036.46, found: *m/z* 1036.13 [M]$^+$. UV-vis (nm, (ε ×10^4 /M^{-1}cm^{-1})): 425 (47.4), 550 (0.6), 590 (0.2). See Fig. S8b for NMR spectra and MALDI-ToF mass spectra.

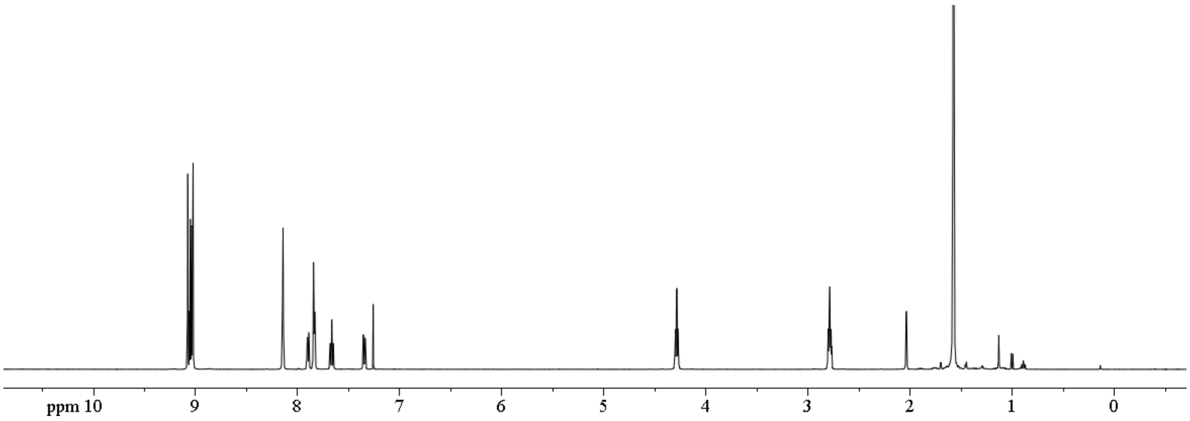

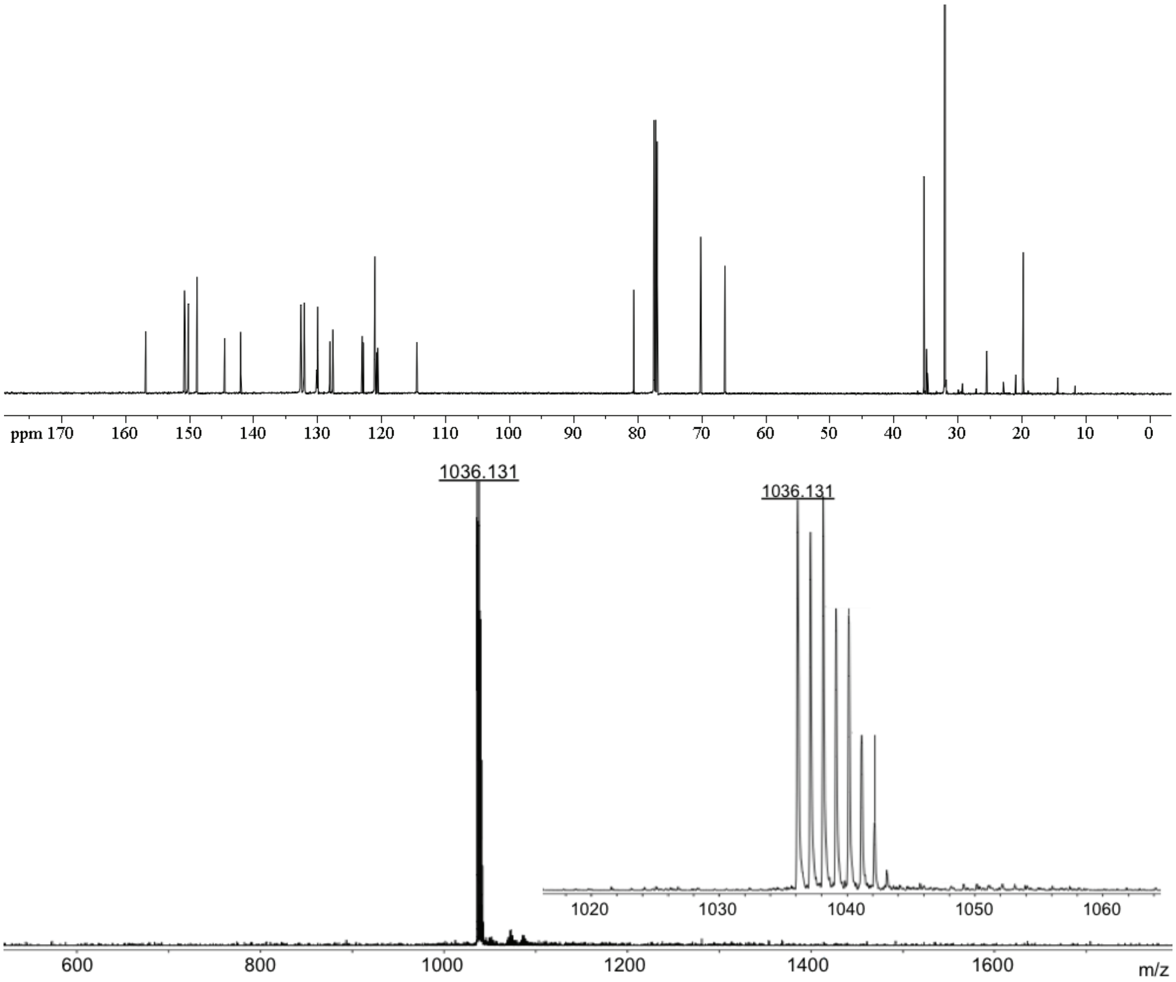

Fig. S8b The ^{1}H (top), ^{13}C NMR (middle), and MALDI-ToF (bottom) spectra for the second compound obtained in the synthesis of **diyne-Zn1**.

IV. Preparation of covalently linked porphyrin dimers possessing 3,5-^{t}Bu$_2$Ph substituents (series 1 catalysts)

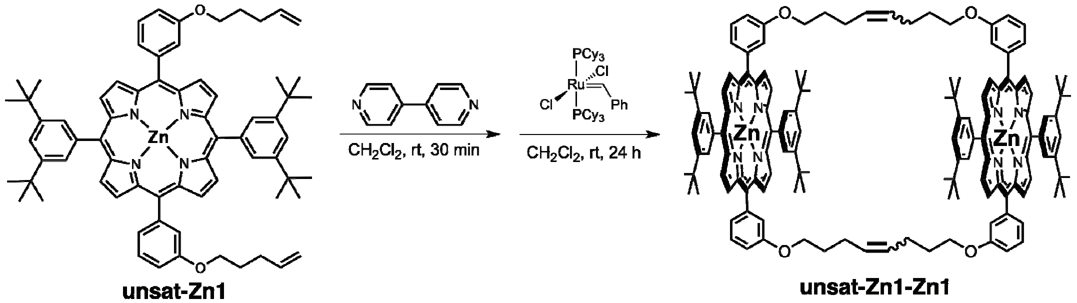

Unsat-Zn1-Zn1. Into a 250 mL Schlenk flask equipped with a magnetic stir bar were combined **unsat-Zn1** (100 mg, 93.6 μmol), CH_2Cl_2 (92 mL), and the 4,4'-dipyridine template (7 mg, 46.8 μmol). The resulting mixture was degassed with a stream of nitrogen for 10 minutes and then allowed to stir under N_2 for an additional 20 minutes. A N_2-degassed CH_2Cl_2 (5 mL) solution of Grubbs' first-generation catalyst (16 mg, 18.7 μmol) was then added via cannula and the resulting mixture was allowed to stir under N_2 for 12 h. A second catalyst aliquot was then added

(16 mg, 18.7 µmol, in 5 mL of N_2-degassed CH_2Cl_2) via cannula and stirring was continued for 12 h more. (Note: without the second catalyst addition, the primary product, as analyzed by MALDI-ToF MS, is a mixture of open and closed dimers.) The reaction was then quenched by adding ethyl vinyl ether (15 mL) and opening to air. Solvent was removed from the quenched reaction mixture under reduced pressure using a rotary evaporator and the resulting residue was subjected to size-exclusion chromatography (Bio-Rad Bio-Beads S-X1, column dimensions = 50 mm × 250 mm, eluent = CH_2Cl_2). The dimer was collected from the second band, which was further purified by silica gel column chromatography (column dimensions = 20 mm × 200 mm, eluent = hexanes/CH_2Cl_2 1:1 v/v) to yield the product as a purple solid (82 mg, 39.3 µmol, 84% yield). Due to the presence of conformational isomers, **unsat-Zn1-Zn1** displays a complicated ^{1}H NMR spectrum, which is simplified upon addition of 4,4'-bipyridyl template:[S4] ^{1}H NMR (499.4 MHz, $CDCl_3$): δ 1.46 (s, 36H, $C(CH_3)_3$), 1.49 (s, 36H, $C(CH_3)_3$), 1.91 (m, 8H, OCH_2CH_2), 2.16 (bs, 8H, $C{=}CHCH_2$), 2.28 (bs, 4H, α-pyridyl), 4.05 (t, J = 6 Hz, 8H, OCH_2), 4.84 (bs, 4H, β-pyridyl), 5.46 (s, vinyl-*H*), 5.49 (s, vinyl-*H*), 7.25 (m, 4H, Ar-*H*), 7.56 (m, 8H, Ar-*H*), 7.74 (s, 8H, Ar-*H*), 7.88 (s, 4H, Ar-*H*), 7.97 (s, 4H, Ar-*H*), 8.83 (s, 16H, β-*H*). $\{^1H\}^{13}C$ NMR (125.8 MHz, $CDCl_3$): δ 24.1, 28.8, 29.8, 31.8, 35.2, 67.5, 114.0, 120.3, 120.6, 120.9, 122.1, 127.3, 127.8, 129.5, 129.8, 130.4, 131.5, 132.0, 142.4, 144.9, 148.2, 148.5, 149.8, 150.3, 157.2. MALDI-ToF (reflective positive mode, pyrene matrix): Calcd for $C_{136}H_{140}N_8O_4Zn_2$: 2081.38, found: *m/z* 2081.95 $[M]^+$. UV-vis (nm, (ε ×10^4 /$M^{-1}cm^{-1}$)): 420 (36.8), 550 (1.5), 591 (0.3). See Fig. S9 for ^{1}H NMR spectrum.

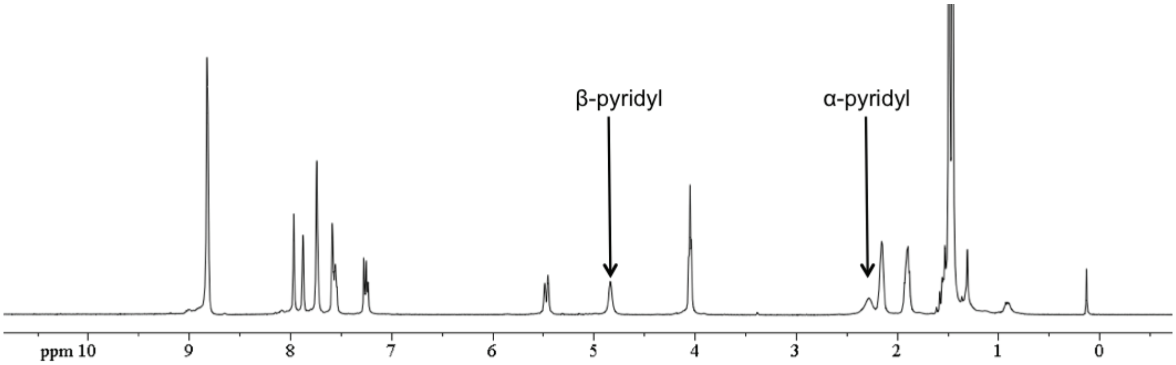

Fig. S9 The ^{1}H NMR spectrum for **unsat-Zn1-Zn1** incorporating 4,4'-bipyridyl template.

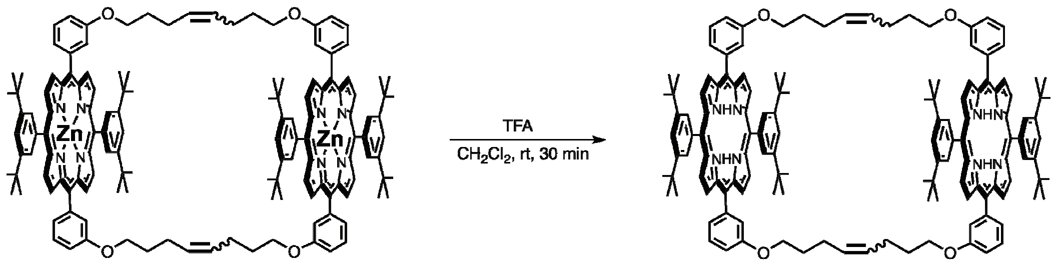

unsat-Zn1-Zn1 **unsat-H$_2$1-H$_2$1**

Unsat-H$_2$1-H$_2$1. **Unsat-Zn1-Zn1** (57 mg, 27.4 µmol) was demetallated following the general demetallation strategy using TFA. The free-base dimer, **unsat-H$_2$1-H$_2$1**, was isolated as a purple solid (53 mg, 27.1 µmol, 99% yield). As characteristic of cyclic dimers of porphyrins and metalloporphyrins, **unsat-H$_2$1-H$_2$1** displays a complicated ^{1}H NMR spectrum due to the presence of conformational isomers:[S5] ^{1}H NMR (499.4 MHz, $CDCl_3$): δ -2.69 (m, 4H, N*H*), 0.9-1.61 (m, 72H, $C(CH_3)_3$), 1.95 (m, 8H, OCH_2CH_2), 2.22 (m, 8H, $C{=}CHCH_2$), 4.15 (m, J = 6

Hz, 8H, OC*H*$_2$), 5.48 (m, 4H, vinyl-*H*), 7.37-7.76 (m, 8H, Ar-*H*), 7.78 (m, 8H, Ar-*H*), 8.02 (m, 4H, Ar-*H*), 8.13 (m, 8H, Ar-*H*), 8.93 (m, 16H, β-*H*). $\{^1H\}^{13}C$ NMR (125.8 MHz, CDCl$_3$): δ 14.5, 20.1, 23.1, 24.1, 27.5, 29.2, 29.8, 30.1, 30.6, 32.1, 35.4, 67.8, 114.4, 115.6, 119.9, 121.2, 122.0, 127.7, 130.3, 141.6, 143.9, 149.0, 157.6. MALDI-ToF (reflective positive mode): Calcd for $C_{136}H_{144}N_8O_4$: 1954.65, found: *m/z* 1954.78 $[M]^+$. UV-vis (nm, (ε ×10^4 /M^{-1}cm^{-1})): 425 (50.8), 550 (1.7), 591 (0.5). See Fig. S10 for ^1H NMR spectrum.

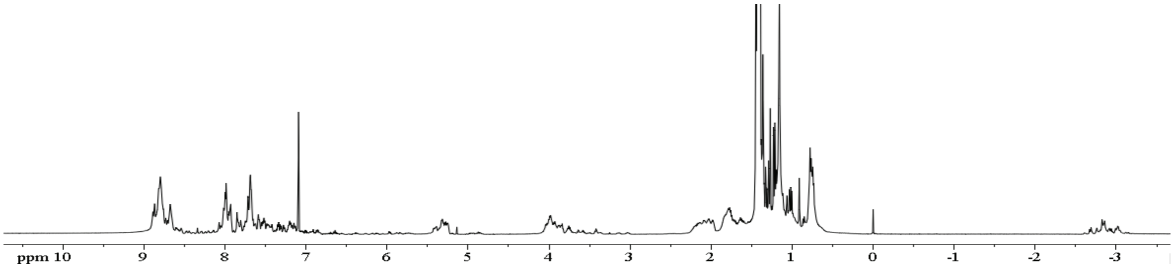

Fig. S10 The ^1H NMR spectrum for **unsat-H$_2$1-H$_2$1**.

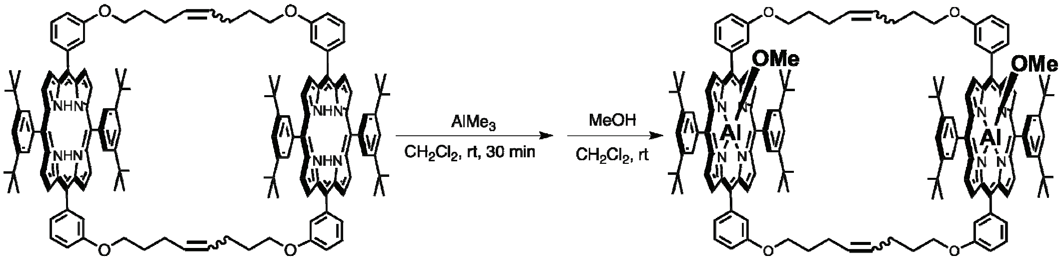

unsat-H$_2$1-H$_2$1 **unsat-Al1-Al1**

Unsat-Al1-Al1. **Unsat-H$_2$1-H$_2$1** (46 mg, 23.5 μmol) was metallated according to the general metallation strategy using AlMe$_3$. Pure **unsat-Al1-Al1** was isolated as a purple solid (48 mg, 23.1 μmol, 98% yield). As characteristic of cyclic dimers of porphyrins and metalloporphyrins, **unsat-Al1-Al1** displays a broad complicated ^1H NMR spectrum due to the presence of conformational isomers:[S5] ^1H NMR (499.4 MHz, CDCl$_3$): δ 1.26-1.69 (m, 72H, C(C*H*$_3$)$_3$), 1.88 (bs, 8H, OCH$_2$C*H*$_2$), 2.23 (bs, 8H, C=CHC*H*$_2$), 4.07 (bs, J = 6 Hz, 8H, OC*H*$_2$), 5.48 (bs, 2H, vinyl-*H*), 5.74 (bs, 2H, vinyl-*H*), 7.31 (bs, 6H, Ar-*H*), 7.79 (m, 16H, Ar-*H*), 8.61 (m, 6H, Ar-*H*), 9.09 (bs, 16H, β-*H*). $\{^1H\}^{13}C$ NMR (125.8 MHz, CDCl$_3$): δ 16.1, 28.3, 28.7, 30.0, 31.5, 32.0, 32.3, 32.5, 35.1, 35.6, 67.5, 115.4, 117.0, 120.1, 121.1, 121.5, 127.4, 129.8, 131.2, 132.6, 140.7, 146.3, 149.4, 157.8. MALDI-ToF (reflective positive mode): Calcd for $C_{138}H_{150}N_8O_6Al_2$: 2070.68, found: *m/z* 2038.53 $[M\text{-}OMe]^+$, 2023.55 $[M\text{-}OMe\text{-}CH_3]^+$, 2009.55 $[M\text{-}OMe\text{-}OMe]^+$. The use of the neutral pyrene matrix is critical; if another matrix containing acidic proton (such as 2-hydroxy-1-naphthoic acid matrix) was used, complete loss of the Al-OMe moieties is observed. UV-vis (nm, (ε ×10^4 /M^{-1}cm^{-1})): 408 (30.5), 551 (0.9), 603 (0.2). See Fig. S11 for ^1H NMR spectrum.

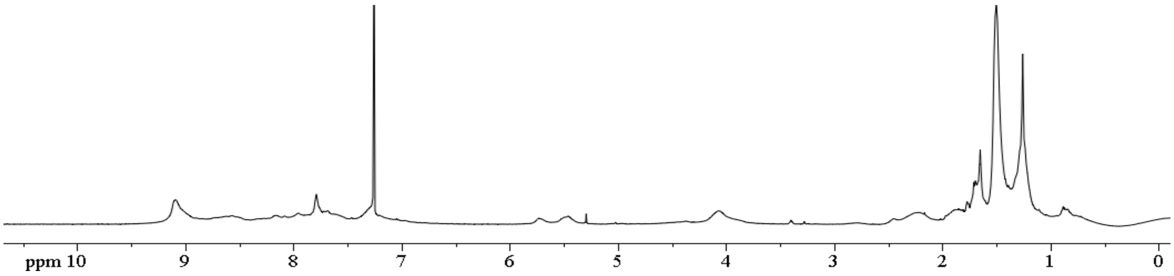

Fig. S11 The ^1H NMR spectrum for **unsat-Al1-Al1**.

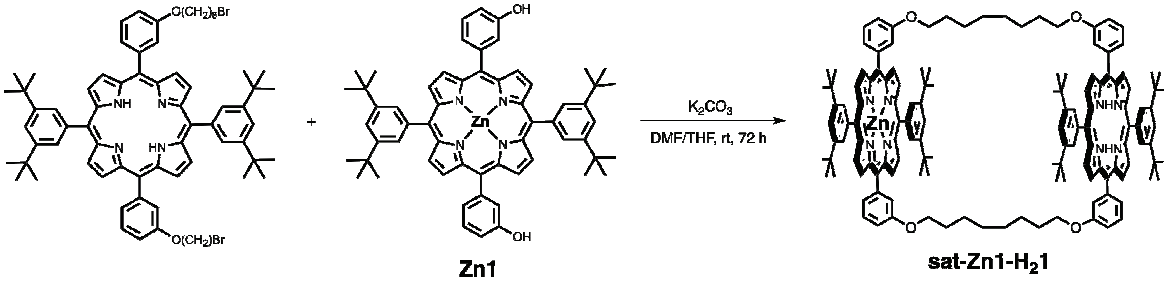

Sat-Zn1-H$_2$1. To a magnetically stirred DMF suspension (95 mL) of K_2CO_3 (375 mg, 2.7 mmol) in a 250 mL round-bottom flask was added dropwise a DMF/THF solution (12 mL 1:1 v/v) of **Zn1** (126 mg, 0.14 mmol) and [5,15-bis-(3-(1-bromooctanyloxy)phenyl)-10,20-bis-(3,5-di-*tert*-butyl-phenyl)]porphine (169 mg, 0.14 mmol) over a period of 24 h using a syringe pump. After the addition was completed, the reaction mixture was allowed to stir for an additional 48 h. The mixture was then poured into toluene (200 mL), washed with water (3 × 150 mL), and dried over Na_2SO_4. After removing the solvent via rotary evaporation, the dimer was purified by silica gel column chromatography (column dimensions = 50 mm × 250 mm, eluent = hexanes/CH_2Cl_2 2:1 v/v), where the second fraction was collected and evaporated to dryness to afford a purple solid (71 mg, 35.1 μmol, 26% yield). As characteristic of cyclic dimers of porphyrins and metalloporphyrins, **sat-Zn1-H$_2$1** displays a complicated ^{1}H NMR spectrum due to the presence of conformational isomers:[S5] ^{1}H NMR (499.4 MHz, $CDCl_3$): δ -2.85 (m, 2H, N*H*), 1.17-1.60 (m, 36, C(CH_3)$_3$), 1.68 (m, 8H, CH_2), 1.78 (m, 8H, CH_2), 1.88 (m, 8H, CH_2), 3.81-4.16 (m, 8H, OCH_2) 7.23-7.36 (m, 6H, Ar-*H*) 7.51-7.75 (m, 8H, Ar-*H*), 7.83 (m, 6H, Ar-*H*), 7.94-8.22 (m, 8H, Ar-*H*), 8.65-9.12 (m, 16H, β-*H*). {^{1}H}^{13}C NMR (125.8 MHz, $CDCl_3$): δ 14.5, 25.8, 26.1, 26.2, 29.3, 29.5, 29.7, 29.9, 30.1, 31.4, 32.1, 35.4, 68.4, 114.1, 114.9, 119.7, 120.9, 121.8, 122.9, 127.4, 128.8, 130.1, 132.3, 142.1, 144.4, 148.9, 150.4, 157.6. MALDI-ToF (reflective positive mode): Calcd for $C_{136}H_{146}N_8O_4Zn$: 2022.05, found: *m/z* 2023.58 $[M]^+$. UV-vis (nm, (ε ×10^4 /$M^{-1}cm^{-1}$)): 423 (39.4), 550 (1.4), 591 (0.3). See Fig. S12 for ^{1}H NMR spectrum.

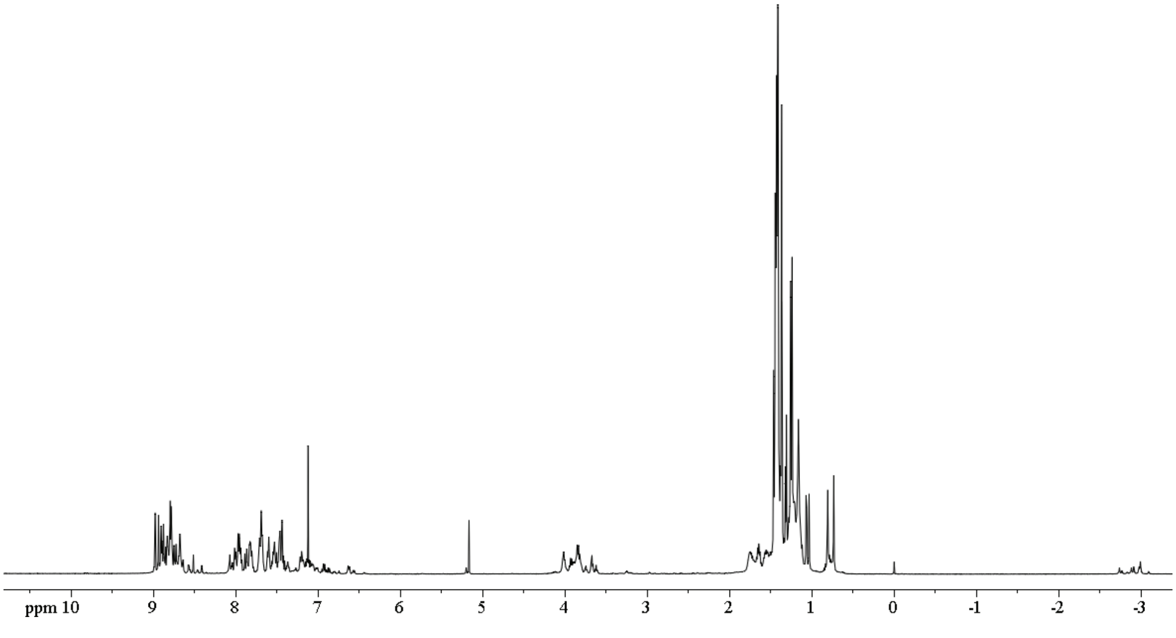

Fig. S12 The ^{1}H NMR spectrum for **sat-Zn1-H$_2$1**.

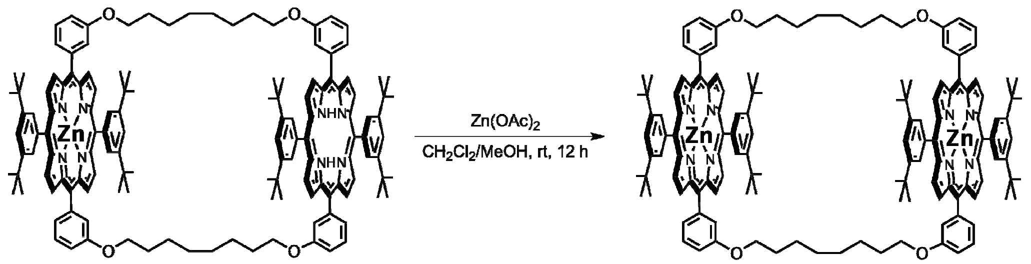

sat-Zn1-H$_2$1 **sat-Zn1-Zn1**

Sat-Zn1-Zn1. To a magnetically stirred solution of **sat-Zn1-H$_2$1** (20 mg, 9.9 µmol) in CH_2Cl_2 (10 mL) in a 50 mL round-bottom flask was added a solution of $Zn(OAc)_2$ (4 mg, 21.9 µmol) in methanol (2 mL). The resulting mixture was allowed to stir at room temperature for 12 h. Solvent was then removed under reduced pressure using a rotary evaporator and the residue was purified by silica gel column chromatography (column dimensions = 20 mm × 200 mm, eluent = hexanes/CH_2Cl_2 2:1 v/v) to give **sat-Zn1-Zn1** as a purple solid (20 mg, 9.8 µmol, 99% yield). Due to the presence of conformational isomers, **sat-Zn1-Zn1** displays a complicated ^{1}H NMR spectrum, which is simplified upon addition of 4,4'-bipyridyl template:[S4] ^{1}H NMR (499.4 MHz, $CDCl_3$): δ 1.36 (m, 16H, C*H*$_2$), 1.47 (m, 72H, C(C*H*$_3$)$_3$), 1.84 (t, *J* = 6.5 Hz, 8H, C*H*$_2$), 2.27 (d, *J* = 6Hz, 4H, α-pyridyl), 4.04 (t, *J* = 6.5Hz, 8H, OC*H*$_2$), 4.81 (d, *J* = 6Hz, 4H, β-pyridyl), 7.22 (d, *J* = 9Hz, 4H, Ar-*H*), 7.54 (m, 6H, Ar-*H*), 7.66 (m, 2H, Ar-*H*), 7.73 (bs, 4H, Ar-*H*), 7.79 (m, 4H, Ar-*H*), 7.87 (m, 4H, Ar-*H*), 7.96 (m, 2H, Ar-*H*), 8.04 (bs, 2H, Ar-*H*), 8.85 (m, 16H, β-*H*). {^{1}H}^{13}C NMR (125.8 MHz, $CDCl_3$): δ 14.5, 23.1, 26.1, 29.7, 30.1, 32.0, 35.3, 68.4, 114.0, 119.9, 120.8, 122.3, 127.5, 128.2, 129.6, 130.4, 131.6, 132.2, 142.5, 143.6, 145.0, 148.3, 150.1, 157.4. MALDI-ToF (reflective positive mode, pyrene matrix): Calcd for $C_{136}H_{144}N_8O_4Zn_2$: 2085.41, found: *m/z* 2085.23 $[M]^+$. UV-vis (nm, (ε ×10^4 /M^{-1}cm^{-1})): 421 (48.3), 550 (1.5), 591 (0.4). See Fig. S13 for ^{1}H NMR spectrum.

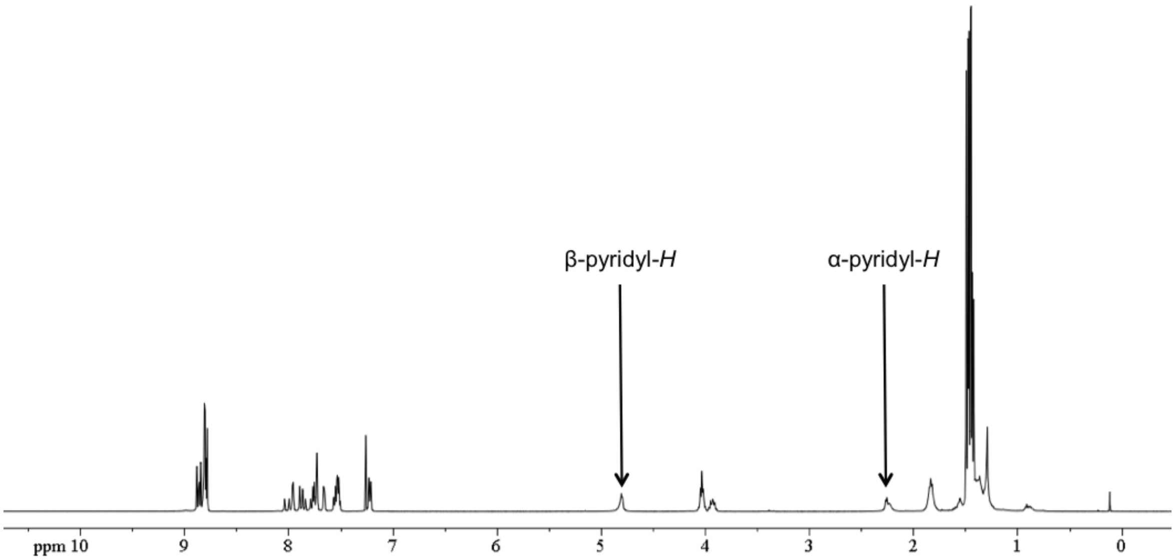

Fig. S13 The ^{1}H NMR spectrum for **sat-Zn1-Zn1** incorporating 4,4'-bipyridyl template.

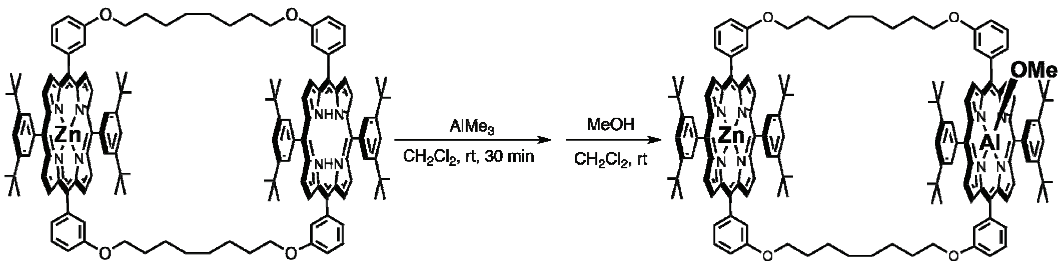

sat-Zn1-H$_2$1 **sat-Zn1-Al1**

Sat-Zn1-Al1. **Sat-Zn1-H$_2$1** (20 mg, 9.9 μmol) was metallated according to the general metallation strategy using AlMe$_3$. However, only 1.1 equiv of AlMe$_3$ was used to prevent transmetallation of the Zn porphyrin. Pure **sat-Zn1-Al1** was isolated as a purple metallic solid (20 mg, 9.6 μmol, 97% yield). As characteristicss of cyclic dimers of porphyrins and metalloporphyrins, **sat-Zn1-Al1** displays a broad complicated ^{1}H NMR spectrum due to the presence of conformational isomers:^{S5} ^{1}H NMR (499.4 MHz, CDCl$_3$): δ 1.33 (m, 16H, C*H*$_2$), 1.53 (m, 72H, C(C*H*$_3$)$_3$), 1.73 (m, 8H, C*H*$_2$), 4.06 (m, 8H, OC*H*$_2$), 7.06 (m, 8H, Ar-*H*), 7.54-7.81 (m, 12H, Ar-*H*), 8.08 (m, 8H, Ar-*H*), 8.95 (m, 16H, β-*H*). {^{1}H}^{13}C NMR (125.8 MHz, CDCl$_3$): δ 23.0, 26.1, 29.2, 30.0, 32.3, 35.3, 68.4, 114.7, 120.1, 120.5, 121.3, 125.5, 127.3, 128.7, 130.0, 132.5, 148.7, 150.1, 150.8, 158.1. MALDI-ToF (reflective positive mode): Calcd for $C_{137}H_{151}N_8O_5AlZn$: 2082.08, found: *m/z* 2082.62 [M]$^+$, 2067.64 [M-CH$_3$]$^+$, 2048.64 [M-OMe]$^+$. The use of the neutral pyrene matrix is critical; if another matrix containing acidic proton (such as 2-hydroxy-1-naphthoic acid matrix) was used, complete loss of the Al-OMe moiety is observed. UV-vis (nm, (ε ×10^4 /M^{-1}cm^{-1})): 417 (40.3), 550 (1.1), 591 (0.4). See Fig. S14 for ^{1}H NMR spectrum.

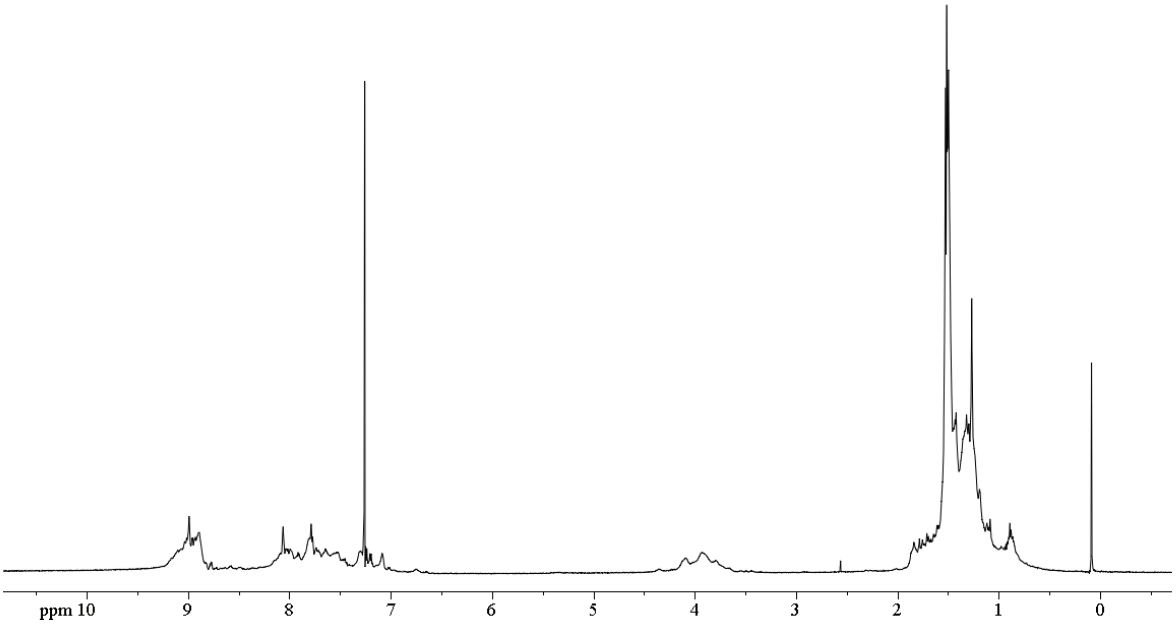

Fig. S14 The ^{1}H NMR spectrum for **sat-Zn1-Al1**.

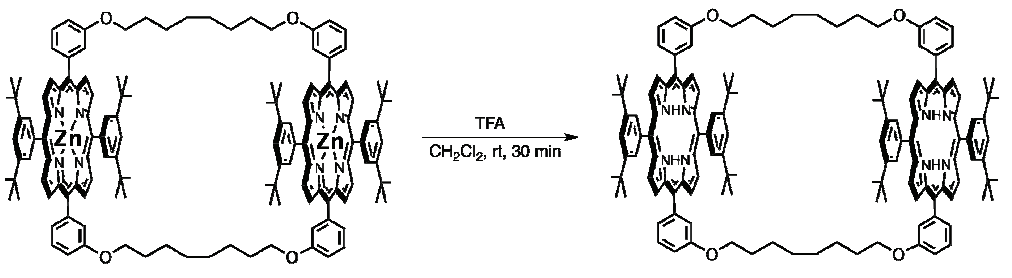

sat-Zn1-Zn1 **sat-H$_2$1-H$_2$1**

Sat-H$_2$1-H$_2$1. **Sat-Zn1-Zn1** (20 mg, 9.6 μmol) was demetallated following the general demetallation strategy using TFA. The free-base dimer, **sat-H$_2$1-H$_2$1**, was isolated as a purple solid (19 mg, 9.3 μmol, 97% yield). As characteristicss of cyclic dimers of porphyrins and metalloporphyrins, **sat-H$_2$1-H$_2$1** displays a complicated ^{1}H NMR spectrum due to the presence of conformational isomers:[S5] ^{1}H NMR (499.4 MHz, $CDCl_3$): δ -2.77 (m, 4H, N*H*), 1.37 (m, 16H, C*H*$_2$), 1.55 (m, 72H, C(C*H*$_3$)$_3$), 1.87 (m, 8H, C*H*$_2$), 4.04 (m, 8H, OC*H*$_2$), 7.28-7.36 (m, 8H, Ar-*H*), 7.50-7.86 (m, 12H, Ar-*H*), 7.97-8.22 (m, 8H, Ar-*H*), 8.91 (m, 16H, β-*H*). {^{1}H}^{13}C NMR (125.8 MHz, $CDCl_3$): δ 23.0, 25.6, 26.3, 29.3, 29.8, 30.1, 31.4, 32.1, 35.4, 68.5, 114.1, 115.5, 119.7, 121.1, 121.9, 127.5, 130.2, 141.5, 143.9, 149.0, 157.7. MALDI-ToF (reflective positive mode): Calcd for $C_{136}H_{148}N_8O_4$: 1958.68, found: *m/z* 1958.78 $[M]^+$. UV-vis (nm, (ε ×10^4 /$M^{-1}cm^{-1}$)): 425 (56.5), 550 (2.0), 591 (0.7). See Fig. S15 for ^{1}H NMR spectrum.

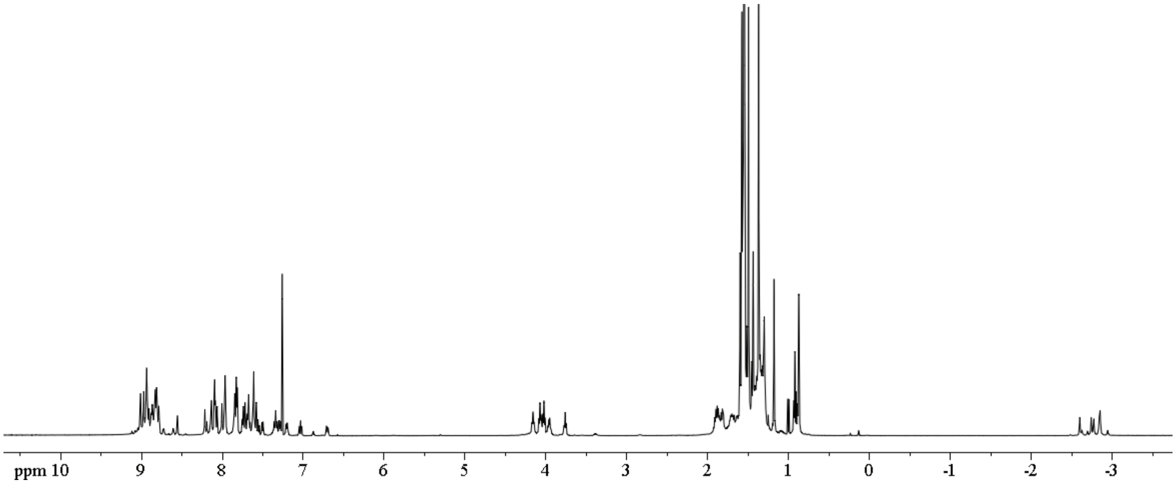

Fig. S15 The ^{1}H NMR spectrum for **sat-H$_2$1-H$_2$1**.

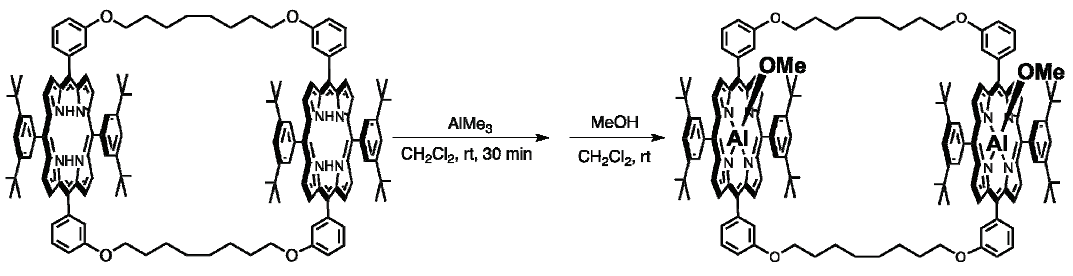

sat-H$_2$1-H$_2$1 **sat-Al1-Al1**

Sat-Al1-Al1. **Sat-H$_2$1-H$_2$1** (19 mg, 9.7 μmol) was metallated according to the general metallation strategy using AlMe$_3$. Pure **sat-Al1-Al1** was isolated as a purple metallic solid (19 mg, 9.5 μmol, 98% yield). As characteristicss of cyclic dimers of porphyrins and metalloporphyrins, **sat-Al1-Al1** displays a broad complicated ^{1}H NMR spectrum due to the presence of conformational isomers:[S5] ^{1}H NMR (499.4 MHz, CDCl$_3$): δ 1.23 (m, 16H, C*H*$_2$) 1.46 (m, 72H, C(C*H*$_3$)$_3$), 1.81 (m, 8H, C*H*$_2$), 4.11 (m, 8H, OC*H*$_2$), 7.31 (bs, 8H, Ar-*H*), 7.89 (m, 16H, Ar-*H*), 8.62 (m, 8H, Ar-*H*), 9.12 (m, 16H, β-*H*). {^{1}H}^{13}C NMR (125.8 MHz, CDCl$_3$): δ 24.1, 26.3, 27.1, 30.2, 30.9, 31.5, 33.8, 66.3, 114.8, 119.5, 120.4, 126.6, 127.8, 129.3, 131.1, 139.2, 147.4, 156.5. MALDI-ToF (reflective positive mode): Calcd for $C_{138}H_{154}N_8O_6Al_2$: 2074.71, found: *m/z* 2043.55 [M-OMe]$^+$, 2027.57 [M-OMe-CH$_3$]$^+$, 2011.43 [M-OMe-OMe]$^+$. The use of the neutral pyrene matrix is critical; if another matrix containing acidic proton (such as 2-hydroxy-1-naphthoic acid matrix) was used, complete loss of the Al-OMe moieties is observed. UV-vis (nm, (ε ×10^4 /M^{-1}cm^{-1})): 408 (36.6), 550 (0.9), 591 (0.3). See Fig. S16 for ^{1}H NMR spectrum.

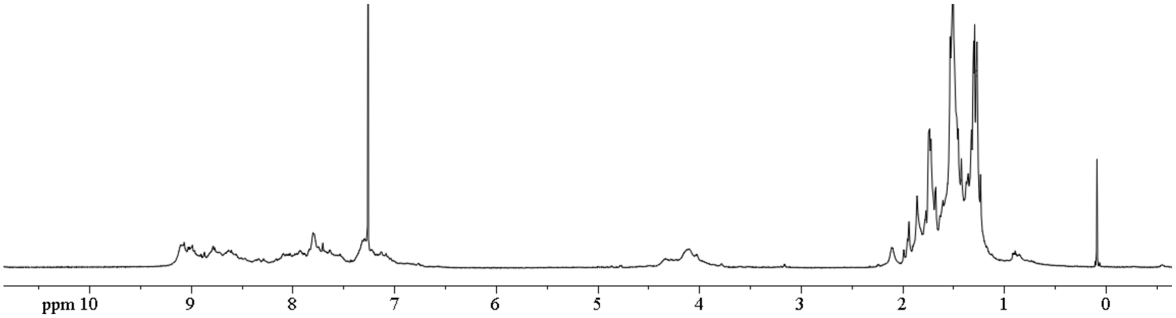

Fig. S16 The ^{1}H NMR spectrum for **sat-Al1-Al1**.

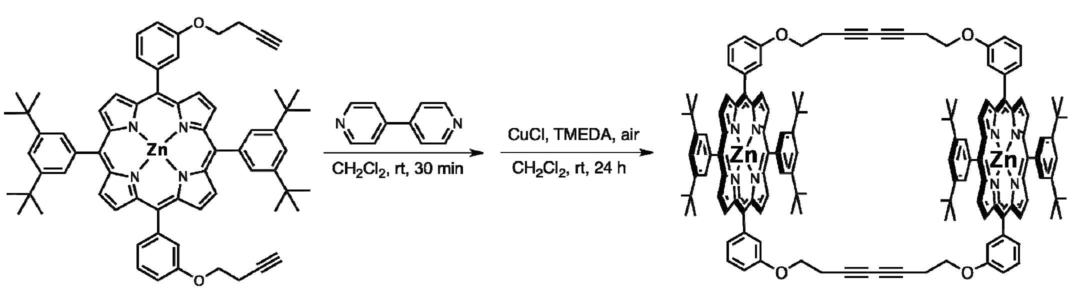

diyne-Zn1 **diyne-Zn1-Zn1**

Diyne-Zn1-Zn1. To a magnetically stirred solution of **diyne-Zn1** (131 mg, 0.1 mmol) in CH$_2$Cl$_2$ (190 mL) in a 500 mL round-bottom flask was added the template 4,4'-bipyridyl (19 mg, 0.1 mmol) as a solid. After an additional 30 minutes of stirring, CuCl (857 mg, 8.7 mmol) and TMEDA (1.0 g, 8.7 mmol) were added to the reaction mixture, which was allowed to stir under air for 24 h. Second portions of CuCl (857 mg, 8.7 mmol) and TMEDA (1.0 g, 8.7 mmol) were added and stirring continued for another 24 h. The reaction mixture was evaporated to dryness via rotary evaporation and the residue thus obtained was redissolved in CH_2Cl_2 (50 mL), washed with water (3 × 100 mL) and brine (100 mL), dried over Na_2SO_4, filtered, and concentrated to dryness. The remaining residue was purified by size-exclusion chromatography (Bio-Rad Bio-Beads S-X1, column dimensions = 50 mm × 250 mm, eluent = CH_2Cl_2), where the first fraction was collected and concentrated to dryness. Further purification was done by silica gel column chromatography (column dimensions = 20 mm × 200 mm, eluent = hexanes/CH_2Cl_2 1:1 v/v) to yield the desired porphyrin dimer as a purple solid (26 mg, 12.4 μmol, 16% yield). Due to the presence of conformational isomers, **diyne-Zn1-Zn1** shows a complicated ^{1}H NMR spectrum, which is simplified upon addition of 4,4'-bipyridyl template:[S4] ^{1}H NMR (499.4 MHz, $CDCl_3$): δ 1.43 (s, 36H , $\mathrm{C(C}H_3)_3$, 1.46 (s, 36H, $\mathrm{C(C}H_3)_3$, 2.81 (t, J = 7 Hz, 8H, $\mathrm{CCC}H_2$), 4.11 (t, J = 7.5 Hz, 8H, $\mathrm{OC}H_2$), 7.16 (dd, J_1 = 8.5 Hz, J_2 = 2 Hz, 2H, Ar-*H*), 1.18 (dd, J_1 = 8.5 Hz, J_2 = 2 Hz, 2H, Ar-*H*), 7.52, (t, J = 8 Hz, 4H, Ar-*H*), 7.57, (s, 4H, Ar-*H*), 7.71 (m, 8H, Ar-*H*), 7.85, (s, 4H, Ar-*H*), 7.94 (s, 4H, Ar-*H*), 8.78, (m, 16H, β-*H*). {^{1}H}^{13}C NMR (125.8 MHz, $CDCl_3$): δ 20.6, 31.9, 35.2, 53.7, 65.6, 66.5, 73.8, 114.3, 119.8, 120.1, 120.6, 122.3, 127.4, 128.2, 129.5, 130.1, 131.3, 131.5, 131.9, 132.1, 142.4, 145.0, 148.2, 149.8, 150.2, 156.4. MALDI-ToF (reflective positive mode): Calcd for $C_{136}H_{128}N_8O_4Zn_2$: 2069.28, found: *m/z* 2070.13 $[M]^+$. UV-vis (nm, (ε ×10^4 /$M^{-1}cm^{-1}$)): 425 (46.7), 552 (0.8), 590 (0.5). See Fig. S17 for ^{1}H NMR spectrum.

We note that the second compound isolated from the synthesis of **diyne-Zn1** (page S11) did not yield the desired dimer when being subjected to the same conditions described above.

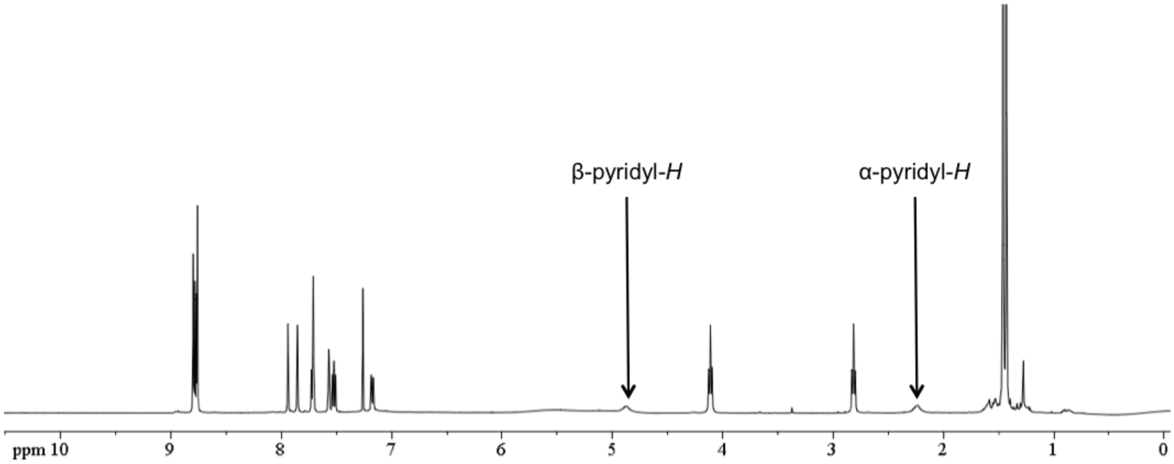

Fig. S17 The ^{1}H NMR spectrum for **diyne-Zn1-Zn1** incorporating 4,4'-bipyridyl template.

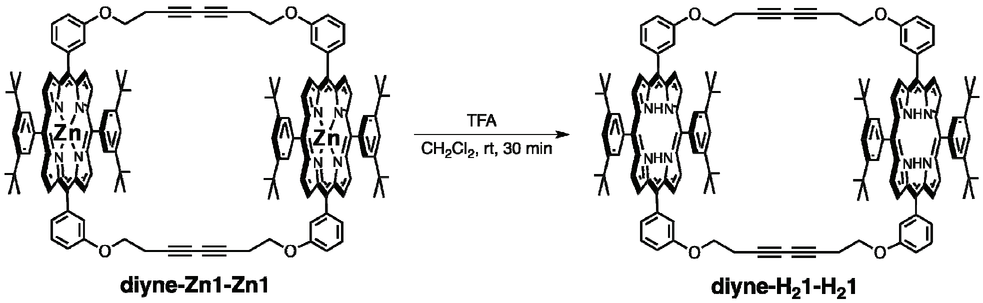

diyne-Zn1-Zn1 **diyne-H$_2$1-H$_2$1**

Diyne-H$_2$1-H$_2$1. **Diyne-Zn1-Zn1** (20 mg, 9.7 μmol) was demetallated following the general demetallation strategy using TFA. The free-base dimer, **diyne-H$_2$1-H$_2$1**, was isolated as a purple solid (18 mg, 9.4 μmol, 97% yield). As characteristicss of cyclic dimers of porphyrins and metalloporphyrins, **diyne-H$_2$1-H$_2$1** displays a complicated ^{1}H NMR spectrum due to the presence of conformational isomers:[S5] ^{1}H NMR (499.4 MHz, CDCl$_3$): δ -2.75 (m, 4H, N*H*), 1.54 (m, 72H, C(C*H*$_3$)$_3$, 2.81 (m, 8H, CCC*H*$_2$), 4.23 (m, 8H, OC*H*$_2$), 7.30 (m, 4H, Ar-*H*), 7.56-7.64 (m, 4H, Ar-*H*), 7.74 (bs, 4H, Ar-*H*), 7.83 (m, 8H Ar-*H*), 8.09 (m, 8H, Ar-*H*), 8.89 (m, 16H, β-*H*). {^{1}H}^{13}C NMR (125.8 MHz, CDCl$_3$): δ 20.7, 21.1, 23.1, 25.6, 30.1, 32.1, 35.4, 66.1, 114.7, 119.6, 121.3, 122.1, 127.9, 128.2, 130.2, 141.5, 144.0, 149.0, 156.9. MALDI-ToF (reflective positive mode): Calcd for C$_{136}$H$_{132}$N$_8$O$_4$: 1942.55, found: *m/z* 1942.49 [M]$^+$. UV-vis (nm, (ε ×10^4 /M^{-1}cm^{-1})): 425 (53.3), 552 (1.2), 590 (0.5). See Fig. S18 for ^{1}H NMR spectrum.

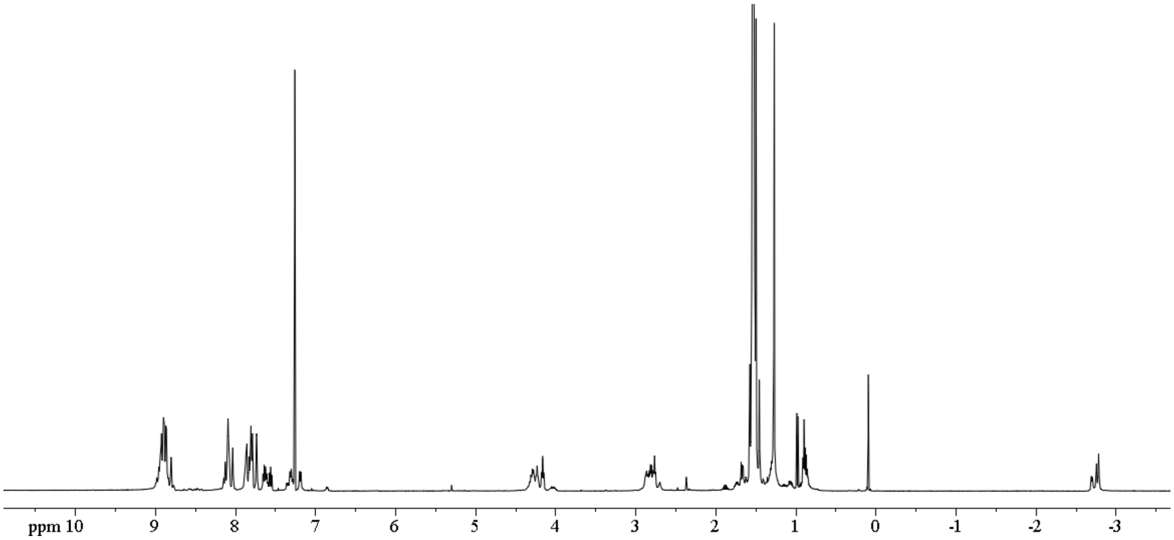

Fig. S18 The ^{1}H NMR spectrum for **diyne-H2-H2**.

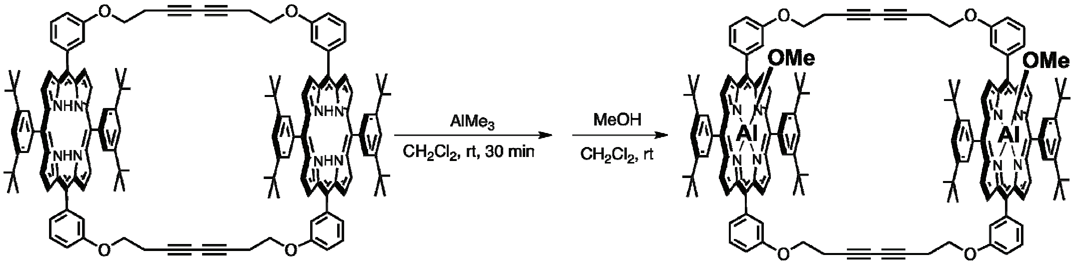

Diyne-Al1-Al1. **Diyne-H$_2$1-H$_2$1** (18 mg, 9.4 μmol) was metallated according to the general metallation strategy using AlMe$_3$. Pure **diyne-Al1-Al1** was isolated as a purple metallic solid (19 mg, 9.2 μmol, 98% yield). As characteristicss of cyclic dimers of porphyrins and metalloporphyrins, **diyne-Al1-Al1** displays a broad complicated ^{1}H NMR spectrum due to the presence of conformational isomers:[S5] ^{1}H NMR (499.4 MHz, CDCl$_3$): δ 1.16-1.97 (m, 72H, C(C*H*$_3$)$_3$, 2.87 (m, 8H, CCC*H*$_2$), 4.39 (m, 8H, OC*H*$_2$), 7.1-7.4 (m, 8H, Ar-*H*), 7.73-7.82 (m, 8H, Ar-*H*), 8.36 (m, 4H, Ar-*H*), 8.85 (m, 8H, Ar-*H*), 9.13 (m, 16H, β-*H*). {^{1}H}^{13}C NMR (125.8 MHz, CDCl$_3$): δ 21.4, 22.1, 23.0, 25.2, 30.1, 31.9, 32.5, 35.3, 35.9, 64.3, 114.5, 120.3, 121.5, 122.7, 126.1, 127.4, 132.2, 140.5, 142.5, 146.7, 148.3, 157.4. MALDI-ToF (reflective positive mode, pyrene matrix): Calcd for C$_{138}$H$_{134}$N$_8$O$_6$Al$_2$: 2058.55, found: *m/z* 2026.25 [M-OMe]$^+$, 2012.24 [M-OMe-CH$_3$]$^+$. The use of the neutral pyrene matrix is critical; if another matrix containing acidic proton (such as 2-hydroxy-1-naphthoic acid matrix) was used, complete loss of the Al-OMe moieties is observed. UV-vis (nm, ($\varepsilon \times 10^4$ /$M^{-1}cm^{-1}$)): 408 (38.3), 550 (1.0), 591 (0.3). See Fig. S19 for ^{1}H NMR spectrum.

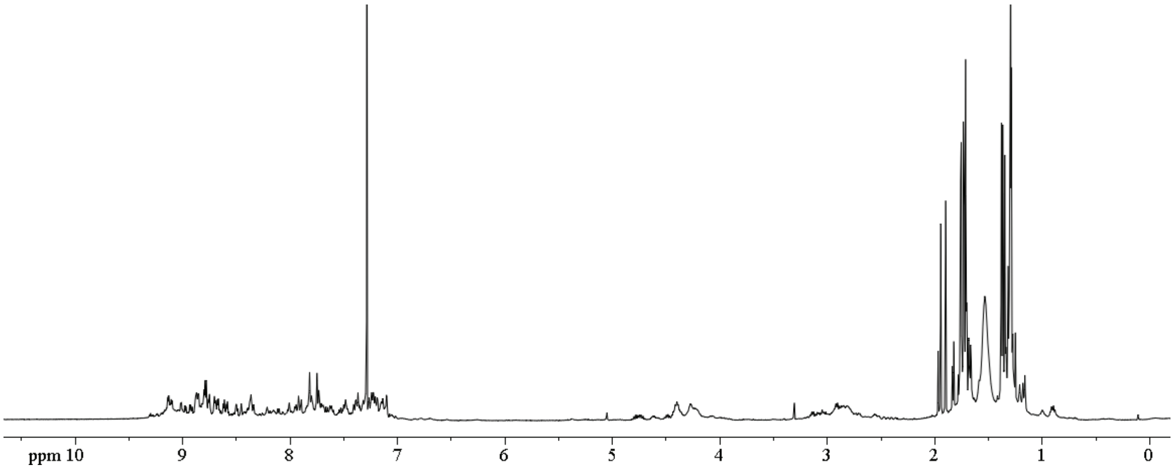

Fig. S19 The ^{1}H NMR spectrum for **diyne-Al1-Al1**.

V. Preparation of porphyrins possessing trihexyl silyl substituents.

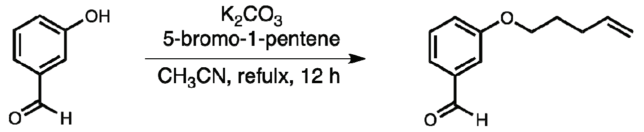

4

3-(1-Pentenyloxy)benzaldehyde (4). This compound was synthesized following a modified literature procedure.[S6] Into a 250 mL round bottom flask equipped with a magnetic stir bar and a water-cooled reflux condenser were combined 3-hydroxybenzaldehyde (3.0 g, 24.6 mmol), K_2CO_3 (7.1 g, 51.6 mmol), anhydrous acetonitrile (90 mL) and 5-bromo-1-pentene (5.5 g, 36.9 mmol). The resulting mixture was then refluxed overnight under N_2. The solution was then cooled to room temperature, filtered, and washed with dichloromethane (100 mL). The combined organics were evaporated to dryness under reduced pressure and the resultant residue was redissolved in dichloromethane (100 mL) and washed with water (50 mL). The organic layer was dried over $MgSO_4$, filtered, and concentrated under reduced pressure. Purification via silica gel column chromatography (column dimensions = 60 mm × 250 mm, eluent = EtOAc/hexanes 1:3 v/v) afforded the product as a pale yellow oil (4.5 g, 23.8 mmol, 97% yield). Spectroscopic data for 3-(1-pentenyloxy)benzaldehyde was in good agreement with literature data.[S7] ^{1}H NMR (499.4 MHz, $CDCl_3$): δ 1.90 (quintet, J = 6.5 Hz, 2H, CH_2CH_2O), 2.24 (q, J = 7 Hz, 2H, $CH_2{=}CHCH_2$), 4.02 (t, J = 6 Hz, 2H, CH_2CH_2O), 5.03 (dd, J_1 = 29 Hz, J_2 = 10.5 Hz, 1H, $CH_2{=}CHCH_2$), 5.08 (dd, J_1 = 29 Hz, J_2 = 17.5 Hz, 1H, $CH_2{=}CHCH_2$), 5.85 (m, 1H, $CH_2{=}CHCH_2$), 7.16 (m, 1H, Ar-*H*), 7.37 (d, 1H, Ar-*H*), 7.43 (m, 2H, Ar-*H*), 9.96 (s, 1H, C*H*O). {^{1}H}^{13}C NMR (125.8 MHz, $CDCl_3$): δ 28.5, 30.3, 67.7, 112.9, 115.7, 122.2, 123.9, 130.3, 138.0, 159.9, 192.5.

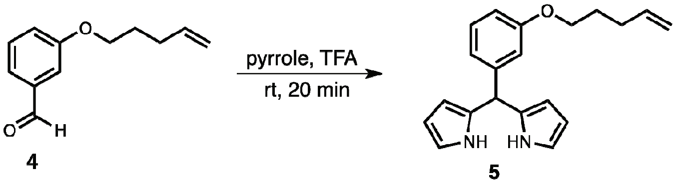

(3-(1-Pentenyloxy)phenyl)dipyrromethane (5). In a 250 mL round bottom flask equipped with a magnetic stir bar and a water-cooled reflux condenser, 3-(1-pentenyloxy)benzaldehyde (3.0 g, 15.8 mmol) was dissolved in freshly distilled pyrrole (110 mL) and degassed with N_2 for 10 min. TFA (0.1 mL, 1.6 mmol) was then added and the resulting mixture was allowed to stir under N_2 for 30 min. The reaction mixture was diluted with CH_2Cl_2 (125 mL) and washed with aq. NaOH (150 mL of a 0.1 M solution). The combined organic layer was dried over Na_2SO_4, filtered, and evaporated to dryness by rotary evaporation. Excess pyrrole was removed by vacuum distillation at 60 °C and 20 mm Hg. The resulting viscous brown oil was purified by silica gel column chromatography (column dimensions = 60 mm × 250 mm, eluent = hexanes/CH_2Cl_2/EtOAc 7:2:1 v/v/v) to afford the pure product as a yellow oil (3.4 g, 11.1 mmol, 71% yield). ^{1}H NMR (499.4 MHz, $CDCl_3$): δ 1.76 (quintet, J = 6.5 Hz, 2H, CH_2CH$_2$O), 2.12 (q, J= 6.5 Hz, 2H, CH$_2$=CHCH_2), 3.83 (t, J = 6.5 Hz, 2H, CH$_2$CH_2O), 4.91 (dd, J_1 = 29.75 Hz, J_2 = 10.5 Hz, 1H, CH_2=CHCH$_2$), 4.97 (dd, J_1 = 29.75 Hz, J_2 = 17.0 Hz, 1H, CH_2=CHCH$_2$), 5.32 (s, 1H, CH), 5.76 (m, 1H, CH$_2$=CHCH$_2$), 5.85 (s, 2H, pyrrole CH), 6.07 (q, J = 3.0 Hz, 2H, pyrrole CH), 6.58 (q, J = 2.5 Hz, 2H, pyrrole CH), 6.70 (m, 2H, Ar-H), 7.13 (m, 2H, Ar-H), 7.80 (br s, 2H, NH). {^{1}H}^{13}C NMR (125.8 MHz, $CDCl_3$): δ 28.7, 30.4, 44.3, 67.4, 107.5, 108.7, 113.0, 115.2, 115.5, 117.5, 120.9, 129.9, 132.6, 138.1, 143.9, 159.6.

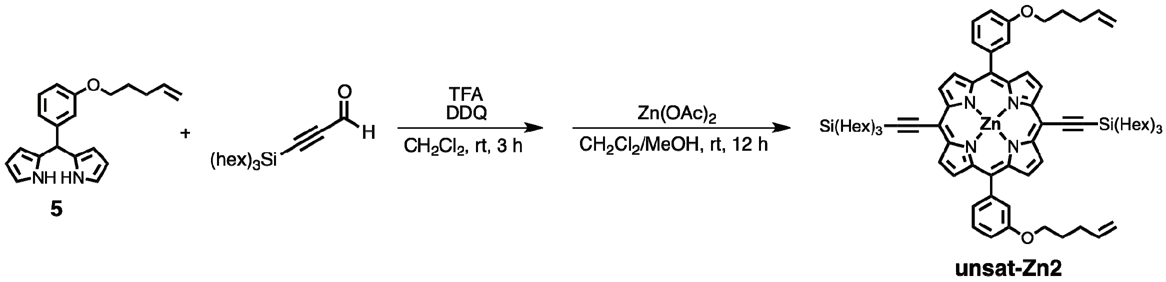

[5,15-Bis(3-(1-pentenyloxy)phenyl)-10,20-bis((trihexylsilyl)ethynyl)porphinato]zinc(II) (unsat-Zn2). In a 1 L round-bottom flask equipped with a magnetic stir bar were combined (3-(1-pentenyloxy)phenyl)dipyrromethane (1.1 g, 3.6 mmol), 3-trihexylsilyl-2-propynal (1.2 g, 3.6 mmol), and CH_2Cl_2 (350 mL). The resulting mixture was degassed with N_2 for ten minutes before TFA (0.2 mL, 2.3 mmol) was added. After stirring under N_2 at room temperature for an additional 2 h, DDQ (1.6 g, 7.1 mmol) was added as a solid and stirring was continued for an additional 2 h. A solution of Zn(OAc)$_2$ (1.0 g, 5.3 mmol) in MeOH (30 mL) was then added and the reaction mixture was allowed to stir for 12 h more before being evaporated to dryness using a rotary evaporator. The crude product was purified by silica gel chromatography (column dimensions = 50 mm × 250 mm, eluent = hexanes/EtOAc 40:1 v/v) to yield the desired product as a purple solid (0.2 g, 0.2 mmol, 9% yield). ^{1}H NMR (499.4 MHz, $CDCl_3$): δ 0.93 (t, J = 7.0 Hz, 18H, ^{n}Hex CH_3), 1.04 (m, 12H, ^{n}Hex CH_2), 1.36-1.46 (m, 24H, ^{n}Hex CH_2), 1.57 (quintet, J = 7 Hz, 12H, ^{n}Hex CH_2), 1.80 (m, 12H, ^{n}Hex CH_2), 1.99 (quintet, J = 7 Hz, 4H, CH_2CH$_2$O), 2.32 (q, J = 7 Hz, 4H, CH$_2$=CHCH_2), 4.16 (t, J = 6.5 Hz, 4H, CH$_2$CH_2O), 5.02 (dd, J_1 = 42.5 Hz, J_2 = 10 Hz, 2H, CH_2=CHCH$_2$), 5.10 (dd, J_1 = 42.5 Hz, J_2 = 17.5 Hz, 2H, CH_2=CHCH$_2$), 5.90 (m, 2H, CH$_2$=C*H*CH$_2$), 7.33 (d, *J* = 8 Hz, 2H, Ar-*H*), 7.66 (t, *J* = 8.5 Hz, 2H, Ar-*H*), 7.74 (s, 2H, Ar-*H*), 7.79 (d, *J* = 7.5 Hz, 2H, Ar-*H*), 8.98 (d, *J* = 4.5 Hz, 4H, β-*H*), 9.74 (d, *J* = 4.5 Hz, 4H, β-*H*). $\{^1H\}^{13}C$ NMR (125.8 MHz, CDCl$_3$): δ 14.2, 14.6, 23.1, 24.7, 28.9, 30.5, 32.0, 33.7, 68.8, 100.9, 102.1, 108.7, 114.5, 115.6, 121.2, 122.7, 127.8, 131.7, 133.1, 138.2, 143.7, 150.4, 152.7, 157.7. MALDI-ToF (reflective positive mode): Calcd for $C_{82}H_{112}N_4O_2Si_2Zn$: 1304.76, found: *m/z* 1304.72 $[M]^+$. UV-vis (nm, (ε ×10^4 /$M^{-1}cm^{-1}$)): 436 (41.3), 538 (0.4), 577 (1.3), 625 (3.3). See Fig. S20 for NMR spectra.

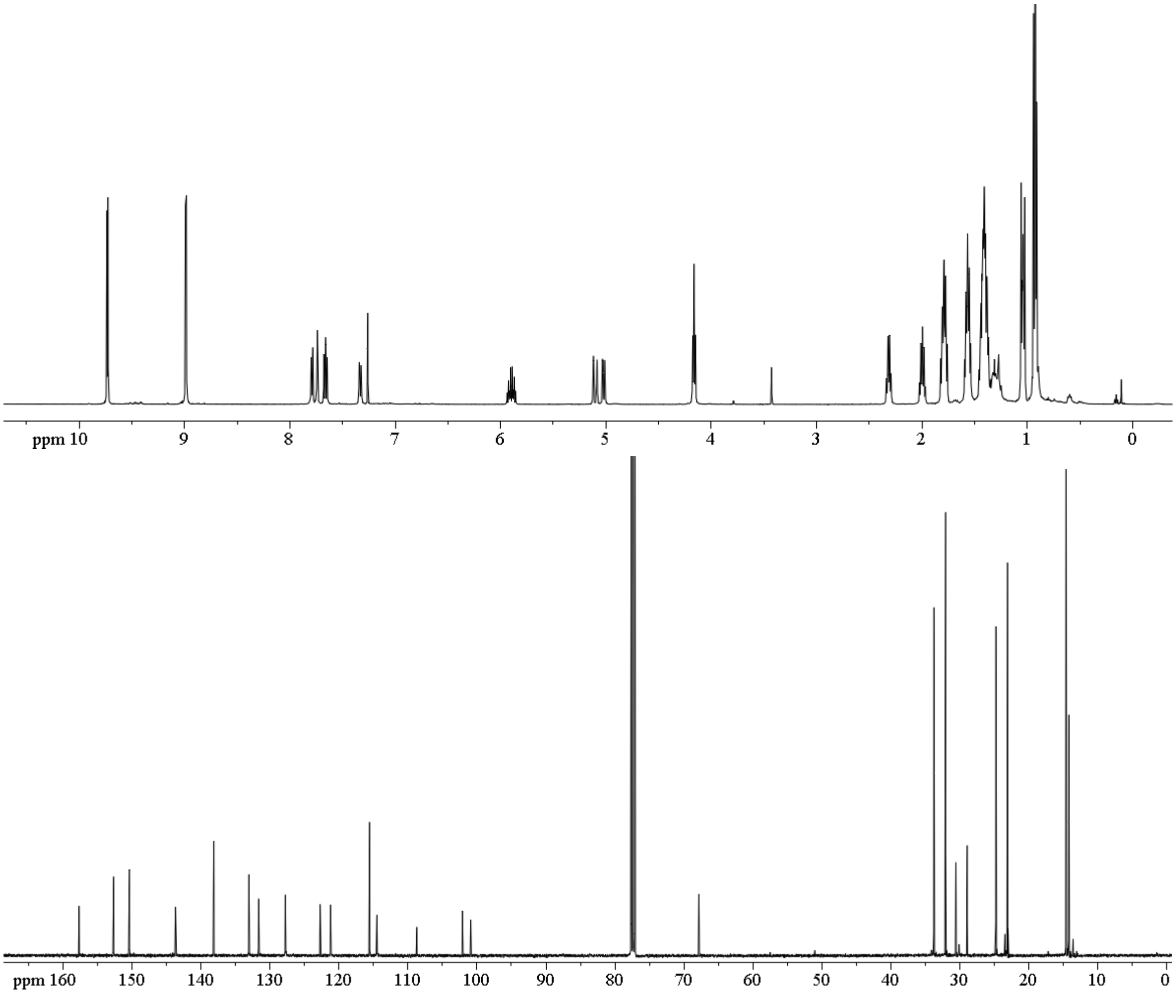

Fig. S20 The ^1H (top) and ^{13}C NMR (bottom) spectra for [5,15-Bis(3-(1-pentenyloxy)phenyl)-10,20-bis((trihexylsilyl)ethynyl)porphinato]zinc(II) (**unsat-Zn2**).

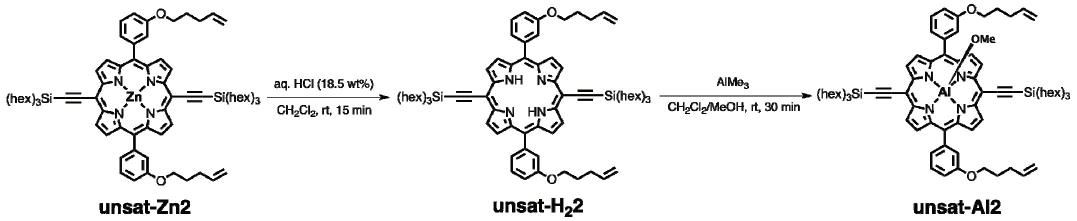

[5,15-Bis(3-(1-pentenyloxy)phenyl)-10,20-bis((trihexylsilyl)ethynyl)porphinato]aluminum(III) methoxide (unsat-Al2). To a magnetically stirred solution of **unsat-Zn2** monomer (20 mg, 15.3 μmol) in CH$_2$Cl$_2$ (20 mL) in a 50 mL round bottom flask was added aqueous HCl (2 mL of an 18.5 wt% solution). After stirring for 15 min at room temperature, the resulting mixture was washed consecutively with water (50 mL), saturated $NaHCO_3$ (30 mL), and brine (30 mL) before being dried over Na_2SO_4 and filtered. The filtrate was then evaporated to dryness using a rotary evaporator and the remaining residue was subjected to silica gel column chromatography (column dimensions = 20 mm × 200 mm, eluent = hexanes/CH_2Cl_2 3:2 v/v) to yield the demetallated product as a purple solid (18 mg, 14.4 μmol, 94% yield). ^1H NMR (499.4 MHz, $CDCl_3$): δ -2.14 (s, 2H, N*H*), 0.93 (t, *J* = 7.0 Hz, 18H, ^{n}Hex CH_3), 1.05 (m, 12H, ^{n}Hex CH_2), 1.28-1.42 (m, 24H, ^{n}Hex CH_2), 1.57 (quintet, *J* = 7.5 Hz, 12H, ^{n}Hex CH_2), 1.79 (m, 12H, ^{n}Hex CH_2), 2.03 (quintet, *J* = 7.5 Hz, 4H, C$H_2$$CH_2$O), 2.35 (q, *J* = 7 Hz, 4H, CH_2=CHCH_2), 4.20 (t, *J* = 6.5 Hz, 4H, CH_2CH_2O), 5.04 (dd, J_1 = 41.75 Hz, J_2 = 10.5 Hz, 2H, CH_2=CHCH_2), 5.13 (dd, J_1 = 41.75 Hz, J_2 = 17 Hz, 2H, CH_2=CHCH_2), 5.91 (m, 2H, CH_2=C*H*CH_2), 7.26 (s, 2H, Ar-*H*), 7.68 (t, *J* = 8 Hz, 2H, Ar-*H*), 7.77 (m, 2H, Ar-*H*), 7.80 (d, *J* = 6.5 Hz, 2H, Ar-*H*), 8.91 (d, *J* = 4.5 Hz, 4H, β-*H*), 9.65 (d, *J* = 4.5 Hz, 4H, β-*H*). $\{^1H\}^{13}C$ NMR (125.8 MHz, $CDCl_3$): δ 13.6, 14.5, 23.1, 24.7, 28.9, 30.1, 30.6, 32.0, 33.7, 67.8, 101.4, 101.7, 108.2 114.7, 115.6, 121.3, 121.8, 127.8, 128.1, 138.2, 142.9, 157.9. MALDI-ToF (reflective positive mode, pyrene matrix): Calcd for $C_{82}H_{114}N_4O_2Si_2$: 1243.98, found: *m/z* 1243.89 $[M]^+$. UV-vis (nm, (ε ×10^4 /$M^{-1}cm^{-1}$)): 434 (56.3), 546 (1.9), 586 (7.8), 623 (1.2), 682 (3.3). See Fig. S21 for NMR spectra.

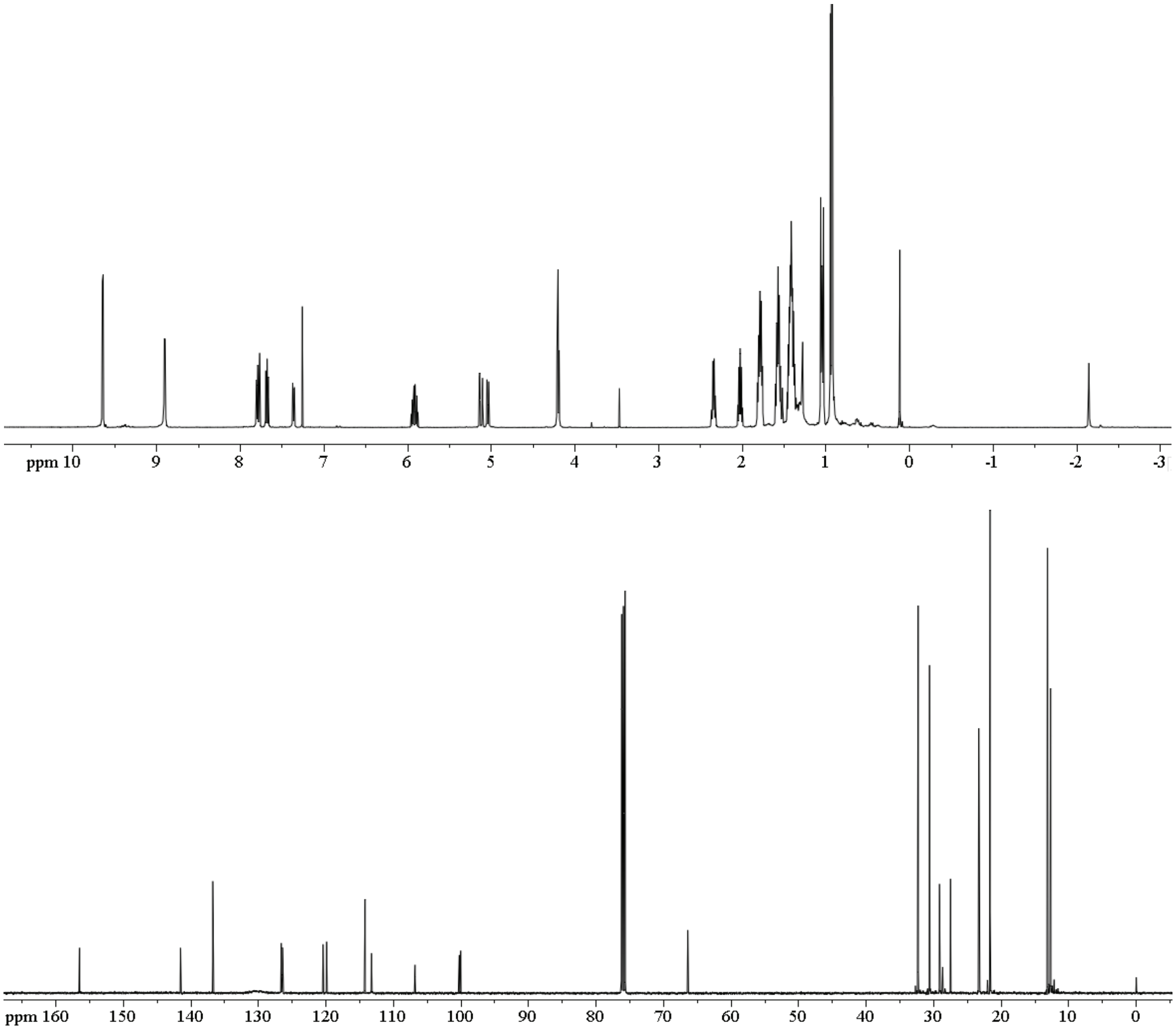

Fig. S21 The ^1H (top) and ^{13}C NMR (bottom) spectra for [5,15-Bis(3-(1-pentenyloxy)phenyl)-10,20-bis((trihexylsilyl)ethynyl)]porphine (**unsat-$H_2$2**).

Unsat-H$_2$2 porphyrin monomer (18 mg, 14.4 μmol) was metallated according to the general metallation strategy using AlMe$_3$. Pure **unsat-Al2** was isolated as a purple solid (18 mg, 14.1 μmol, 98% yield). ^{1}H NMR (499.4 MHz, CDCl$_3$): δ 0.99 (t, *J* = 6.5 Hz, 18H, ^{n}Hex $\mathrm{C}H_3$), 1.14 (br s, 12H, ^{n}Hex $\mathrm{C}H_2$), 1.26 (s, 3H, $\mathrm{OC}H_3$), 1.46-1.52 (br m, 27H, ^{n}Hex $\mathrm{C}H_2$), 1.67 (br s, 12H, ^{n}Hex $\mathrm{C}H_2$), 1.88 (br s, 12H, ^{n}Hex $\mathrm{C}H_2$), 2.14 (br s, 4H, $\mathrm{C}H_2\mathrm{CH_2O}$), 2.47 (br s, 4H, $\mathrm{CH_2{=}CHC}H_2$), 4.30 (br m, 4H, $\mathrm{CH_2C}H_2\mathrm{O}$), 5.15 (dd, J_1 = 43.5 Hz, J_2 = 10.0 Hz, 2H, $\mathrm{C}H_2\mathrm{{=}CHCH_2}$), 5.25 (dd, J_1 = 43.5 Hz, J_2 = 16.0 Hz, 2H, $\mathrm{C}H_2\mathrm{{=}CHCH_2}$), 6.04 (br m, 2H, $\mathrm{CH_2{=}C}H\mathrm{CH_2}$), 6.97 (br s, 4H, Ar-*H*), 7.61 (br s, 2H, Ar-*H*), 8.47 (br s, 4H, β-H_2), 8.91 (br s, 2H, Ar-*H*), 9.12 (br s, 4H, β-H_1). {^{1}H}^{13}C NMR (125.8 MHz, CDCl$_3$): δ 13.8, 14.4, 22.9, 24.6, 28.6, 30.3, 31.9, 33.8, 67.5, 98.9, 107.4, 115.0, 115.8, 119.5, 130.3, 131.8, 138.1, 145.5, 147.5, 157.4. MALDI-ToF (reflective positive mode, pyrene matrix): Calcd for $C_{83}H_{115}N_4O_3Si_2Al$: 1298.83, found: *m/z* 1302.50 [M]$^+$, 1284.50 [M-CH$_3$]$^+$, 1267.50 [M-OMe]$^+$. ESIMS: Calcd for $C_{83}H_{115}N_4O_3Si_2Al$: 1298.83, found: *m/z* 1299.32 [M+H]$^+$. UV-vis (nm, (ε ×10^4 /M^{-1}cm^{-1})): 437 (35.5), 535 (0.5), 586 (1.4), 637 (4.1). See Fig. S22 for NMR spectra.

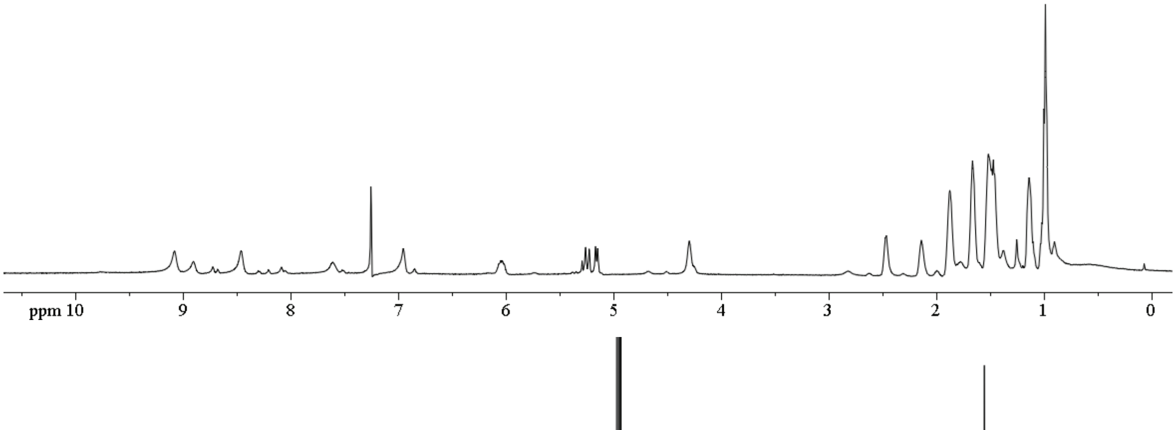

Fig. S22 The ^{1}H (top) and ^{13}C NMR (bottom) spectra for [5,15-Bis(3-(1-pentenyloxy)phenyl)-10,20-bis((trihexylsilyl)ethynyl)porphinato]aluminum(III) methoxide (**unsat-Al2**).

VI. Preparation of covalently linked porphyrin dimers possessing trihexyl silyl substituents (series 2 catalysts)

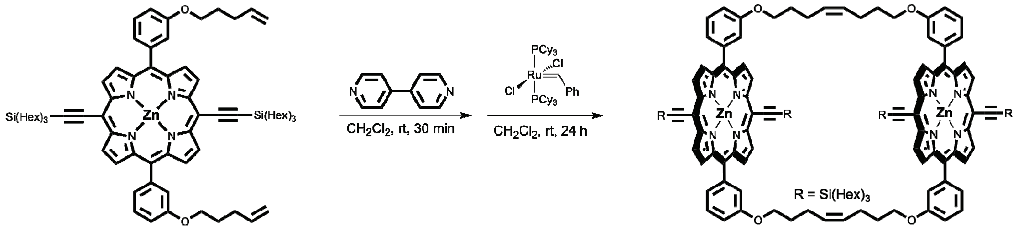

unsat-Zn2 **unsat-Zn2-Zn2**

Unsat-Zn2-Zn2. Into a 100 mL Schlenk flask equipped with a magnetic stir bar were combined **unsat-Zn2** (50 mg, 38.3 μmol), anhydrous CH_2Cl_2 (38 mL), and the 4,4'-dipyridine template (3 mg, 19.1 μmol). The resulting mixture was degassed with N_2 for 10 min and then allowed to stir under N_2 for an additional 20 min. A degassed CH_2Cl_2 (2 mL) solution of Grubbs' first generation catalyst (6 mg, 7.7 μmol) was then added via cannula to the reaction mixture and the resulting mixture was allowed to stir under N_2 for 12 h. A second catalyst aliquot was then added (3 mg, 3.9 μmol, in 2 mL of N_2-degassed CH_2Cl_2) via cannula and stirring was continued for 12 h more. (Note: without the second catalyst addition, the primary product, as analyzed by MALDI-ToF MS, is a mixture of open and closed dimers.) The reaction was then quenched by adding ethyl vinyl ether (10 mL) and opening to air. Solvents were removed from the quenched reaction mixture under reduced pressure using a rotary evaporator and the resulting residue was purified by silica gel column chromatography (column dimensions = 20 mm × 200 mm, eluent = hexanes/CH_2Cl_2 3:2 v/v). The first fraction was collected and concentrated to obtain the pure product as a purple solid (42 mg, 16.3 μmol, 85% yield). Due to the presence of conformational isomers, **unsat-Zn2-Zn2** displays a complicated ^{1}H NMR spectrum, which is simplified upon addition of 4,4'-bipyridyl template:^{S4} ^{1}H NMR (499.4 MHz, $CDCl_3$): δ 0.86 (t, *J* = 7Hz, 36H, ^{n}Hex C*H*$_3$), 0.94 (t, *J* = 8.5 Hz, 24H, ^{n}Hex C*H*$_2$), 1.33 (m, 48H, ^{n}Hex C*H*$_2$), 1.48 (q, *J* = 7 Hz, 24H, ^{n}Hex C*H*$_2$) 1.69 (m, 24H, ^{n}Hex CH_2), 1.92 (bs, 8H, OCH_2C*H*$_2$), 2.19 (bs, 8H, CH=CHC*H*$_2$), 2.28 (bs, 4H, α-pyridyl), 4.07 (q, *J* = 6Hz, 8H, OC*H*$_2$), 4.78 (bs, 4H, β-pyridyl), 5.50 (m, 4H, vinyl-*H*), 7.25 (m, 4H, Ar-*H*), 7.51 (m, 4H, Ar-*H*) 7.56 (m, 4H, Ar-*H*), 7.66 (t, *J* = 8Hz, 4H, Ar-*H*), 8.77 (d, *J* = 4.5Hz, 8H, β-*H*), 9.52 (d, *J* = 4.5Hz, 8H, β-H). {^{1}H}^{13}C NMR (125.8 MHz, $CDCl_3$): δ 13.9, 14.4, 22.9, 24.5, 28.9, 29.8, 29.9, 31.8, 33.5, 67.5, 67.9, 99.7, 100.9, 109.3, 113.7, 121.5, 122.2, 127.5, 127.8, 129.9, 130.4, 130.9, 132.5, 143.6, 143.9, 149.9, 152.3, 157.4. MALDI-ToF (reflective positive mode): Calcd for $C_{160}H_{216}N_8O_4Si_4Zn_2$: 2558.58, found: *m/z* 2558.42 $[M]^+$. UV-vis (nm, (ε ×10^4 /$M^{-1}cm^{-1}$)): 436 (33.7), 633 (3.2), 621 (2.2) 582 (1.3). See Fig. S23 for ^{1}H NMR spectrum.

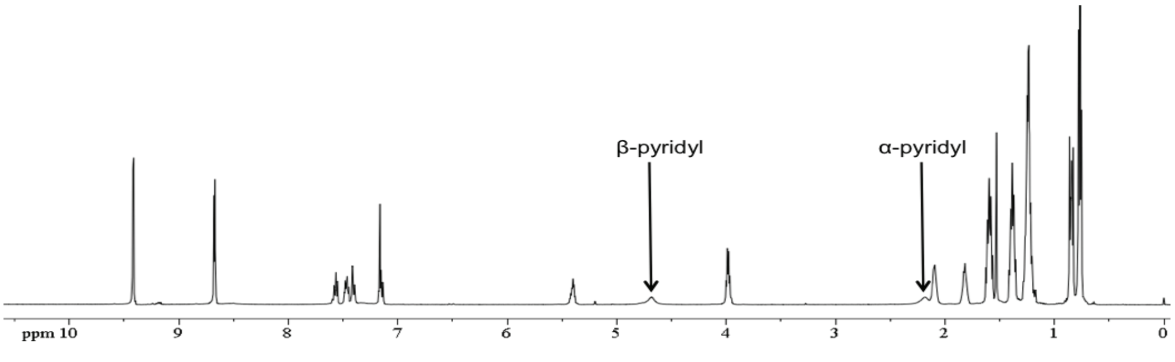

Fig. S23 The ^{1}H NMR spectrum for **unsat-Zn2-Zn2** incorporating 4,4'-bipyridyl template.

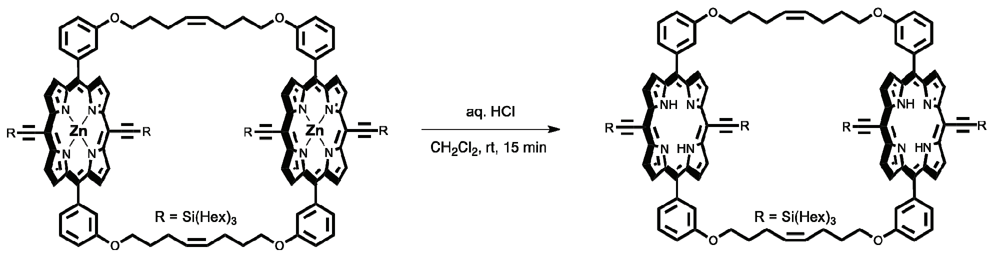

unsat-Zn2-Zn2 **unsat-H$_2$2-H$_2$2**

Unsat-H$_2$2-H$_2$2. To a magnetically stirred solution of **unsat-Zn2-Zn2** (30 mg, 12.0 μmol) in CH_2Cl_2 (20 mL) in a 50 mL round-bottom flask was added aqueous HCl (2 mL of an 18.5 wt% solution). After 15 min of stirring at room temperature, the resulting mixture was washed consecutively with water (50 mL), saturated $NaHCO_3$ (30 mL), and brine (30 mL) before being dried over Na_2SO_4 and filtered. The filtrate was evaporated to dryness using a rotary evaporator and the remaining residue was subjected to column chromatography over silica gel (column dimensions = 20 mm × 200 mm, eluent = hexanes/CH_2Cl_2 3:2 v/v) to yield the demetallated product as a purple solid (26 mg, 11.2 μmol, 93% yield). As characteristicss of cyclic dimers of porphyrins and metalloporphyrins, **unsat-H$_2$2-H$_2$2** displays a complicated ^{1}H NMR spectrum due to the presence of conformational isomers:[S5] ^{1}H NMR (499.4 MHz, $CDCl_3$): δ -2.52 (m, 4H, N*H*), 0.90 (m, 36H, ^{n}Hex C*H*$_3$), 1.06 (bs, 24H, ^{n}Hex C*H*$_2$), 1.35 (m, 48H, ^{n}Hex C*H*$_2$), 1.48 (m, 24H, ^{n}Hex C*H*$_2$) 1.66 (m, 24H, ^{n}Hex CH$_2$), 1.95 (bs, 8H, OCH$_2$C*H*$_2$), 2.28 (bs, 8H, CH=CHC*H*$_2$), 4.11 (m, 8H, OC*H*$_2$), 5.56 (m, 4H, vinyl-*H*), 7.34 (m, 4H, Ar-*H*), 7.53 (m, 4H, Ar-*H*) 7.64 (m, 4H, Ar-*H*), 7.76 (m, 4H, Ar-*H*), 8.76 (m, 8H, β-*H*), 9.47 (m, 8H, β-H). {^{1}H}^{13}C NMR (125.8 MHz, $CDCl_3$): δ 13.4, 13.6, 13.9, 14.5, 22.9, 24.7, 29.1, 30.1, 32.0, 33.7, 67.6, 101.4, 108.1, 115.8, 120.6, 121.6, 127.7, 131.2, 142.8, 157.8. MALDI-ToF (reflective positive mode): Calcd for $C_{160}H_{220}N_8O_4Si_4$: 2431.85, found: *m/z* 2431.14 $[M]^+$. UV-vis (nm, (ε ×10^4 /M^{-1}cm^{-1})): 434 (17.6), 545 (0.6), 586 (2.4), 622 (0.4), 681 (1.0). See Fig. S24 for ^{1}H NMR spectrum.

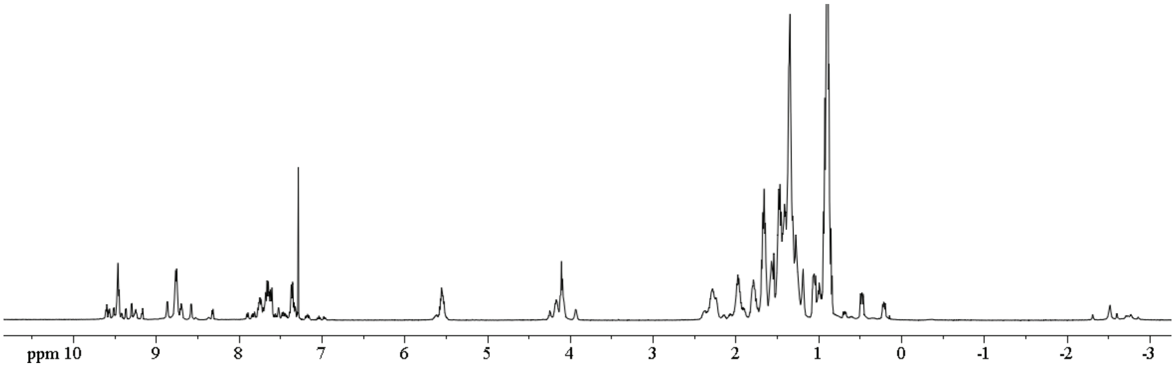

Fig. S24 The ^{1}H NMR spectrum for **unsat-H$_2$2-H$_2$2**.

unsat-H$_2$2-H$_2$2 **unsat-Al2-Al2**

Unsat-Al2-Al2. **Unsat-H$_2$2-H$_2$2** (26 mg, 11.2 μmol) was metallated according to the general metallation strategy using AlMe$_3$. Pure **unsat-Al2-Al2** was isolated as a purple solid (27 mg, 11.0 μmol, 98% yield). As characteristicss of cyclic dimers of porphyrins and metalloporphyrins, **unsat-Al2-Al2** displays a broad complicated ^{1}H NMR spectrum due to the presence of conformational isomers:[S5] ^{1}H NMR (499.4 MHz, CDCl$_3$): δ 0.98 (bs, 36H, ^{n}Hex C*H*$_3$), 1.05 (bs, 24H, ^{n}Hex C*H*$_2$), 1.27 (bs, 48H, ^{n}Hex C*H*$_2$), 1.46 (bs, 24H, ^{n}Hex C*H*$_2$) 1.61 (m, 24H, ^{n}Hex CH$_2$), 1.78 (bs, 8H, OCH$_2$C*H*$_2$), 2.29 (bs, 8H, CH=CHC*H*$_2$), 4.09 (bs, 8H, OC*H*$_2$), 5.85 (m, 4H, vinyl-*H*), 6.7 (m, 4H, Ar-*H*), 7.42 (m, 4H, Ar-*H*) 8.41 (m, 8H, Ar-*H*), 9.21 (m, 8H, β-*H*). {^{1}H}^{13}C NMR (125.8 MHz, CDCl$_3$): δ 14.6, 23.1, 24.7, 29.6, 30.1, 32.0, 33.8, 64.7, 101.7, 106.1, 116.8, 121.6, 122.3, 127.9, 130.6, 142.1, 161.6. MALDI-ToF (reflective positive mode): Calcd for $C_{162}H_{222}N_8O_6Si_4Al_2$: 2543.85, found: *m/z* 2511.03 [M-OMe]$^+$, 2495.98 [M-OMe-CH$_3$]$^+$, 2483.01 [M-OMe-OMe]$^+$. The use of the neutral pyrene matrix is critical; if another matrix containing acidic proton (such as 2-hydroxy-1-naphthoic acid matrix) was used, complete loss of the Al-OMe moieties is observed. UV-vis (nm, (ε ×10^4 /M^{-1}cm^{-1})): 420 (23.9), 637 (1.3), 584 (0.5). See Fig. S25 for ^{1}H NMR spectrum.

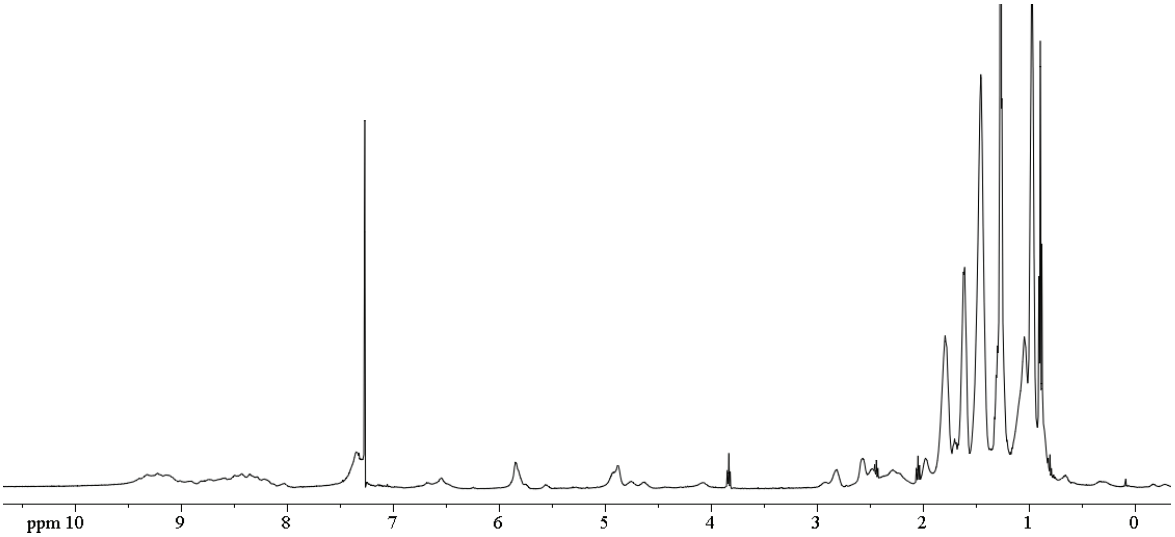

Fig. S25 The ^{1}H NMR spectrum for **unsat-Al2-Al2**.

VII. Synthesis of *para*-nitrophenyl diphenylphosphate.

Para-nitrophenyl diphenylphosphate was synthesized following a modified literature procedure.[S8] To a magnetically stirred solution of titanium tetrachloride (16.3 μL, 148.3 μmol) in anhydrous THF (40 mL) in a 100 mL Schlenk flask was added 4-nitrophenol (1.14 g, 8.2 mmol) at room temperature under N$_2$. A solution of diphenyl chlorophosphate (1.99 g, 7.4 mmol) in anhydrous THF (5 mL) was then added using a gas-tight syringe, followed by triethylamine (2.1 mL, 14.9 mmol), and the resulting mixture was allowed to stir for 1 h more. The resulting yellow solution was quenched by adding water (10 mL) and extracted with EtOAc (3 × 80 mL). The combined organic extracts were dried over $MgSO_4$, filtered, and concentrated under reduced pressure. Purification via silica gel column chromatography (column dimensions = 50 mm × 250 mm, eluent = EtOAc/hexanes 1:3 v/v) afforded PNPDPP as a white solid (2.4 g, 6.4 mmol, 86% yield). ^{1}H NMR (400.6 MHz, $CDCl_3$): δ 7.21-7.24 (m, 6H, Ar-*H*), 7.33-7.38 (m, 6H, Ar-*H*), 8.22 (d, *J* = 9.2 Hz, 2H, Ar-*H*). $\{^1H\}^{13}C$ NMR (100.7 MHz, $CDCl_3$): δ 120.2, 121.0, 125.9, 126.2, 130.2, 150.2, 155.2. $\{^1H\}^{31}P$ NMR (161.9 MHz, $CDCl_3$): δ -17.84. HRESIMS: Calcd for $[C_{18}H_{14}NO_6P+H]^+$: 372.0632, found: *m/z* 372.0670 $[M+H]^+$.

VIII. Representative procedure for the methanolysis of *p*-nitrophenyl diphenyl phosphate (PNPDPP). Under bench-top conditions, a 2 dram vial equipped with a magnetic stir bar was charged with PNPDPP (41.8 mg, 25 mM), the appropriate catalyst (Al or Zn-porphyrin monomer (6 mol%) or dimer (3 mol%)), and anhydrous $CHCl_3$ (2.25 mL). Methanol (2.25 mL to make a 12.3 M solution) was then added to the reaction mixture at room temperature. The reaction vial was sealed with a Teflon-lined cap and allowed to stir at 60 ºC in an oil bath. Aliquots (0.20 mL) were periodically taken and filtered through a pad of silica gel, which was then washed with ethyl acetate (3 × 2 mL). The combined filtrates were concentrated *in vacuo* at room temperature, redissolved in $CDCl_3$, and analyzed via ^{31}P NMR spectroscopy. The conversion of PNPDPP as a function of reaction time was obtained by comparing the integrated areas under the resonances for PNPDPP and methyl diphenyl phosphate (MDPP) (Fig. S26).

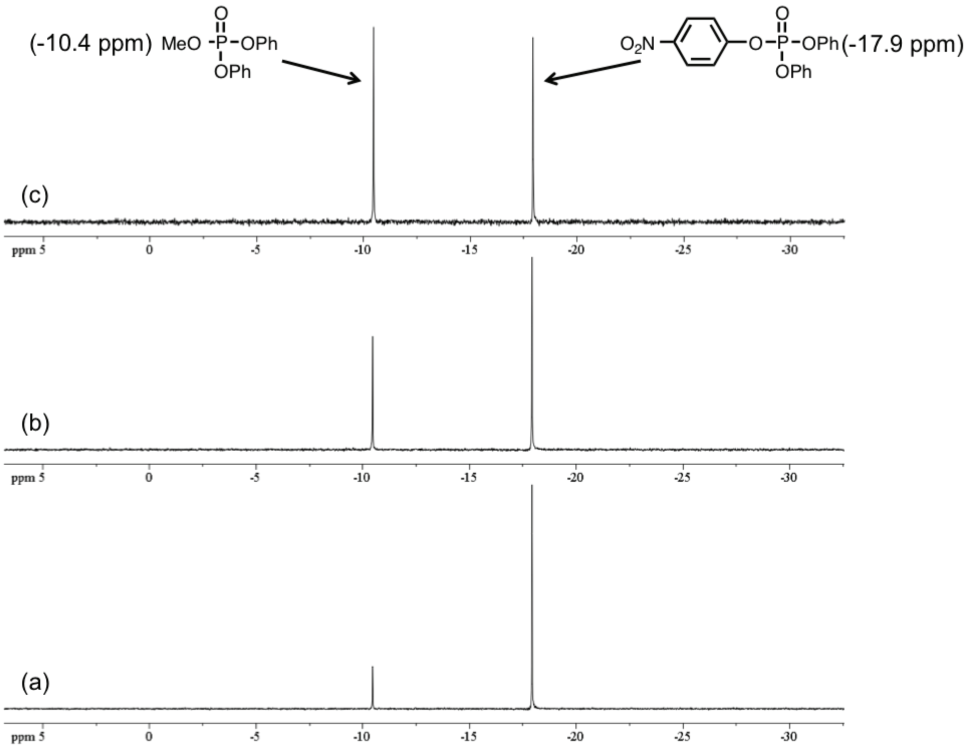

Fig. S26 Progress for the methanolysis of PNPDPP to MDPP in the presence of 3 mol% **unsat-Al1-Al1** at 60 ºC, as monitored by ^{31}P NMR spectroscopy at (a) 6 h, (b) 30 h, and (c) 50 h.

IX. CHELPG charges of aluminum porphyrin monomers. Partial charges of Al and O atoms in each porphyrin were estimated using the CHELPG charge calculation scheme.[S9] B3LYP/6-31+G(d) calculations were performed to estimate the charges and for simplification, alkane side chains were excluded from the simulation experiment.

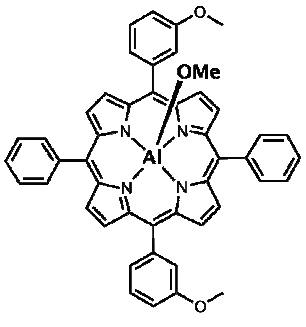

Tetraphenyl porphyrin

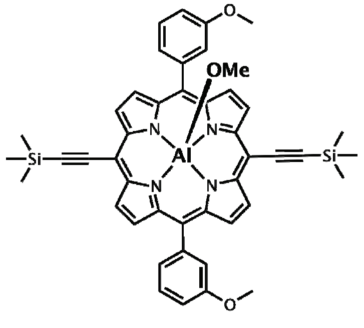

Alkyne-substituted porphyrin

Table S1 Partial charges of Al and O atoms and Al-O bond properties.

Porphyrin Substituent at 10, 20 Position	Al Charge	O Charge	Al-O Bond Length (A)	Al-O Bond Energy (kcal/mol)
Phenyl	1.189	-0.645	1.751	161.6
$-C{\equiv}CSi(CH_3)_3$	1.248	-0.653	1.747	164.0

X. Product formation rates for the methanolysis of PNPDPP catalyzed by series 1 catalysts. Reactions were carried out as described above in section VIII with several porphyrin catalysts and conversion data was collected. As an example, the determination of the product formation rate for **unsat-Al1-Al1** was carried out as follows. To a 2 dram vial equipped with a magnetic stir bar was added PNPDPP (41.8 mg, 25 mM) and **unsat-Al1-Al1** (7.0 mg, 3 mol%). Anhydrous $CHCl_3$ (2.25 mL) and MeOH (2.25 mL to make a 12.3 M solution) were added and the vial was sealed with a Teflon-lined cap and the reaction was allowed to stir at 60 ºC in an oil bath. Aliquots (0.20 mL) were withdrawn after 30, 60, 90, 120, 180, and 270 min and filtered through a pad of silica gel, which was then washed with ethyl acetate (3 × 2 mL). The combined filtrates were concentrated *in vacuo* at room temperature, redissolved in $CDCl_3$, and analyzed via ^{31}P NMR spectroscopy to determine the yield of DPMP (Tables S2 and S3).

Table S2 Product formation rates for the methanolysis of PNPDPP in the presence and absence of porphyrin dimer (**series 1**) catalysts at 12.3 M MeOH. Reported catalyzed rates were background-corrected from uncatalyzed reactions.

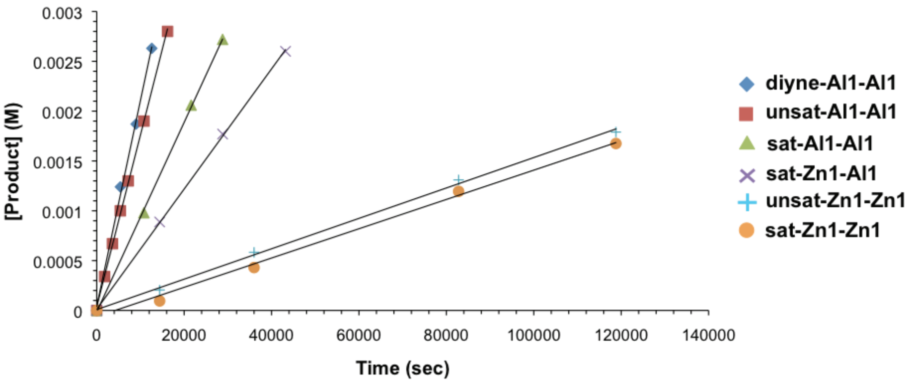

Porphyrin catalyst	Catalyst loading (mol %)	Observed initial rate (M/s)
sat-Zn1-Zn1	3	1.47×10^{-8}
unsat-Zn-Zn1	3	1.53×10^{-8}
sat-Zn1-Al1	3	6.03×10^{-8}
sat-Al1-Al1	3	9.51×10^{-8}
unsat-Al1-Al1	3	1.69×10^{-7}
diyne-Al1-Al1	3	2.05×10^{-7}
unsat-$H_2$1-$H_2$1	3	9.51×10^{-10}
Uncatalyzed reaction	-	9.17×10^{-10}

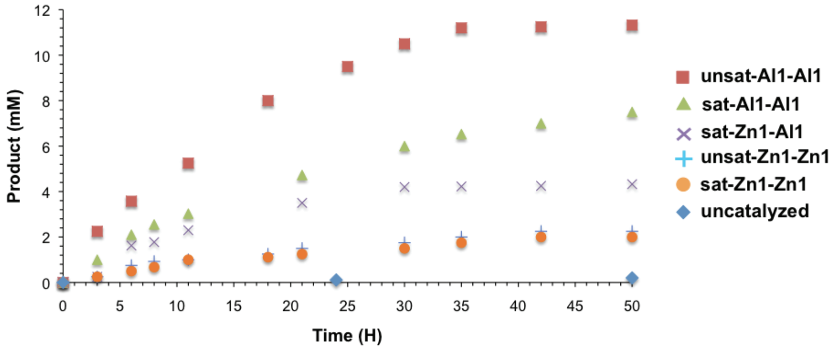

Fig. S27 Overall product formation profiles for the methanolysis of PNPDPP in the presence and absence of the series 1 porphyrin catalysts.

Table S3 Product formation rates for the methanolysis of PNPDPP in the presence of porphyrin monomer (**series 1**) catalysts at 12.3 M MeOH. Reported catalyzed rates were background-corrected from uncatalyzed reactions.

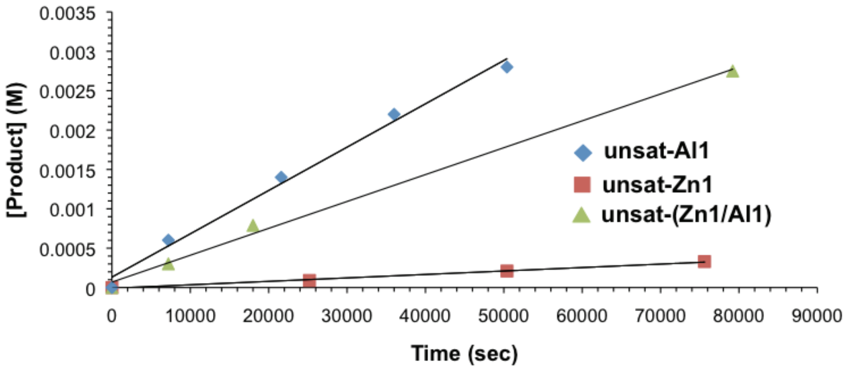

Porphyrin catalyst	Catalyst loading (mol %)	Observed initial rate (M/s)
unsat-Zn1	6	4.4×10^{-9}
unsat-Al1	6	5.47×10^{-8}
unsat-(Zn1/Al1)	6 (3 mol% each)	3.41×10^{-8}

XI. Product formation rates for the methanolysis of PNPDPP catalyzed series 2 catalysts. Reactions were carried out as described above in section X.

Table S4 Product formation rates for the methanolysis of PNPDPP in the presence of porphyrin (**series 2**) catalysts at 12.3 M MeOH. Reported catalyzed rates were background-corrected from uncatalyzed reactions.

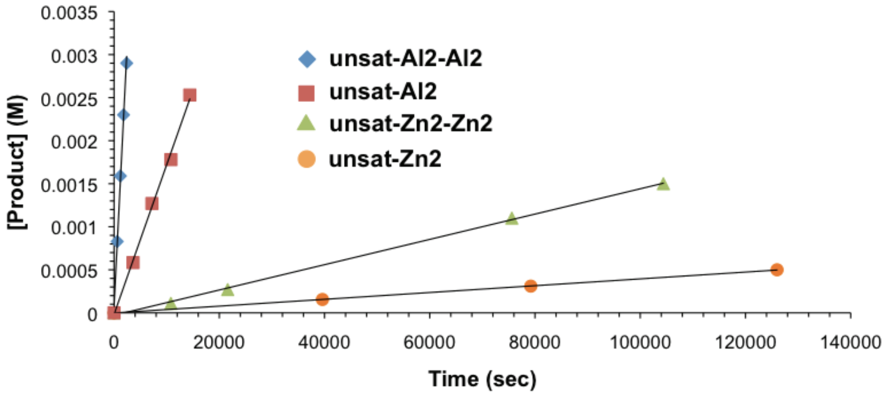

Porphyrin catalyst	Catalyst loading (mol %)	Observed initial rate (M/s)
unsat-Zn2	6	4.0×10^{-9}
unsat-Al2	6	1.67×10^{-7}
unsat-Zn2-Zn2	3	1.47×10^{-8}
unsat-Al2-Al2	3	1.21×10^{-6}

XII. Measurement of binding constants. The UV-vis spectrophotometric titrations were conducted by progressively adding small aliquots (5 μL) of guest solution (15.6 M for neat MeOH or 1.3 M for PNPDPP in $CHCl_3$), using a 25 μL microsyringe, to a cuvette containing the porphyrin dimer solution (2.5 mL of a 0.5 μM solution in $CHCl_3$). To minimize the change of the solution volume, the maximum total added volume for all aliquots of the guest solution was less than 100 μL. As an example for the analysis of UV-vis titration data, the change in absorbance (A) of **unsat-Al1-Al1** in the presence of the guest was calculated and the data were plotted against [guest] (guest = MeOH or PNPDPP, Figs. S28 and S29). Simultaneous binding of the guest to the host was assumed to vary following the 1:n stoichiometries (**unsat-Al1-Al1**:guest) and the binding constants K_a for these species were derived using the Marquardt least-squares minimization[S10] based on the equations:

$$\textbf{unsat-Al1-Al1} + n\mathrm{L} \overset{K_a}{\rightleftharpoons} (\textbf{unsat-Al1-Al1})\cdot \mathrm{L}_n$$

$$K_a = \frac{[(\textbf{unsat-Al1-Al1})\cdot \mathrm{L}_n]}{[\textbf{unsat-Al1-Al1}][\mathrm{L}]^n} \quad (S1)$$

$$C_{\text{unsat-Al1-Al1}} = [\textbf{unsat-Al1-Al1}] + [(\textbf{unsat-Al1-Al1})\cdot \mathrm{L}_n] \quad (S2)$$

$$C_L \approx [\mathrm{L}] \quad (S3)$$

$$[(\textbf{unsat-Al1-Al1})\cdot \mathrm{L}_n] = \frac{C_{\text{unsat-Al1-Al1}} K_a}{K_a + (1/C_L)^n} \quad (S4)$$

K_a : Binding constant of MeOH or PNPDPP to **unsat-Al1-Al1**
n : Binding number of MeOH or PNPDPP to **unsat-Al1-Al1**
[**unsat-Al1-Al1**] : Concentration of **unsat-Al1-Al1**
[L] : Concentration of MeOH or PNPDPP
$C_{\text{unsat-Al1-Al1}}$: Total concentration of **unsat-Al1-Al1**
C_L : Total concentration of MeOH or PNPDPP

Eq S4 indicates that [**unsat-Al1-Al1**$\cdot L_n$] is the function of n (the number of guest binding) and K_a when C_L and $C_{(\text{unsat-Al1-Al1})}$ are known. Two unknown parameters (n and K_a) in Eq S4 for single guest (n = 1), two guests (n = 2), three guests (n = 3), and four guests (n = 4) binding model were fitted from the UV titration data. The quality of the fitting between calculated curve and experimental titration data indicates that single-guest binding mode are reasonable in $CHCl_3$ for both **unsat-Al1-Al1**:MeOH and **unsat-Al1-Al1**:PNPDPP.

Plotting A versus [PNPDPP] for the binding of PNPDPP to **unsat-Al1-Al1** gave a binding constant of K_a = 70.7 M^{-1} (n = 1, Fig. S28) for the 1:1 complex of **unsat-Al1-Al1**:PNPDPP, indicating that one PNPDPP is coordinating to one **unsat-Al1-Al1**. Additionally, plotting A versus [MeOH] for the binding of MeOH to **unsat-Al1-Al1** gave a good fit for the 1:1 complex of **unsat-Al1-Al1**:MeOH, with a binding constant of K_a = 5.6 M^{-1} (n = 1, Fig. S29).

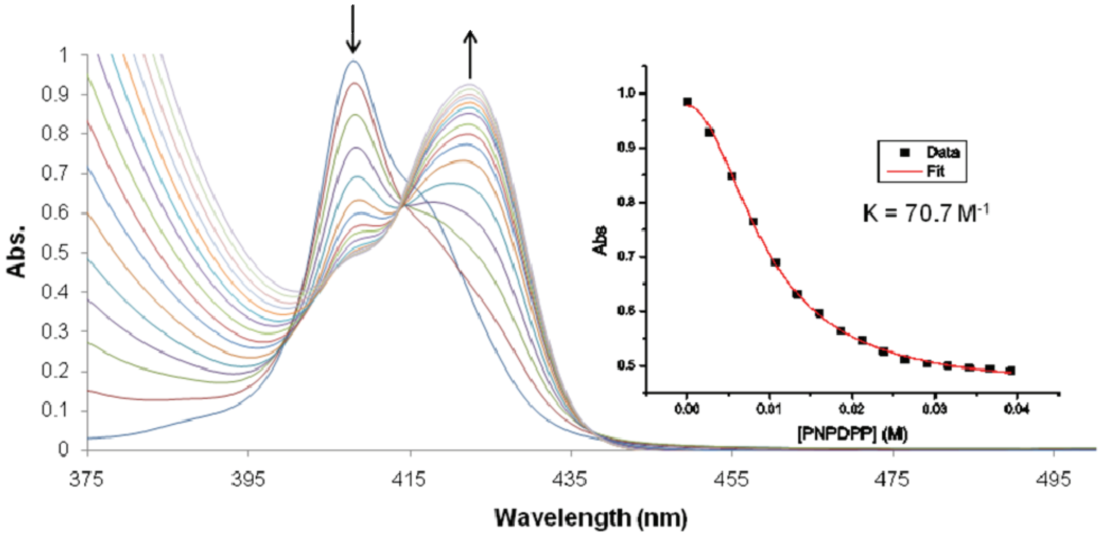

Fig. S28 The changes in the absorption spectra of **unsat-Al1-Al1** in $CHCl_3$ upon titration with PNPDPP at rt. Arrows show the directions of change in absorption with increasing PNPDPP concentration. Inset: The absorption changes at 408 nm and the result of fitting the data to Eq S4.

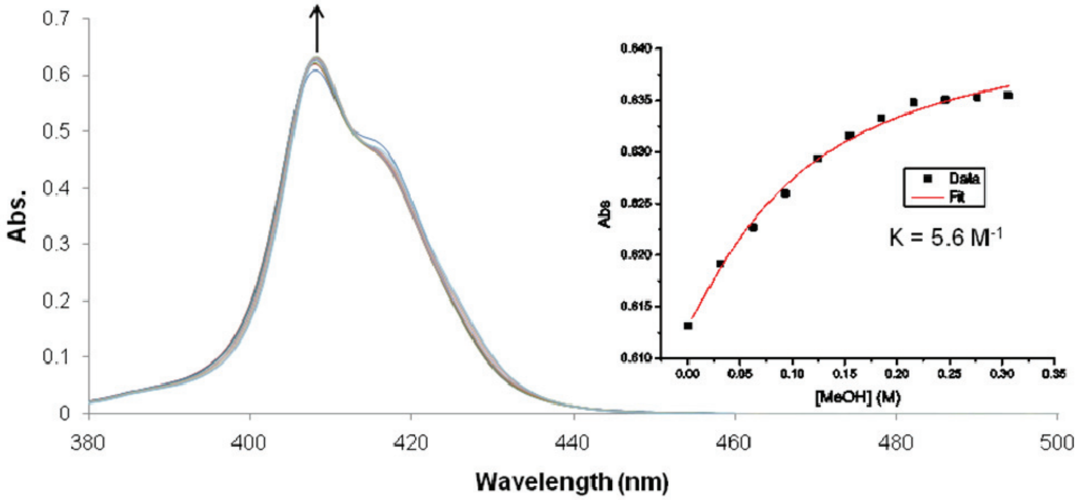

Fig. S29 The changes in the absorption spectra of **unsat-Al1-Al1** in $CHCl_3$ upon titration with MeOH at rt. The arrow shows the direction of change in absorption with increasing MeOH concentration. Inset: The absorption changes at 408 nm and the result of fitting the data to Eq S4.

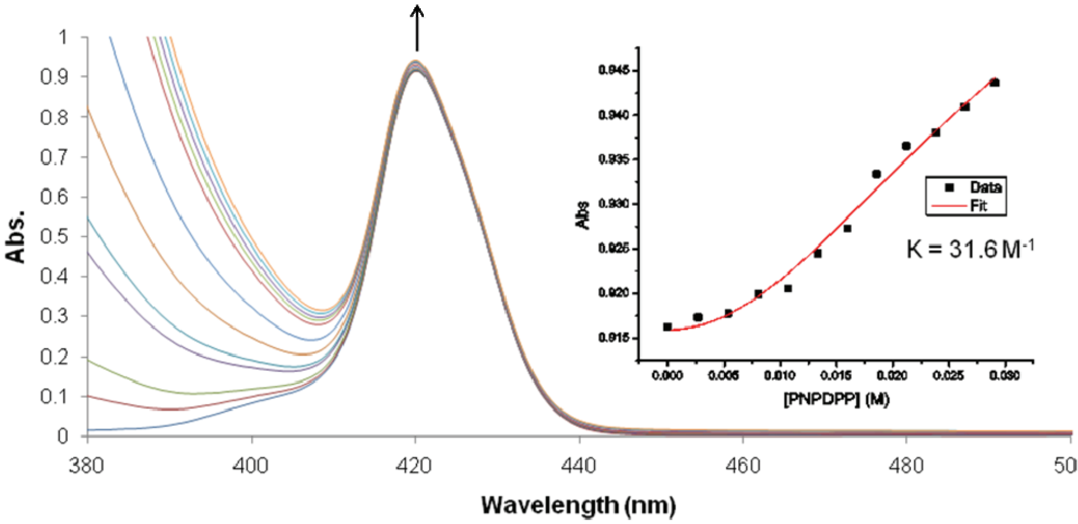

Fig. S30 The changes in the absorption spectra of **unsat-Zn1-Zn1** in $CHCl_3$ upon titration with PNPDPP at rt. The arrow shows the direction of change in absorption with increasing PNPDPP concentration. Inset: The absorption changes at 420 nm and the result of fitting the data to Eq S4.

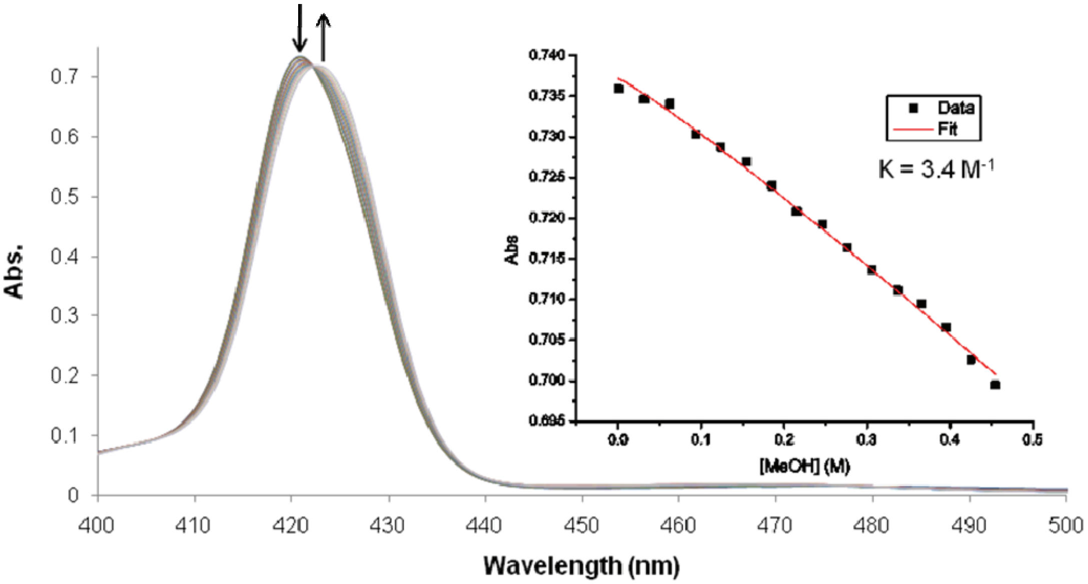

Fig. S31 The changes in the absorption spectra of **unsat-Zn1-Zn1** in $CHCl_3$ upon titration with MeOH at rt. Arrows show the directions of change in absorption with increasing MeOH concentration. Inset: The absorption changes at 420 nm and the result of fitting the data to Eq S4.

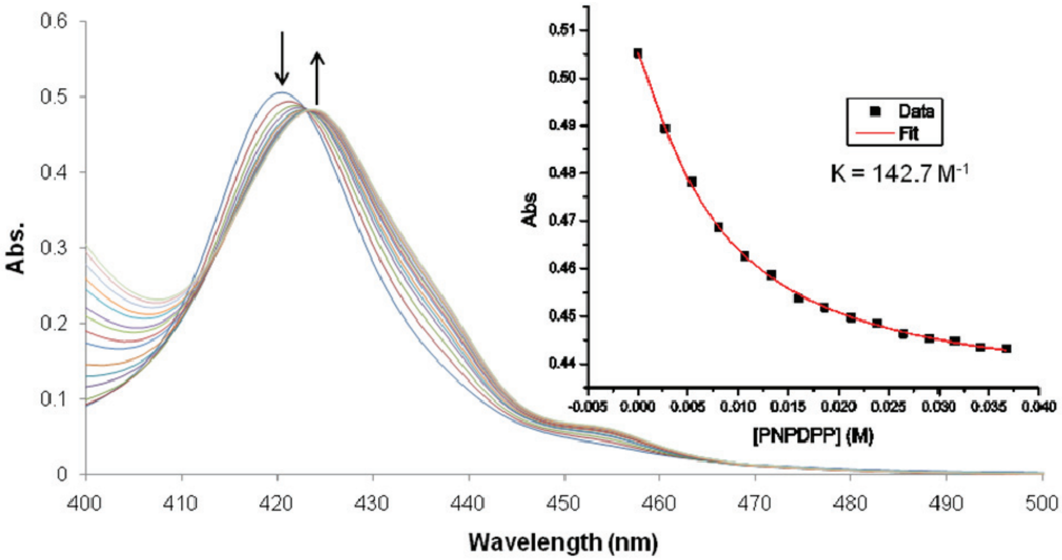

Fig. S32 The changes in the absorption spectra of **unsat-Al2-Al2** in $CHCl_3$ upon titration with PNPDPP at rt. Arrows show the directions of change in absorption with increasing PNPDPP concentration. Inset: The absorption changes at 420 nm and the result of fitting the data to Eq S4.

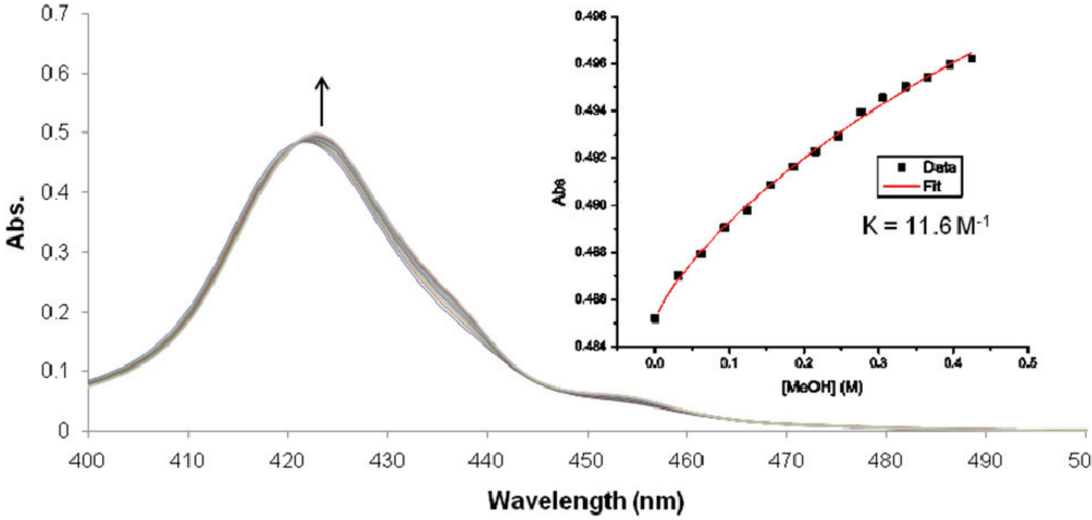

Fig. S33 The changes in the absorption spectra of **unsat-Al2-Al2** in $CHCl_3$ upon titration with MeOH at rt. The arrow shows the direction of change in absorption with increasing MeOH concentration. Inset: The absorption changes at 420 nm and the result of fitting the data to Eq S4.

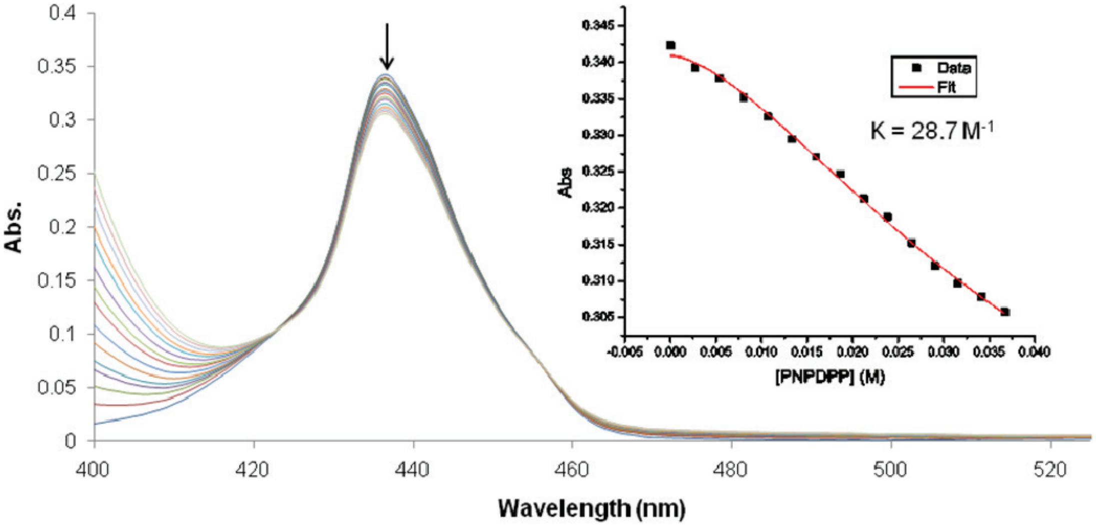

Fig. S34 The changes in the absorption spectra of **unsat-Zn2-Zn2** in $CHCl_3$ upon titration with PNPDPP at rt. The arrow shows the direction of change in absorption with increasing PNPDPP concentration. Inset: The absorption changes at 436 nm and the result of fitting the data to Eq S4.

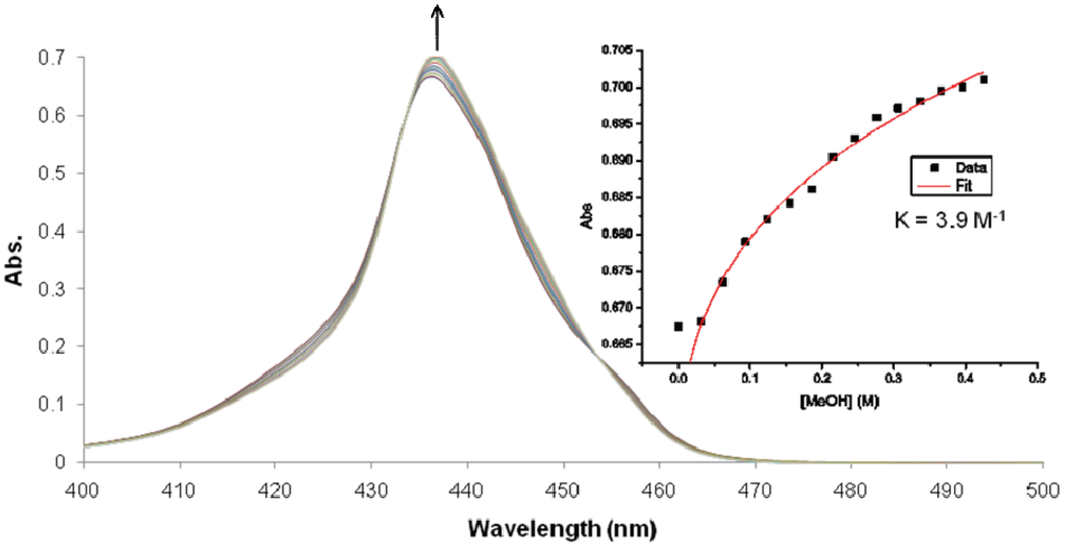

Fig. S35 The changes in the absorption spectra of **unsat-Zn2-Zn2** in $CHCl_3$ upon titration with MeOH at rt. The arrow shows the direction of change in absorption with increasing MeOH concentration. Inset: The absorption changes at 436 nm and the result of fitting the data to Eq S4.

Table S5 UV-vis-measured binding constants of MeOH and PNPDPP to various porphyrin dimers in $CHCl_3$.

Porphyrin species	Binding constant of MeOH ($K_{a(MeOH)}$, M^{-1})^a	Binding constant of PNPDPP ($K_{a(PNPDPP)}$, M^{-1})^a
unsat-Al1-Al1	5.6	70.7
unsat-Zn1-Zn1	3.4	31.6
unsat-Al2-Al2	11.6	142.7
unsat-Zn2-Zn2	3.9	28.7

[a] UV-vis titration experiments of MeOH and PNPDPP were carried out at room temperature in $CHCl_3$. The solutions of the porphyrin dimers were 0.5 μM.

The fluorescence titrations were carried out by progressively adding small aliquots (5 μL) of PNPDPP solution (1.3 M, PNPDPP stock solutions in $CHCl_3$/MeOH (1:1 v/v)), using a 25 μL microsyringe, to a quartz fluorescence cuvette containing the porphyrin dimer solution (1 mL of a 2 μM solution in $CHCl_3$/MeOH (1:1 v/v)) or the porphyrin monomer solution (1 mL of a 5 μM solution in $CHCl_3$/MeOH (1:1)). To minimize the change of the solution volume, the maximum total added volume for all aliquots of the guest solution was less than 100 μL. The solution was excited at 442 nm and the fluorescent emission intensity was recorded from 500 to 800 nm after each addition of PNPDPP. A plot of intensity versus [PNPDPP] was carried out to yield the binding constant (K_a) by the nonlinear fitting method described above.[S10]

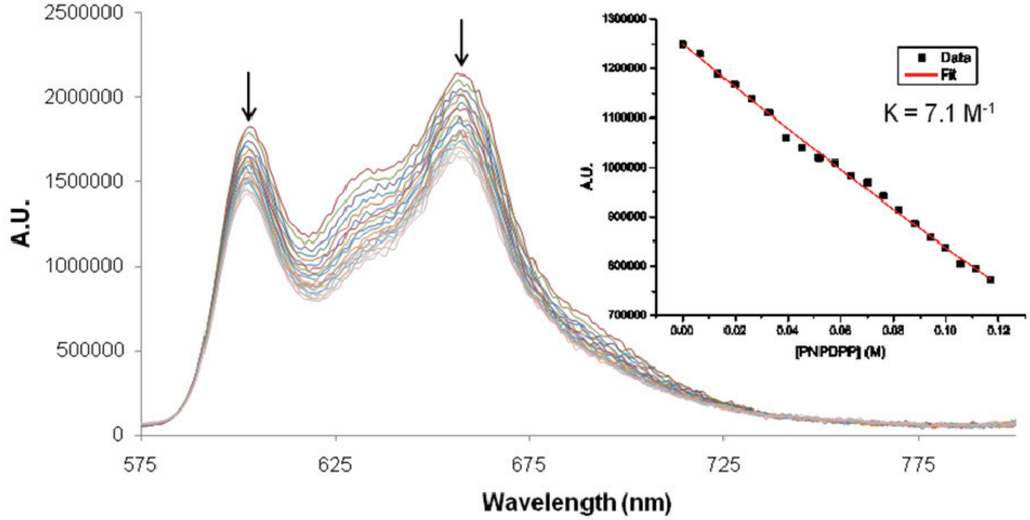

Fig. S36 The changes in the fluorescence emission spectra of **unsat-Al1** in $CHCl_3$/MeOH upon titration with PNPDPP at rt. Arrows show the directions of change in fluorescence emission with increasing PNPDPP concentration. Inset: the fluorescence emission changes at 605 nm and the result of fitting the data to Eq S4.

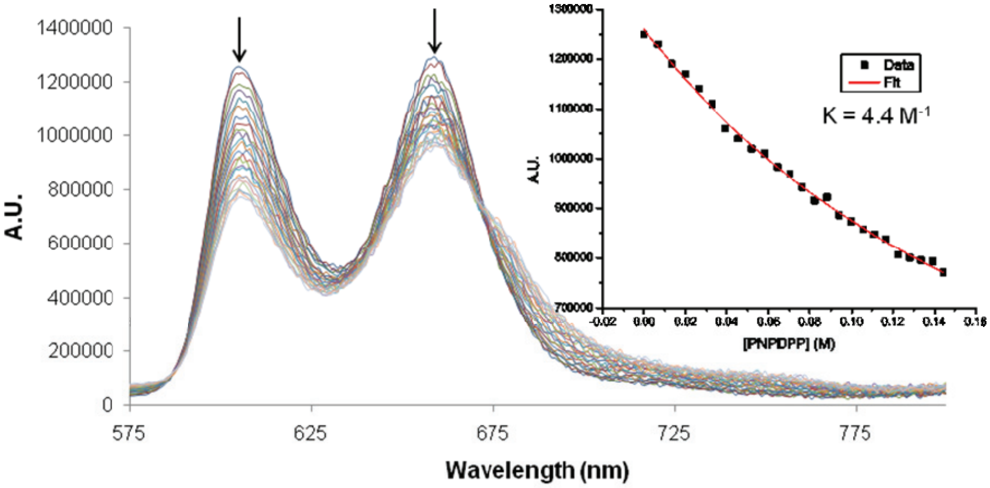

Fig. S37 The changes in the fluorescence emission spectra of **unsat-Zn1** in $CHCl_3$/MeOH upon titration with PNPDPP at rt. Arrows show the directions of change in fluorescence emission with increasing PNPDPP concentration. Inset: the fluorescence emission changes at 605 nm and the result of fitting the data to Eq S4.

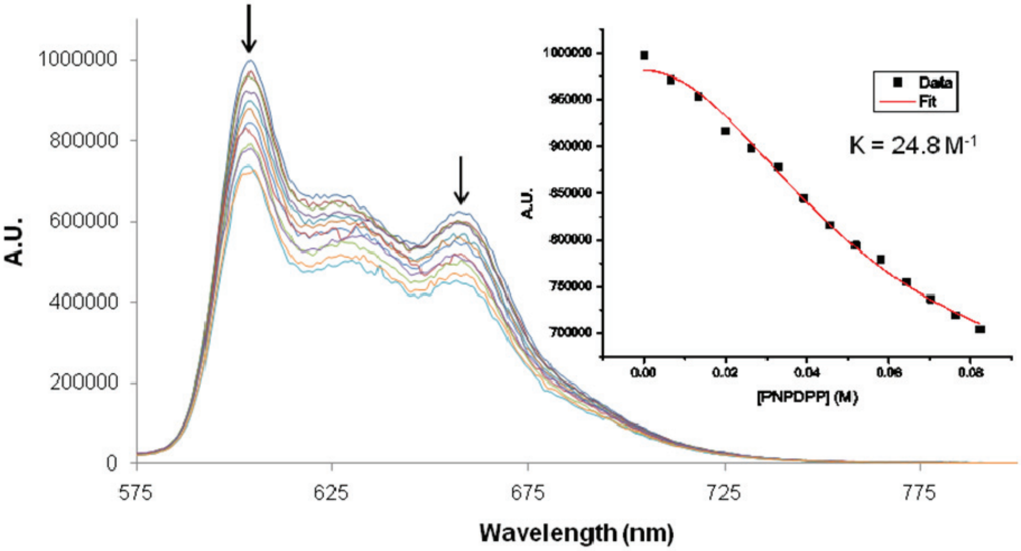

Fig. S38 The changes in the fluorescence emission spectra of **unsat-Al1-Al1** in $CHCl_3$/MeOH upon titration with PNPDPP at rt. Arrows show the directions of change in fluorescence emission with increasing PNPDPP concentration. Inset: the fluorescence emission changes at 605 nm and the result of fitting the data to Eq S4.

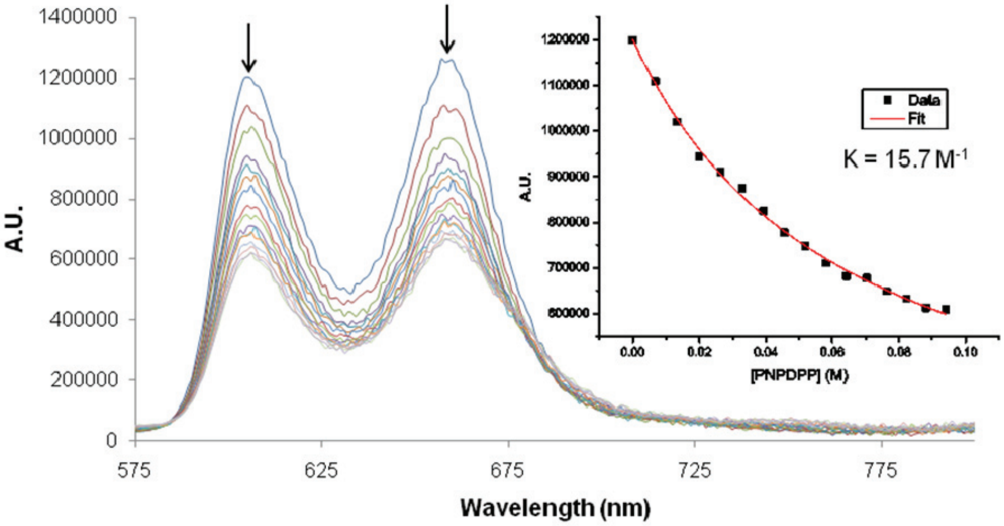

Fig. S39 The changes in the fluorescence emission spectra of **unsat-Zn1-Zn1** in $CHCl_3$/MeOH upon titration with PNPDPP at rt. Arrows show the directions of change in fluorescence emission with increasing PNPDPP concentration. Inset: the fluorescence emission changes at 605 nm and the result of fitting the data to Eq S4.

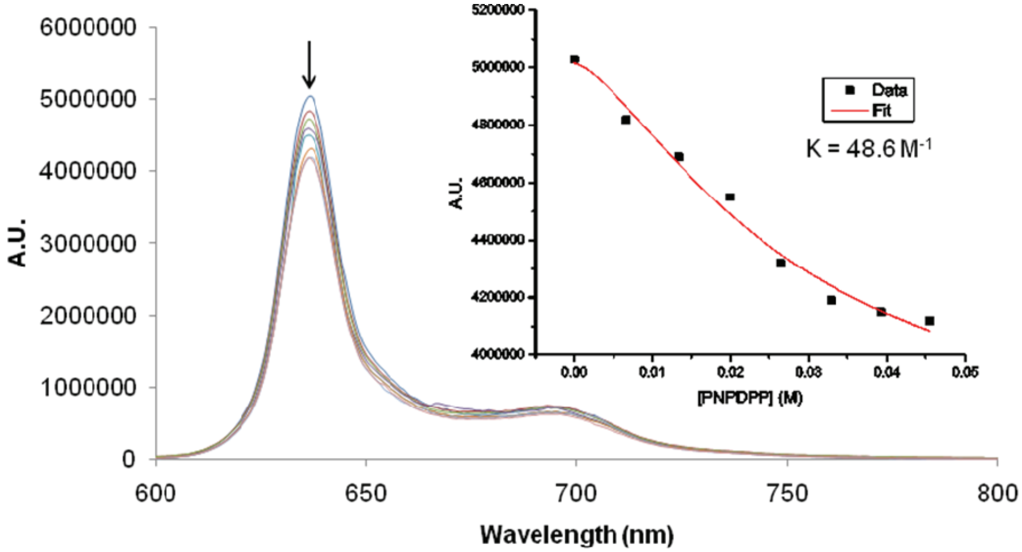

Fig. S40 The changes in the fluorescence emission spectra of **unsat-Al2-Al2** in $CHCl_3$/MeOH upon titration with PNPDPP at rt. The arrow shows the direction of change in fluorescence emission with increasing PNPDPP concentration. Inset: the fluorescence emission changes at 637 nm and the result of fitting the data to Eq S4.

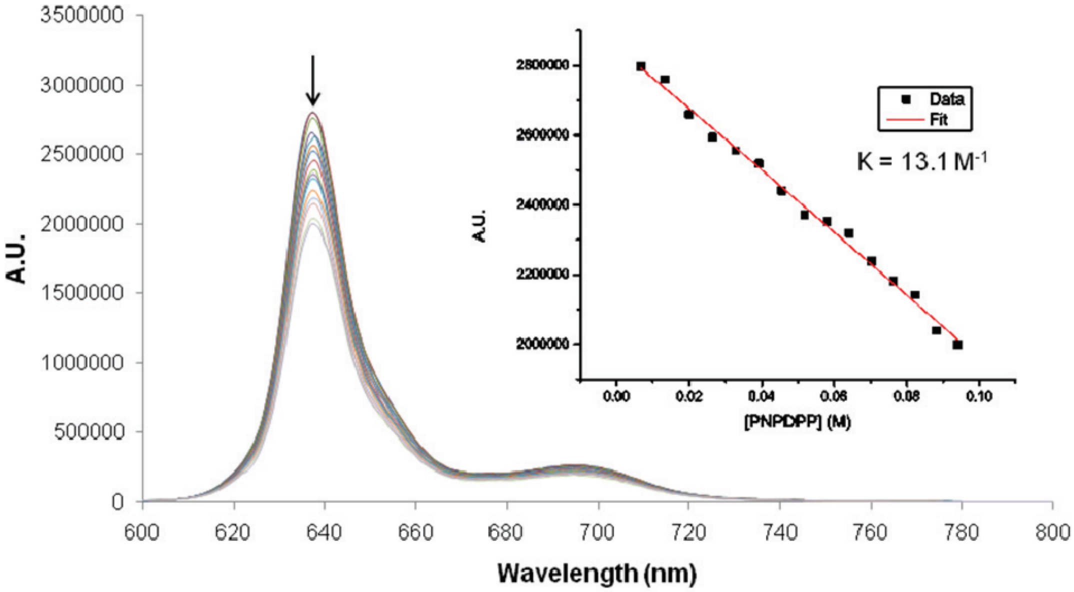

Fig. S41 The changes in the fluorescence emission spectra of **unsat-Zn2-Zn2** in $CHCl_3$/MeOH upon titration with PNPDPP at rt. The arrow shows the direction of change in fluorescence emission with increasing PNPDPP concentration. Inset: the fluorescence emission changes at 637 nm and the result of fitting the data to Eq S4.

Table S6 Fluorescence-based binding constants of PNPDPP to various porphyrin dimers in a mixture of $CHCl_3$/MeOH (1:1 v/v).

Porphyrin species	Binding constant of PNPDPP ($K_{a(\mathrm{PNPDPP})}$, M^{-1})^a
unsat-Al1	7.1
unsat-Zn1	4.4
unsat-Al1-Al1	24.8
unsat-Zn1-Zn1	15.7
unsat-Al2-Al2	48.6
unsat-Zn2-Zn2	13.1

^{a}Fluorescence titration experiments of PNPDPP were carried out at room temperature in a mixture of $CHCl_3$/MeOH (1:1 v/v). The solutions of the porphyrin dimers were 2 μM and the solutions of the porphyrin monomers were 5 μM.

The predicted binding constants of PNPDPP ($K_{a(PNPDPP)}$) to porphyrin dimers in a mixture of $CHCl_3$/MeOH (1:1 v/v) based on the $K_{a(PNPDPP)}$ and $K_{a(MeOH)}$ in pure $CHCl_3$. The quality of the fitting between calculated curve and experimental UV-vis titration data indicates that single-guest binding mode is reasonable in $CHCl_3$ for both PNPDPP and MeOH to porphyrin dimer hosts (**H**). (Figs. S28-S35). Thus, the binding constant of PNPDPP to the porphyrin dimer host (**H**) in pure $CHCl_3$ ($K_{PNPDPP}(CHCl_3)$) can be calculated as follows:

$$\mathbf{H} + \mathrm{PNPDPP} \overset{K_{PNPDPP}}{\rightleftharpoons} \mathbf{H}\cdot\mathrm{PNPDPP}$$

$$K_{PNPDPP}(CHCl_3,\ M^{-1}) = \frac{[\mathbf{H}\cdot\mathrm{PNPDPP}]}{[\mathbf{H}][\mathrm{PNPDPP}]} \qquad \text{(S5)}$$

The binding constants of MeOH to the porphyrin dimer host (**H**) in pure $CHCl_3$ ($K_{MeOH}(CHCl_3)$) can be calculated as follows:

$$\mathbf{H} + \mathrm{MeOH} \overset{K_{MeOH}}{\rightleftharpoons} \mathbf{H}\cdot\mathrm{MeOH}$$

$$K_{MeOH}(CHCl_3,\ M^{-1}) = \frac{[\mathbf{H}\cdot\mathrm{MeOH}]}{[\mathbf{H}][\mathrm{MeOH}]}$$

$$\frac{[\mathbf{H}\cdot\mathrm{MeOH}]}{[\mathbf{H}]} = K_{MeOH}[\mathrm{MeOH}] \qquad \text{(S6)}$$

In a mixture of $CHCl_3$/MeOH (1:1 v/v), the association constant of PNPDPP to the porphyrin dimer (**H**) at room temperature ($K_{PNPDPP}(CHCl_3/MeOH)$) can be expressed as:

$$(\mathbf{H} + \mathbf{H}\cdot\mathrm{MeOH}) + \mathrm{PNPDPP} \overset{K_{PNPDPP}}{\rightleftharpoons} \mathbf{H}\cdot\mathrm{PNPDPP}$$

$$\begin{aligned} K_{PNPDPP}(CHCl_3/MeOH,\ M^{-1}) &= \frac{[\mathbf{H}\cdot\mathrm{PNPDPP}]}{([\mathbf{H}]+[\mathbf{H}\cdot\mathrm{MeOH}])[\mathrm{PNPDPP}]} \\ &= \frac{[\mathbf{H}\cdot\mathrm{PNPDPP}]}{(1+K_{MeOH}(CHCl_3)[\mathrm{MeOH}])[\mathbf{H}][\mathrm{PNPDPP}]} \\ &= \frac{K_{PNPDPP}(CHCl_3)}{(1+K_{MeOH}(CHCl_3)[\mathrm{MeOH}]} \qquad \text{(S7)} \end{aligned}$$

As an example, the predicted binding constant of PNPDPP to **unsat-Al1-Al1** in a mixture of $CHCl_3$/MeOH (1:1 v/v, 12.3 M MeOH) can be calculated as follows:

$K_{PNPDPP}(CHCl_3/MeOH)$ for **unsat-Al1-Al1** = $(70.7\ M^{-1})/(1 + (5.6\ M^{-1} \times 12.3\ M)) = 1.0\ M^{-1}$

The predicted binding constants of PNPDPP to **unsat-Zn1-Zn1**, **unsat-Al2-Al2**, and **unsat-Zn2-Zn2** can be calculated in the same manner (Table S7).

Table S7 The predicted binding constants of PNPDPP ($K_{a(PNPDPP)}$) to porphyrin dimers in a mixture of $CHCl_3$/MeOH (1:1 v/v) based on the $K_{a(PNPDPP)}$ and $K_{a(MeOH)}$ in pure $CHCl_3$.

Porphyrin species	**Binding constant of PNPDPP ($K_{a(PNPDPP)}$)**	
	Predicted $K_{a(PNPDPP)}$ (M^{-1})	**Experimental $K_{a(PNPDPP)}$ (M^{-1})[a]**
unsat-Al1-Al1	1.0	24.8
unsat-Zn1-Zn1	0.7	15.7
unsat-Al2-Al2	1.0	48.6
unsat-Zn2-Zn2	0.6	13.1

[a] Experimental $K_{a(PNPDPP)}$ values were obtained from the room-temperature fluorescence titration of PNPDPP to 2 μM solutions of the porphyrin dimers in a mixture of $CHCl_3$/MeOH (1:1 v/v). See complete data set in Table S4.

Author contributions audit: R.K.T., S.J.L., J.T.H., and S.T.N. conceived the experiments presented herein. R.K.T. synthesized all compounds except *para*-nitrophenyl diphenylphosphate, which was synthesized by B.K. R.K.T carried out the characterization of all compounds, the catalysis experiments, and the UV-vis and fluorescence titration experiments. P.R. carried out the CHELPG calculations. B.K. carried out several control experiments. J.T.H. and S.T.N. supervised the project. R.K.T wrote the initial draft of the paper and received inputs and corrections from all co-authors. R.K.T., B.K., and S.T.N. finalized the manuscript.

XII. References

S1. A. B. Pangborn, M. A. Giardello, R. H. Grubbs, R. K. Rosen and F. J. Timmers, *Organometallics*, 1996, **15**, 1518-1520.

S2. M. J. Plater, S. Aiken and G. Bourhill, *Tetrahedron*, 2002, **58**, 2405-2413.

S3. M. J. Plater, S. Aiken and G. Bourhill, *Tetrahedron*, 2002, **58**, 2415-2422.

S4. K. Tashiro and T. Aida, *Chem. Soc. Rev.*, 2007, **36**, 189-197.

S5. A. Ouchi, K. Tashiro, K. Yamaguchi, T. Tsuchiya, T. Akasaka and T. Aida, *Angew. Chem., Int. Ed.*, 2006, **45**, 3542-3546.

S6. G. Subramaniam and R. K. Gilpin, *Macromolecules*, 1990, **23**, 693-697.

S7. K. C. Nicolaou, S. Y. Cho, R. Hughes, N. Winssinger, C. Smethurst, H. Labischinski and R. Endermann, *Chem. Eur. J.*, 2001, **7**, 3798-3823.

S8. S. Jones and D. Selitsianos, *Org. Lett.*, 2002, **4**, 3671-3673.

S9. C. M. Breneman and K. B. Wiberg, *J. Comput. Chem.*, 1990, **11**, 361-373.

S10. OriginPro 8.0, OriginLab Corp., Northampton, MA, USA.